PRELIMINARY DESIGN REPORT
PROTOTYPE STEAM GENERATOR

Report No
BAW-1280-28

VOL. 3 - EFFECTS OF SODIUM-WATER REACTION ON STEAM GENERATOR

Volume 3
of 4 Volumes

U.S. Atomic Energy Commission
Chicago Operations Office
Lemont, Illinois

MASTER

November 15, 1965

SODIUM-HEATED STEAM GENERATOR
DEVELOPMENT

AEC CONTRACT NO. AT (11-1) - 1280
B&W CONTRACT NO. 610 - 0067

THE BABCOCK & WILCOX CO.
BOILER DIVISION

Barberton, Ohio

This report has not been [redacted] for publication. It is [redacted] the recipient [redacted] official [redacted] purposes only [redacted] should not be [redacted] further disseminated until officially [redacted] reviewed [redacted] released for publication.

DISCLAIMER

This report was prepared as an account of work sponsored by an agency of the United States Government. Neither the United States Government nor any agency Thereof, nor any of their employees, makes any warranty, express or implied, or assumes any legal liability or responsibility for the accuracy, completeness, or usefulness of any information, apparatus, product, or process disclosed, or represents that its use would not infringe privately owned rights. Reference herein to any specific commercial product, process, or service by trade name, trademark, manufacturer, or otherwise does not necessarily constitute or imply its endorsement, recommendation, or favoring by the United States Government or any agency thereof. The views and opinions of authors expressed herein do not necessarily state or reflect those of the United States Government or any agency thereof.

DISCLAIMER

Portions of this document may be illegible in electronic image products. Images are produced from the best available original document.

Report No. BAW - 1280 - 28

PRELIMINARY DESIGN REPORT
PROTOTYPE STEAM GENERATOR

Volume 3
of 4 Volumes

VOL. 3 - EFFECTS OF SODIUM-WATER REACTION ON STEAM GENERATOR

to

U.S. Atomic Energy Commission
Chicago Operations Office
Lemont, Illinois

November 15, 1965

AEC Contract No. AT (11-1)-1280
B&W Contract No. 610-0067

SODIUM-HEATED STEAM GENERATOR
DEVELOPMENT

Prepared By: J.E. Hocking

Approved By: P.B. Probert

Date: November 15, 1965

THE BABCOCK & WILCOX CO.
BOILER DIVISION
BARBERTON, OHIO

TABLE OF CONTENTS

		PAGE
1.0	INTRODUCTION	1
2.0	CONCLUSIONS	6
3.0	PREDICTION OF THE MAXIMUM CREDIBLE SODIUM-WATER REACTION PRESSURES & VOLUMES	11
4.0	THE DYNAMIC STRENGTH OF THE STEAM GENERATOR SHELL	16
	INTRODUCTION.	
	4.1 IMPULSE-MOMENTUM METHOD OF ANALYSIS	19
	APPENDIX - SAMPLE CALCULATIONS - IMPULSE - MOMENTUM METHOD	
	4.2 WORK-ENERGY METHOD OF ANALYSIS	44
	APPENDIX - SAMPLE CALCULATIONS - WORK - ENERGY METHOD	
5.0	LOCALIZED BULGE FAILURE ANALYSIS	59
6.0	CORROSION OF MATERIALS OF CONSTRUCTION IN PRODUCTS OF A SODIUM-WATER REACTION	87
7.0	STRAIN HARDENING DATA	94
8.0	STRUCTURAL ANALYSIS OF THE CENTER PIPE ASSEMBLY UNDER EXTERNAL PRESSURE LOADING.	102
9.0	STRUCTURAL ANALYSIS OF THE BOILER COIL SUPPORTS UNDER SODIUM-WATER REACTION CONDITIONS	107
10.0	ANALYSIS OF TUBE VIBRATION SUPPORTS AND BAFFLES DURING A SODIUM-WATER REACTION CONDITION	124
11.0	CREDIBILITY OF OVERHEATING THE SHELL AND LINER DURING A SODIUM-WATER REACTION	135

1.0 INTRODUCTION

ANALYSIS OF THE PRESSURE EFFECTS AND SHELL STRENGTH FOR THE PROTOTYPE SODIUM HEATED STEAM GENERATOR.

INTRODUCTION:

In any steam generator heated by sodium one must face the possibility of a sodium-water reaction. Designing the boiler with double tube walls does not insure against a sodium-water reaction. As an example, Adams, et al, KAPL - P-1512, describes sodium-water reaction in a double tube steam generator having mercury in the annulus.

One of the objectives of this Contract is to develop an economical, practical, reliable, large central station steam generator. Since double tube wall construction does not insure against a sodium-water reaction and does multiply the cost of the heating surface by a factor of about four, the steam generator under this Contract is being designed with a single tube wall separating the sodium and water. It is felt that if sodium-heated steam generators are ever to be economical, ways must be found to provide adequate safety from sodium-water reactions using single tube walls.

Experience with sodium-water reactions in actual steam generators is generally optimistic. Two small once-through steam generators built for the Fermi program and for SRE have had no leaks. A tabulation of experience with leaks in steam generators is shown in Table III of "Literature Review of Sodium-Water Reactions", by J.A. Ford, APDA-167. With the exception of the Fermi Steam generator wear failures and re-

sulting reaction, pressure rises and mechanical damage were either not observed or were very minor. Local high temperatures, corrosion, and stress corrosion were observed in several instances, however. In the absence of more operating experience with sodium-heated steam generators the designer must consider the worst credible accident.

It is considered credible that sometime during the test life of the Prototype Steam Generator some type of leak may develop in which water will react with the sodium. This condition must be taken into account in designing the Sodium-Heated Steam Generator. The design of the Full-Size and Prototype Steam Generator is such that the steam generator shell in each case is protected by a liner separated from the shell by an inert gas annulus. A gas cushion is provided over the sodium in each steam generator, and relief valves and rupture discs are provided for the safe relief of the products of a sodium-water reaction.

There are two areas of concern in providing for the safe handling of a sodium-water reaction in a steam generator. These are:

1. Small leaks - It is important to detect small leaks as early as possible and take corrective action before corrosion resulting from the sodium-water reaction has damaged the steam generator and before the small leak has had a chance to become a large leak. Reliable detection techniques are extremely important. The Commission has an active program on the development of leak detection techniques not under this Contract.

2. Large leaks - In the case of large leaks it is important to isolate the steam generator from the feedwater and steam headers and vent the water to dump system. The more water that is removed through an isolation and dump system the less water will be available to react with the sodium. Relief devices must be provided to vent the products of the sodium-water reaction safely without allowing the pressure in the steam generator to build-up higher than the steam generator can safely withstand. The steam generator shell must be capable of withstanding the maximum pressure peaks that may occur at any time during the reaction. This is imperative for the safety of personnel and equipment and is a prime design objective.

Generally, the problems of handling sodium-water reaction products in the B&W Full-Size and the Prototype Steam Generators will be quite similar. The tubes in both the Full-Size and Prototype Steam Generator are the same size so that the size of leak and quantity of reaction products to handle will be the same. The transient pressure peaks during the first few milliseconds will be similar in the Prototype Steam Generator.

A co-operative effort program has been carried out by Atomic Power Development Associates and the Babcock & Wilcox Company to analyze the Full-Size and Prototype Steam Generators under conditions of a sodium-water reaction accident. This program is divided into two parts. The

first part of this study concerns itself with analyzing the Full-Size Steam Generator to determine the credible maximum number of tubes that may fail as a result of an initial leak from a single tube, and to demonstrate that the products from this reaction can be safely contained and safely relieved. The second portion of the study is the somewhat easier task of demonstrating that the Prototype Steam Generator will be adequately safe to operate at SCTI.

Background work to both steam generator systems has been done by APDA under Subcontract No. 1 to this Contract. This has provided predictions of the credible pressures and temperatures resulting from a sodium-water reaction.

B&W has analyzed the strength of the steam generators to determine the extent of damage due to APDA's predicted pressures and temperatures. The analysis for the Prototype Steam Generator is described herein. The analysis of the sodium-water problems in the Full-Size Steam Generator are included in the Addendum to the Preliminary Design Report, Full-Size Steam Generator Report, BW 67-2 (a).

2.0 CONCLUSIONS

CONCLUSIONS:

As a result of this study it is concluded that the Full-Size Steam Generator will withstand a credible number of tubes failing simultaneously without becoming a hazard to nearby personnel and equipment. Very conservative assumptions have been used throughout, from the prediction of pressures and temperatures by APDA to the dynamic analyses of the Steam Generator shell and internal parts.

A short summary of the results of the several analyses are as follows:

DYNAMIC STRENGTH OF STEAM GENERATOR SHELL -- IMPULSE-MOMENTUM METHOD OF ANALYSIS:

From this analysis it is concluded that the Full-Size Steam Generator can withstand at least the simultaneous failure of 25 tubes in the worst location in the Steam Generator at the pressure condition resulting in the highest leak rate.

DYNAMIC STRENGTH OF STEAM GENERATOR SHELL -- WORK-ENERGY METHOD OF ANALYSIS:

The work-energy type of analysis has shown that the Full-Size Steam Generator will withstand the simultaneous failure of 25 tubes in the worst location in the steam generator at the worst case pressure condition.

LOCALIZED BULGE FAILURE ANALYSIS:

If a large number of tubes are assumed to fail near the liner wall the liner and steam generator shell can withstand the simultaneous failure of 25 tubes. Analyses were made of from one to 25 simultaneous tube ruptures and the 25 tube ruptures in the worst case. The greater number

of tubes spreads the pressure over more of the shell and the analysis approaches the work-energy analysis for the whole shell.

CORROSION OF MATERIALS OF CONSTRUCTION IN PRODUCTS OF A SODIUM-WATER REACTION:

In addition to the safe containing and relieving of the products from a large leak there is a problem of local corrosion resulting from a leak that may be so small that no change in shell side pressure or average temperature occurs.

As a portion of Subcontract No. 1 to this Contract APDA demonstrated experimentally severe thinning of tubes adjacent to a leak in a tube array simulating the B&W Steam Generator. This thinning took place in a few seconds under the worst case conditions. A separate general corrosion test program at B&W Research Center showed very rapid corrosion in aqueous NaOH at elevated temperatures, but not as high as the APDA tests.

Because of the possible severe corrosion damage to a tube bundle adjacent to an initial leak it is very important to provide means in the plant control system to detect water to sodium leaks early and reliable , and to isolate and dump the water from the leaking steam generator.

STRAIN HARDENING DATA FOR THE FULL-SIZE STEAM GENERATOR:

The effect of strain hardening on material properties is considered in the dynamic analyses of the steam generator shell. Experimental data for strain hardening co-efficients from Lehigh University, at ambient temperature, and from the B&W Research Center, at elevated temperature,

shows that strain hardening decreases as temperature increases.

The liner and vessel temperature were used to predict the amount of strain hardening to be expected during deflection of the liner and shell.

STRUCTURAL ANALYSIS OF CENTER PIPE ASSEMBLY:

Analysis of the possible collapse of the center pipe has shown that for failure of 1 tube (at the worst case operating condition), the center pipe is likely to collapse. Whether the center pipe is full of sodium or arranged to be full of gas does not significantly affect the credibility of collapse. If the center pipe does collapse and seal off this escape path the pressure predicted by the APDA computer program is almost unchanged. The reason for this is that the APDA mathematical model is limited to two parallel escape paths. The reaction products actually have more than two parallel paths of escape in the steam generator. When it is assumed that the center pipe is plugged another escape path can be selected for the computer solution. The net result is almost no change in the predicted pressure.

STRUCTURAL ANALYSIS OF THE BOILER COIL SUPPORTS:

Based on the predicted pressure differentials across the coil support bars it can be concluded that the weld connecting the clamping bars to the support bars will be satisfactory, in tension, for 25 tubes rupturing simultaneously. It has been established that the welds on the clamping bars will fail before the tubes are affected in shear or before the applied moment causes failure stresses in the tubes.

ANALYSIS OF TUBE VIBRATION SUPPORTS AND BAFFLES:

The vibration plates and baffles will be satisfactory for the simultaneous rupture of 25 tubes with a factor of safety of one and a half. This has been shown to be true by solving the problem with static methods of analysis and correlating this with the results of the dynamic strength analysis of the shells to obtain the apparent dynamic strength capabilities of these plates & baffles.

CREDIBILITY OF OVERHEATING THE SHELL AND LINER DURING A SODIUM-WATER REACTION:

For the time intervals of interest, (10^{-4} to 1 sec.), the high temperature of the reaction will have penetrated the liner wall less than 10 per cent of the liner thickness, and will not have significantly affected its overall strength. The steam generator shell will not have been affected at all. At longer times the rupture disc will have operated to relieve the pressure within the steam generator.

3.0 PREDICTION OF THE MAXIMUM CREDIBLE SODIUM-WATER REACTION PRESSURES & VOLUMES.

PREDICTION OF THE MAXIMUM CREDIBLE SODIUM-WATER REACTION PRESSURES:

The APDA analysis made to determine the pressure effects of the sodium-water reaction in the Prototype Steam Generator is given in the following reports:

1. APDA - 167 - Ford, J.A., "Literature Review of Sodium-Water Reactions," March 15, 1965.
2. APDA - 175 - "Analysis of the Babcock & Wilcox Company Prototype Steam Generator for a Sodium-Water Reaction".

Only a very brief summary of the general methods of approach and worst case pressure vs. time curves from the APDA analysis is included here. For further details the reader is referred to the APDA reports.

A mathematical model was used to determine the maximum credible pressure for various quantities of instantaneous tube failure, at several locations.

The model takes into account the inertial effect of the sodium above the hydrogen bubble, the compression of the gas in the gas space, the static head of the sodium, the frictional drag on the sodium and the pressure behavior of the hydrogen bubble.

The following assumptions are inherent in the mathematical model.

1. The reaction was considered to be instantaneous.

2. The leak was assumed to occur at "fill" temperature of 350°F with full design pressure of 2625 psig (This condition results in the highest credible leak rate).
3. The leak rate of the water and steam was instantaneous and constant, and not a function of the reaction back pressure.
4. The hydrogen was generated at 1800°F.
5. The hydrogen bubble was assumed to expand isothermally.
6. The hydrogen bubble instantaneously assumes the shape of the cross section of the region being studied and pushed the liquid as a solid slug of sodium.
7. The sodium has two flow paths.
8. The full pressure drop of the sodium as it moved upward was distributed uniformly along the sections considered.

The simultaneous rupture of the 25 downcomer tubes at the top of the downcomer annulus, just below the downcomer boxes, has proven to be the worst credible case. This is APDA case XVI and assumes the center pipe to be collapsed blocking the flow; with relief for the reaction up through the boiler and superheater tube bundle. Both boiler downcomer boxes are considered to be ruptured providing further relief through these channels.

Figure 1 shows the maximum bubble pressure & bubble volume for Case XVI as used throughout the calculation for the Dynamic Analysis of the Steam Generator.

HYDROGEN BUBBLE PRESSURE AND VOLUME, WORST CASE

(APDA CASE XVI, DOWNCOMER ANNULUS)

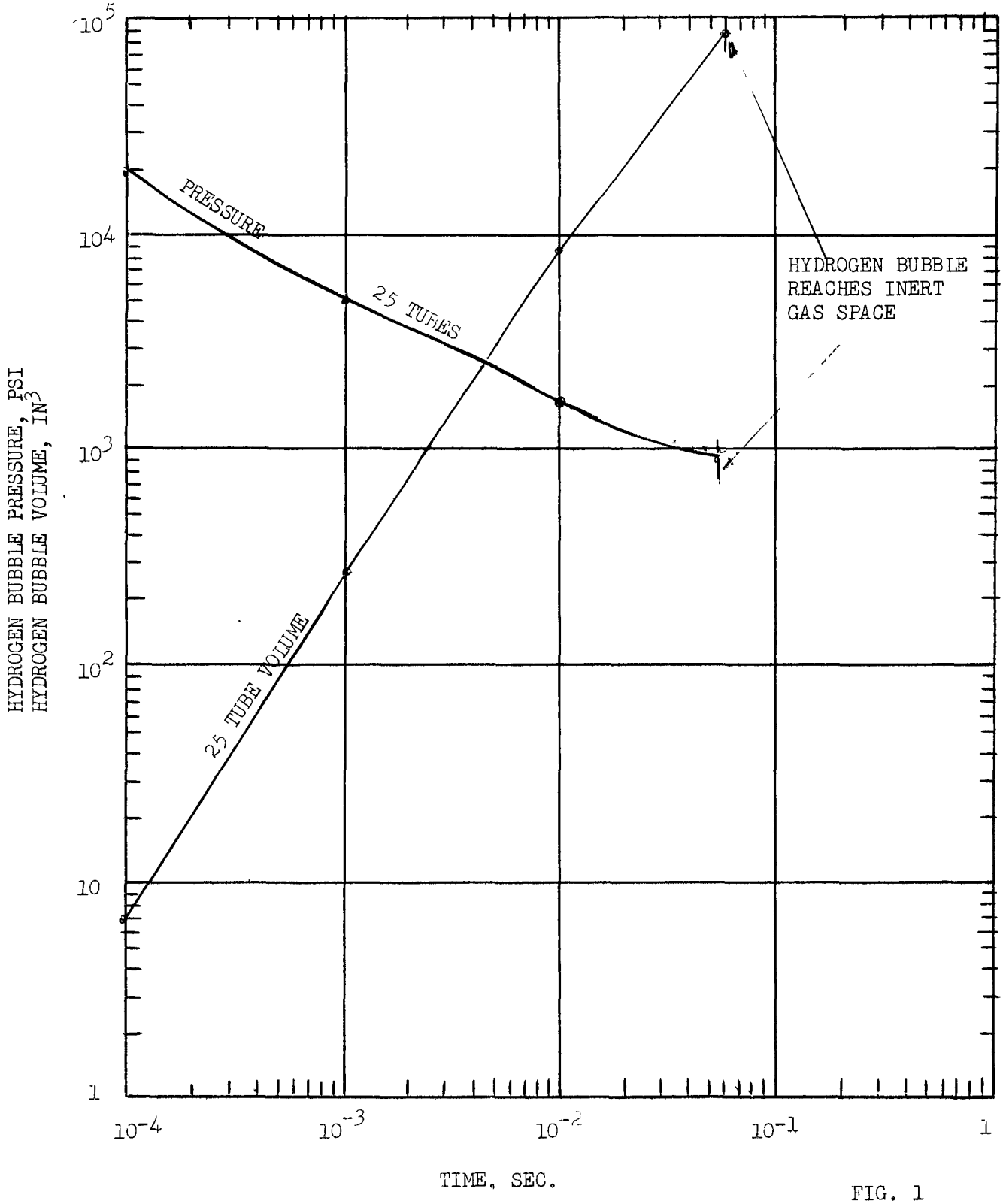

FIG. 1

4. THE DYNAMIC STRENGTH OF THE STEAM GENERATOR SHELL.

INTRODUCTION:

The physical condition of the steam generator shells just prior to a sodium-water reaction is one of equilibrium. During operation the shell deflection or motion will be affected by the operating pressure and temperature and can be assumed to be static for any one point of time. The major question regarding the shells integrity arises from the transient forces and temperatures[1] produced during a sodium-water reaction.

The quantities involved in the Newton's law are: force, mass, and acceleration. Acceleration further involves the use of: time, distance and velocity. Through basic experience with the physical phenomena other quantities have been established which use the basic fundamental laws of Newton. These are work, energy, power, impulse, and momentum. Thus force and distance measure work, mass and velocity measure momentum and kinetic energy; force, distance and time measure power; and force and time measure impulse.

There are three familiar mathematical methods used in obtaining equations that describe the dynamic behavior of mechanical systems. These are (1) the force-acceleration, (2) the work-energy, and (3) the impulse-momentum methods, and all are derivable from Newton's law. In order to get a physical picture of how these methods are related, consider a system (defined as a fixed collection of objects or matter) consisting of

[1]See Section 11.0 for a discussion on the Credibility of Overheating the Vessel and Liner.

a constant concentrated mass acted on by a single external force F (not necessarily constant) in the direction of motion. For this case Newton's law states that: $F = m \frac{dv}{dt}$

$$\begin{bmatrix}\text{Instantaneous}\\ \text{external force}\end{bmatrix} = m \begin{bmatrix}\text{Instantaneous}\\ \text{acceleration}\end{bmatrix} \qquad (1)$$

This equation is the basis for the well-known <u>force-acceleration</u> method.

If the small increment of displacement dx occurs in time increment dt, equation (1) can be multiplied by dx and manipulated as follows:

$$Fdx = m \frac{dv}{dt} \quad dx = m \frac{dx}{dt} \quad dv$$

$$= m\ v\ dv = d\ (\tfrac{1}{2}\ m\ v^2)$$

Since the equation now has force-length dimensions and Fdx is by definition the work of force F it is recognized that -

$$Fdx = d\ (\tfrac{1}{2}\ m\ v^2)$$

$$\begin{bmatrix}\underline{\text{work}}\text{ done on}\\ \text{system by F}\\ \text{during dx}\end{bmatrix} = \begin{bmatrix}\text{increase of}\\ \text{kinetic }\underline{\text{energy}}\\ \text{of system in dt}\end{bmatrix} \qquad (2)$$

Thus Newton's law can be used as the basis for a <u>work-energy</u> approach to dynamics problems and Eq. (2) considered to be a restricted form of the general energy equation of physics.

If now equation (1) is multiplied by time increment dt and it is borne in mind that the system by definition has constant mass, the following transformation can be made -

$$Fdt = m\left[\frac{dv}{dt}\right] dt = mdv \qquad (3)$$

$$Fdt = d\ (mv)$$

$$\left[\begin{array}{c}\text{impulse of}\\ \text{external force } F\end{array}\right] = \left[\begin{array}{c}\text{increase of}\\ \text{system momentum}\end{array}\right]$$

In this form Newton's law represents the impulse-momentum point of view in representing dynamic systems.

Although any one or all of the methods represented by the foregoing three equations can be used in handling a given dynamics problem, they are not all equally convenient. That is, a problem might be very simple to set up and solve mathematically with the work-energy method, but extremely laborious using force-acceleration. In general, the force-acceleration method is most useful in cases where acceleration must be calculated and expressed as a function of time. On the other hand, the work energy method is particularly effective where changes of velocity are required as a function of displacement. The impulse-momentum method can be used to advantage in situations where impact loads (large forces of short duration) act on the system and where the mass may vary with time.

This briefly summarizes the theoretical correlation between the work-energy and the impulse momentum methods.

4.1 DYNAMIC STRENGTH OF STEAM GENERATOR SHELL IMPULSE-MOMENTUM METHOD OF ANALYSIS:

In the original calculations for the dynamic bursting strength of the shells the impulse-momentum approach was arbitrarily chosen because of the impulse loading applied during the sodium-water reactions. This reaction produces a hydrogen bubble and a bubble pressure. The bubble will develop rather slowly; however, the

pressure effect will move outward from the reaction zone at the velocity of sound in sodium, or approximately 5000 ft/sec. This implies that the pressure loading will be felt on the shells soon after the reaction.

DESCRIPTION OF ANALYSIS:

To begin with, picture a differential volume (dv) of the shell being acted upon by a force F. This indicates the following classical facts about the portion:

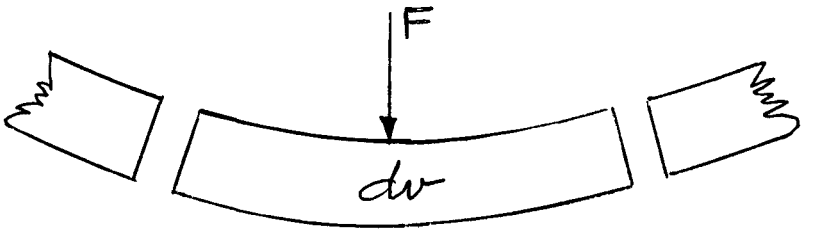

1. The particle has inertia; that is, it will resist having its position changed. (Newton's First Law of Motion).
2. The particle cannot of itself change its position but it regulates this motion through its mass; that is, the change shall always be inversely proportionally to its mass (Newton's Second Law of Motion).
3. The action between the differential volume and the remaining part of the shell is equal and opposite. This implies that the adjoining pieces are being strained by the attempt of each particle in the system to maintain an equilibrium condition.

A change in the position or motion of the differential volume can only occur if there is an unbalance in the system. In this case the unbalance is caused by the sodium-water reaction forces. The reactions working against this force and trying to maintain an equilibrium condition are:

1. The inertial effect of the shell.
2. The mass of the shell as it affects the acceleration.
3. The internal strain in adjoining portions of the shell as they attempt to maintain an equilibrium in the system.

The dynamic strength of the shell and liner has been established by using ASME paper No. 64- WA/APM-16 "The Strength of Thin Walled Cylinders Subjected to Dynamic Internal Pressures" by C.J. Constantino.

The problem involves the ability of the Steam Generator shell and liner to sustain dynamic pressures resulting from a sodium-water reaction within the shells. The displacement of the shells are considered to be quite large and because of this the elastic behavior of the material has been neglected in the analysis. The shells are assumed to deform as ideally plastic strain hardened material and the dynamic strength characteristics are accounted for by the appropriate value for the stress-strain relationships. The internal pressure has been considered a function of time only, and not related to the radius or internal volume of the shell.

Both the liner and shell have been assumed to be displaced by the dynamic pressure to the instability point of the shell, (the

point beyond which no increase in the pressure is required to keep accelerating the shell.) Given the geometry of the shell and the anticipated load duration the dynamic strength of the shell can be evaluated from the curves, included in the aforementioned paper, in the following manner.

1. Establish the maximum strain to the instability limit of the shell.
2. Determine the strain hardening exponent (n) and strength coefficient (K) of the material.
3. Determine the value for τ_o (the time factor) for the times of interest (t_o)
4. Knowing the strain hardening exponent (n) and the strain (ε_c') select the value of $p_1\tau_o$ from Fig. 2 from which p_1 (the impulsively applied pressure) can be calculated.
5. Determine p_2 (the step pulse pressure) from Fig. 3.
6. The ratio of $\frac{p_1}{p_2}$ is used in Fig. 5 to obtain the ratio of $\frac{p_o}{p_2}$ from which p_o (the dimensionless peak dynamic pressure) is obtained.
7. The dimensionless peak dynamic pressure is equal to the dimensionless pressure ratio or

$$p_o = \frac{P_o R_o}{K\ H_o}$$

where P_o = initial peak dynamic pressure, psi.

R_o = initial shell radius, in.

K = the strength coefficient for the material, psi

H_o = initial shell thickness, in.

The peak dynamic pressure the shell can withstand is obtained from this equation by solving for P_o. This value for P_o (#/in^2) must be converted to a specific impulse value by multiplying P_o by the time of interest (t_o). This is necessary in order to directly compare the specific pressure loading (specific impulse, psi-sec.) of the shell, which is a result of the sodium-water reaction hydrogen-bubble pressure. From this it is possible to determine the relationship between the strength of the shell vs. the greatest possible number of simultaneous tube failures.

The static strength of the vessel is solved for a comparison with the dynamic strength of the shell.

The dynamic strength of the shell has been established. It is now necessary to establish the actual pressure loading applied against the shell. This is accomplished by using the impulse momentum method of analysis.

The expression for impulse (from page 18) is:

$$\text{Impulse} = \int F dT = \int P \, dT$$

by substituting the above expression for P in terms of T in the impulse equation and integrating the total impulse from the beginning of a leak to any time can be calculated. If the dynamic strength of the vessel is greater at all times than these values of impulse, the vessel will not fail.

The calculations were based on the following assumptions:

1. The liner & vessel wall is Croloy 2-1/4 in the annealed or normalized condition.
2. The heat generated during a sodium-water reaction will not affect the shell or liner before the pressure pulse has decayed to a value below the static bursting strength. (See Section 11.0 for Temperature Gradients in Shells.)
3. The value of the strength coefficient (K) and hardening constants (n) at design temperature are given in Section 7.0 .
4. The maximum pressure pulse, for any point in time is assumed to act uniformly over the circumference of the liner and vessel wall.
5. The shell and liner are assumed to strain to the maximum established by the instability of the shell.

CONCLUSIONS:

A plot of results is shown below. At each time the dynamic strength capacity of the shell is greater than the applied pressure pulse.

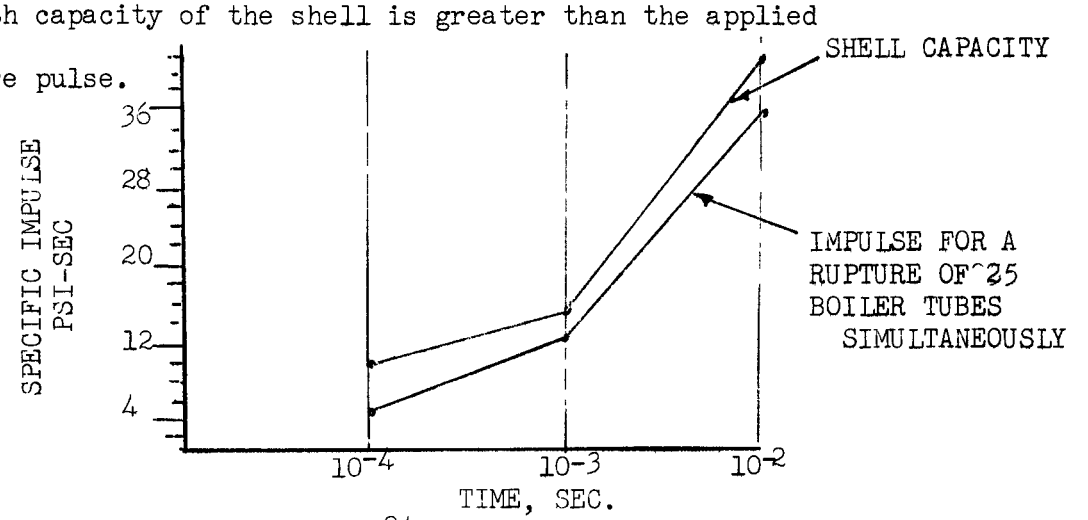

This figure shows through the impulse-momentum method that the shell will withstand a simultaneous rupture of 25 tubes. This is probably very conservative because of the assumptions made in both the APDA, and impulse-momentum calculations.

It has also been established by the calculations of this method that for a static condition of loading the shell-liner combination will withstand a pressure of 3647 psi.

APPENDIX:

SAMPLE CALCULATIONS -- STRENGTH OF STEAM GENERATOR SHELL, IMPULSE-MOMENTUM METHOD:

I CALCULATION OF LINER STRENGTH:

A. Dynamic Analysis (See Ref. (1)

1.) The time scale (τ) will be evaluated according to Ref. (1). For Croloy 2-1/4 material the strain hardening exponent is $n = .044$ as shown in Section 7.0 The strength coefficient K = 96,000 for the annealed and normalized condition (Ref. Section 10.7).

2.) Assume the liner wall will deform to the instability point of the vessel wall.

$$R_o = 37.372''$$

and

$$r = \frac{R}{R_o} = \frac{37.372}{32.625} = 1.145$$

From Ref. (1) Eq. (28) the conventional strain definition is:

$$= \frac{R-R_o}{R_o} = r-1 = 1.145-1 = .145 \text{ or } 14.5\%$$

3.) The dimensionless time scale is $\tau = \frac{t}{T}$ and since the time duration is t_o then:

$$\tau_o = \frac{t_o}{T} = \frac{t}{(\gamma R_o^2/2K)^{\frac{1}{2}}}$$

$$R_o^2 = 32.625^2 = 1.064 \times 10^3$$

For steel:

$$\gamma = \frac{\text{unit weight}}{\text{gravitational constant}} = \frac{.283\ \#/in^3}{386\ in/sec^2} = .733 \times 10^{-3}$$

$$\tau_o = \frac{t_o}{(.733(1.064)/2x0.96x10^5)^{\frac{1}{2}}} = \frac{t_o}{(.406 \times 10^{-5})^{\frac{1}{2}}} = \frac{t_o}{2.018x10^{-3}}$$

4.) The peak dynamic pressure (p_o) will be evaluated for durations of $t_o = 10^{-4}$, 10^{-3}, & 10^{-2}. From Ref. (1) Fig. (2) when:

$$\eta = .044 \ \& \ \varepsilon_c' = .145 \text{ then:}$$

$$p_1 \tau_o = 1.3 \quad \therefore \quad p_1 = \frac{1.3}{\tau_o} = \frac{1.3x2.018x10^{-3}}{t_o}$$

5.) For $t_o = 10^{-4}$ sec.

$$p_1 = \frac{1.3 \times 2.018 \times 10^{-3}}{10-4} = \underline{\underline{26.2}}$$

Also from Ref. (1) (Fig. 3) $p_2 = \underline{\underline{0.9}}$

$$p_1/p_2 = \frac{26.2}{0.9} = 29.1$$

When using Fig. (5) values must be interpolated for $\eta = .044$ where deviation is small for $\eta = .01$ & $\eta = 0.1$ and becomes of no importance. For $p_1/p_2 > 10$ the author of Ref. (1) confirmed the slope to be 45° therefore when $p_1/p_2 = 29.1$ then:

$$p_o/p_2 = 29.1 \text{ and } p_o = 29.1\ p_2 = 29.1\ (0.9) = \underline{\underline{26.2}}$$

6.) For the $t_o = 10^{-3}$ sec.

$$p_1 = 2.62 \ \& \ p_2 = 0.9$$

$$p_1/p_2 = \frac{2.62}{0.9} = 2.92$$

From Fig. (5) $p_o/p_2 = \underline{\underline{5.0}}$

Therefore:

$$p_o = 5.0\ p_2 = 5.0\ (0.9) = \underline{\underline{4.5}}$$

7.) For the $t_o = 10^{-2}$ sec.

$$p_1 = \frac{1.3 \times 2.108 \times 10^{-3}}{10^{-2}} = .262\ \&\ p_2 = 0.9$$

$$p_1/p_2 = \frac{.262}{0.9} = .291$$

$$p_o/p_2 = 1.2\ \&\ p_o = 1.2(0.9) = \underline{\underline{1.08}}$$

8.) The dynamic pressure (P_o) can be obtained from the expression for the dimensionless pressure ratio where:

$$p = \frac{P\ R_o}{K\ H_o} \text{ (Ref. (1) nomenclature)}$$

Adding the appropriate subscripts where p_o is the dimensionless peak dynamic pressure, and P_o the initial peak dynamic pressure and solving for P_o

$$P_o = p_o \quad \frac{K\ H_o}{R_o}$$

Note: K has been substituted here for $_o$ as used in the paper for purposes of consistency.

Where the quantity in the parenthesis for the liner is:

$$\frac{K\ H_o}{R_o} = \frac{96{,}000\ (.5)}{32.625} = 1471$$

Therefore $P_o = 1471\ p_o$ for the liner

9.) The initial peak dynamic pressure, P_o, sustained by the liner at each time duration t_o is as follows,

t_o (sec.)	p_o	$P_o = 1471\ p_o$ (psi)
10^{-4}	26.2	38,540
10^{-3}	4.5	6,620
10^{-2}	1.08	1,589

B. Static Analysis

1.) The static bursting pressure in dimensionless form is established by Equation (12) of Ref. (1) where:

$$p^* = \frac{2}{\sqrt{3}}\left(\frac{n}{\sqrt{3}\,e}\right)^{n} \quad \text{where } n = .044 \ \& \ e = 2.718$$

$$= 1.155\left(\frac{.044}{\sqrt{3}\,(2.718)}\right)^{.044}$$

$$= 1.155\ (.0094)^{.044}$$

$$p^* = .941$$

2.) Using the same expressions as Item A.8 utilizing appropriate subscripts the static bursting pressure at instability is:

$$P_s = 1471\ p^*$$

$$P_s = 1471\ (.941) = \underline{1384\ \text{psi}}$$

II - CALCULATION OF THE VESSEL STRENGTH:

A. Dynamic Analysis

1.) The maximum strain that can be achieved at the point of instability is given by Eq. (12) where $n = .098$

$$r^* = e^{n/2} = 2.718^{.098/2} = 1.052$$

2.) A value of r = 1.052 will be utilized which gives a final strain near the maximum. The final strain is established

by Eq. (28) where:

$$\varepsilon_c' = r - 1 = 1.052 - 1.0 = 0.052 \text{ in/in}$$

3.) The inside radius of the vessel is $R_o = 36.0''$, and for Croloy 2-1/4 K = 103,000, and $\gamma = .733 \times 10^{-3}$. Evaluating the dimensionless time scale where:

$$\tau_o = \frac{t_o}{T} = \frac{t_o}{(\gamma R_o 2/2K)^{\frac{1}{2}}} = \frac{t_o}{(.733 \times 10^{-3}(36)^2/2x1.03x10^5)^{\frac{1}{2}}}$$

$$\tau_o = \frac{t_o}{2.14 \times 10^{-3}}$$

4.) The peak dynamic pressure, p_o, in non-dimensional form will be evaluated for time durations of $t_o = 10^{-4}$, 10^{-3}, and $t_o = 10^{-2}$ sec. From Ref. (1) Fig. (2) when $\eta = .098$ and $\varepsilon_c' = .052$ then:

$$p_1 \tau_o = 0.9 \text{ therefore } p_1 = \frac{0.9}{\tau_o} = \frac{0.9 \times 2.14 \times 10^{-3}}{t_o}$$

5.) For $t_o = 10^{-4}$ sec.

$$p_1 = \frac{0.9x2.14x10^{-3}}{10^{-4}} = 19.6$$

6.) From Ref. (1) Fig. (3) $p_2 = 0.75$

Therefore:

$$p_1/p_2 = \frac{19.26}{0.75} = 25.7$$

and

$$p_o/p_2 = 25.7 \text{ from Fig. (5) as explained in I A.5}$$

$$p_o = 25.7\ p_2 = 25.7\ (0.75) = \underline{\underline{19.26}}$$

7.) For $t_o = 10^{-3}$sec.

$$p_1 = \frac{0.9 \times 2.14 \times 10^{-3}}{10^{-3}} = 1.96 \ \& \ p_2 = 0.75$$

$$p_1/p_2 = \frac{1.96}{0.75} = 2.57$$

and from Fig. (5) $p_o/p_2 = 4.0$

therefore $p_o = 4.0\ (p_2) = 4.0\ (0.75) = \underline{\underline{3.0}}$

8.) For $t_o = 10^{-2}$ sec.

$$p_1 = \frac{0.9 \times 2.14 \times 10^{-3}}{10^{-2}} = .1926 \ \& \ p_2 = 0.75$$

$$p_1/p_2 = \frac{.1926}{6.75} = .257$$

and from Fig. (5) $p_o/p_2 = 1.2$

therefore $p_o = 1.4\ (p_2) = 1.2\ (0.75) = \underline{\underline{0.9}}$

9.) The dynamic pressure (P_o) as set forth previously is:

$$P_o = p_o \quad \frac{KH_o}{R_o}$$

where $K = 103{,}000$, $H_o = 1.0''$ and $R_o = 36''$ for the vessel then

$$\frac{KH_o}{R_o} = \frac{1.03 \times 10^5 \times 1.0}{36} = 2{,}861$$

therefore $P_o = 2861\ (p_o)$ for the vessel

7.) The initial peak dynamic pressure (P_o) sustained by the vessel at each time duration t_o is as follows:

t_o (sec.)	p_o	$P_o = 2861\ p_o$ psi
10^{-4}	19.26	55,103
10^{-3}	3.0	8,583
10^{-2}	0.9	2,574

B. Static Analysis

1.) The static bursting strength (P_s) as determined previously is based on:

$$p^* = \frac{2}{\sqrt{3}} \left(\frac{n}{\sqrt{3}\, e} \right)^{n} \quad \text{where } n = .098$$

$$= 1.155 \left(\frac{.098}{\sqrt{3}(2.718)} \right)^{.098}$$

$$= 1.155\ (.021)\ .098$$

$$P_s = 2861\ (.791)$$

$$= \underline{2263} \text{ psi}$$

IIc - STRENGTH OF LINER AND VESSEL:

A. 1.) It is assumed that the inner liner wall deforms out to contact the vessel wall. The process continues and proceeds to strain further and thereby load the vessel wall. The liner wall and vessel wall pressure strength is combined as follows:

2.) The total static pressure strength (psi) is:

	P_s (psi)
Liner	1384
Vessel	2263
Total	3647 psi

3.) The total dynamic pressure strength (P_o) at the three time durations are:

	10^{-4} sec.	10^{-3} sec.	10^{-2} sec.
Liner (psi)	38,540	6,620	1,589
Vessel (psi)	55,103	8,583	2,574
Total	93,643	15,203	4,163

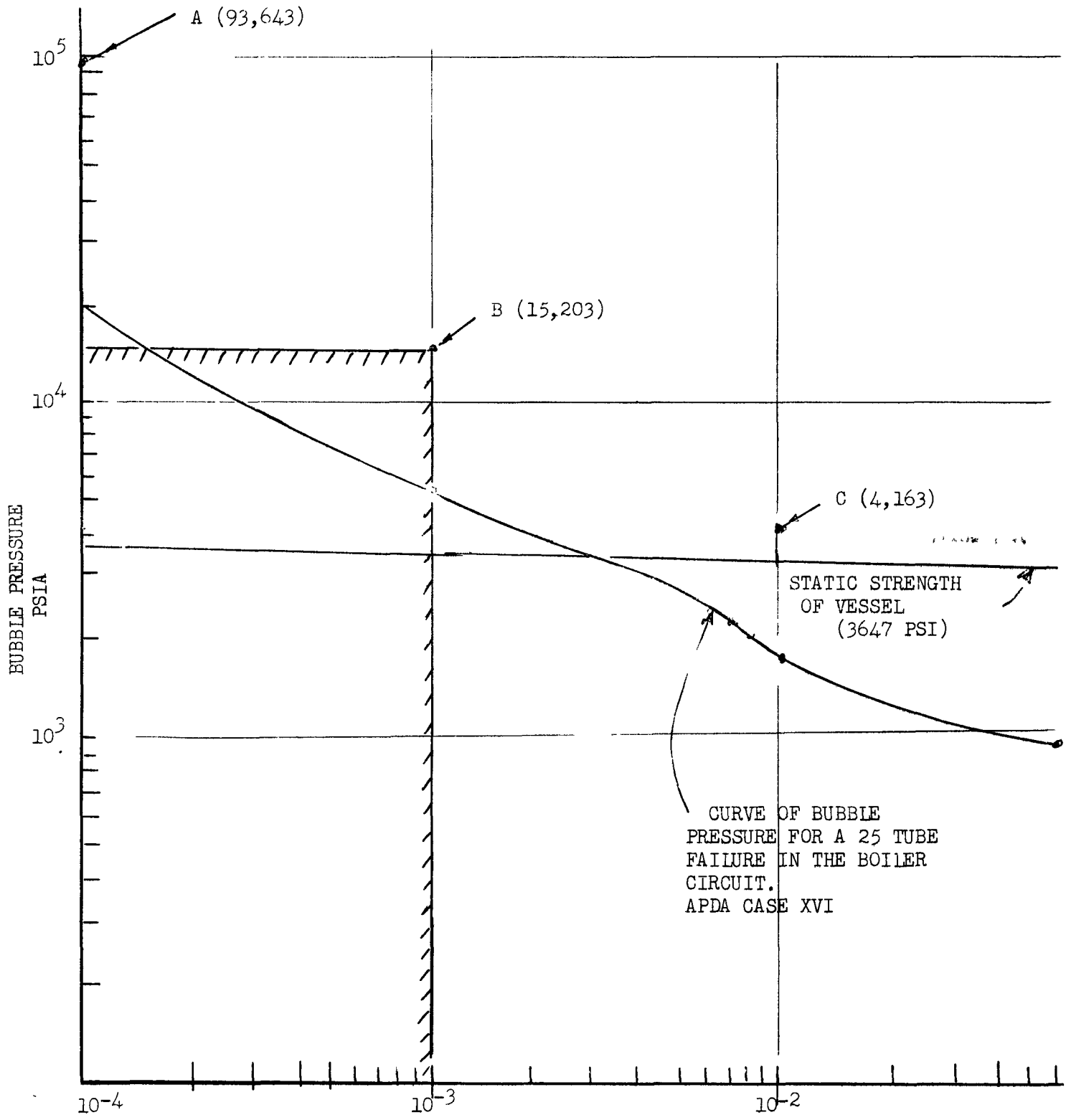

FIG. 1 COMPARISON OF DYNAMIC PRESSURE STRENGTH OF THE VESSEL VS. HYDROGEN BUBBLE PRESSURE OF THE REACTION.

B. 1.) The Log-Log curve of pressure versus time, for a rupture of the 25 tubes in the boiler section (APDA Case XVI) is replotted in Fig. 1.

Superimposed on this plot is a straight line showing the total static pressure strength of the vessel.

Dynamic strength in terms of specific impulse, psi - sec.

10^{-4} = 93,643 (10^{-4}) = 9.364 psi - sec.

10^{-3} = 15,203 (10^{-3}) = 15.203 psi - sec.

10^{-2} = 4,163 (10^{-2}) = 41.63 psi - sec.

2.) The dynamic pressure strength (P_o) vs. time is included on this plot as points A, B, & C. The points represent the computed dynamic pressures which the liner-vessel can withstand for particular finite durations of loading. The points A, B, & C cannot be directly compared to the applied bubble pressure. In order to compare the dynamic pressure strength vs. time of the liner-vessel (represented by Points A, B, & C) to the hydrogen bubble pressure vs. time, one must consider impulse.

At any given time, t_o, the area under the hydrogen bubble pressure curve represents a "specific" impulse. Similarly, we can compute the value of the dynamic pressure pulse that the liner-vessel can withstand over the time duration t_o. If one then calculates the area swept out by this pulse, one gets the specific impulse that corresponds to this pulse. For instance, one can obtain the specific impulse that the liner vessel can withstand @ t_o = 0.001 by computing the area under Point "B" (See swept area for Point B shown

on Fig. 1). One can then compare the area under the hydrogen bubble pressure curve to the area under Point B. As long as the areas under the various points are greater than those under the bubble curve for the same t_o, one can conclude that the dynamic strength of the liner-vessel combination can withstand the applied impulse.

III. CALCULATION OF IMPULSIVE LOADING FROM SODIUM-WATER REACTIONS:

A curve fit for the APDA Curve XVI, which is considered to be the worst credible pressure for the simultaneous rupture of 25 tubes in the downcomer annulus, produces the following equations:

For times between 10^{-4} and 10^{-3} the following equation approximates the curve:

$$P = 106.3T^{-0.568}$$

For times between 10^{-3} and 10^{-2}

$$P = 168.5T^{-0.502}$$

By integrating these equations it is possible to calculate the area under the hydrogen bubble pressure curve and represent a specific impulse. These values can be compared to the dynamic pressure pulse that the liner-vessel shell can withstand over the specific time duration.

The area or specific impulse under the hydrogen bubble curve for times of 10^{-4}, 10^{-3} and 10^{-2} are:

$$P = 106.3 \int_o^t T^{-0.568} dt$$

$$= 106.3 \left[\frac{T^{0.432}}{0.432} \right]_o^t$$

At 10^{-4}

$$P = 106.3\left[\frac{(.0001)^{0.432}}{0.432}\right]$$

$$= \underline{\underline{4.57}} \text{ psi - sec.}$$

At 10^{-3}

$$P = 106.3\left[\frac{(.001)^{0.432}}{0.432}\right]$$

$$P = \underline{\underline{12.3}} \text{ psi - sec.}$$

At 10^{-3} to 10^{-2}

$$P = 168.5\ T^{-0.502}$$

$$= 168.5\left[\frac{T^{0.498}}{0.498}\right]_{.001}^{.01}$$

$$= 168.5\left[\frac{(.01)^{0.498}}{0.498}\right] - 168.5\left[\frac{(.001)^{0.498}}{0.498}\right]$$

$$= 33.87 - 10.78$$

$$= \underline{\underline{23.09}} \text{ psi - sec.}$$

Then the total specific impulse at 10^{-2} is the value equal to the sum of the area for the integration of equation $P = 106.3\ T^{-0.568}$ at 10^{-3} plus the area integrated for equation $P = 168.5\ T^{-0.502}$ from the time interval of 10^{-3} to 10^{-2}.

10^{-3}	= 12.3
10^{-3} to 10^{-2}	= 23.09
Total	35.39 psi - sec (at 10^{-2})

The following table shows the results of the calculation for the specific impulse of the hydrogen bubble pressure and compares this with the values for the dynamic pressure pulse the shells will sustain for the simultaneous rupture of 25 tubes in the downcomer annulus (consider to be a worst case condition).

(time - (sec)					
10^{-4}		10^{-3}		10^{-2}	
Specific Impulse of Bubble Press. psi - sec.	Dynamic Strength of Shell psi - sec.	Specific Impulse of Bubble Press. psi - sec.	Dynamic Strength of Shell psi - sec.	Specific Impulse of Bubble Press. psi - sec.	Dynamic Strength of Shell psi - sec.
4.57	9.36	12.3	15.20	35.39	41.63

CONCLUSION:

With the great conservatism used in both the APDA analysis of the hydrogen bubble pressure and in the assumption used in the impulse momentum method of analyzing the shell it is felt that the liner and shell of the Prototype Steam Generator will sustain a simultaneous rupture of all 25 tubes in the boiler circuit without failure of the shell.

Nomenclature:

n = strain hardening exponent

K or σ_o = strength measure or strength coef. - psi

R_o = initial shell radius (I.R.) - inches

R = shell radius (final) - inches

ε_c' = final or max. strain at end of motion - in/in

γ = unit mass of material

t_o = dynamic load duration - sec.

$T = (R_o^2/2K)^{\frac{1}{2}}$ time factor - sec.

t = time, sec.

τ = t/T dimensionless time scale

$r = R/R_o$, dimensionless shell radius

p_1 = linearly decaying pressure pulse applied to shell ref. (1) eq. (25)

p_2 = step pulse applied to shell ref. (1) eq. (26)

p_o = peak dynamic pressure at max. radius - ref. (1) eq. (19)

P_o = initial peak dynamic pressure - psi

p* = static instability ratio, non-dimensional

P_s = static internal pressure, psi

Published References

Ref. (1) - "The Strength of Thin-Walled Cylinders Subjected to Dynamic Pressures," by C.J. Constantino ASME Paper No. 64-WA/APM-16-Journ. of Applied Mechanics.

Unpublished References

Ref. (2) - "Strength Coefficient and Strain Hardening Data for Croloy 2-1/4"

Unpublished References (Continued)

by Alan W. Pense, Lehigh University, March, 1965 & B&W Research Laboratory (See Section VII).

Ref. (3) - "Sodium-Water Reaction Data by Atomic Power Development Associates, Inc. (APDA).

Paper No.
64—WA/APM-16

The Strength of Thin-Walled Cylinders Subjected to Dynamic Internal Pressures

C. J. COSTANTINO
Research Engineer,
IIT Research Institute,
Chicago, Ill.

CA-5-7630
7118

The equation of motion governing the response of long (infinite) cylinders to dynamic internal pressures is derived. Since large displacements and wall-thinning effects are taken into account, elastic behavior of the material is neglected. The material is assumed to be rigid-plastic, with strain-hardening being taken into account through the Ludwik power strain-hardening law. Numerical results are presented for a range of hardening constants from 0.01 to 1.0, covering the range applicable to most materials of interest. The form of the dynamic pressure considered is an initially peaked, linearly decaying pressure pulse. Charts are presented giving the pressure and duration required to produce a given final radius of the cylinder.

THE purpose of this study has been to obtain an approximate measure of the response of containment shells subjected to blast-type (dynamic) internal pressures. Such information would be of value when attempting to evaluate the protection afforded by the structure against an accident (nuclear excursion, coolant leak, and so on).

Within this framework, the bursting strength of thin-walled infinite cylinders subjected to internal pressures is obtained incorporating the following assumptions:

1 Elastic displacements of the shell are negligible as compared to the large displacements obtained at burst.

2 The shell material deforms as an ideally plastic, strain-hardening solid satisfying the maximum octahedral yield-stress criterion of Mises[1] and the subsequent displacements are determined from the associated flow law.

3 The applied internal pressure is a function of time only, but not of the radius (internal volume) of the shell. This assumption is actually an approximation to the loading felt by the shell as it deforms.

4 Dynamic effects on the stress-strain properties of the material can be accounted for by an appropriate choice of the constants in the static stress-strain laws postulated for the material.

Strain-Hardening Law

In general, the stress-strain behavior of any ductile material may be described analytically as

$$\sigma = \sigma_0 F(\epsilon) \tag{1}$$

where F is some function of the effective strain determined by experiment. For the state of biaxial stress associated with thin-shell problems, the effective stress and strain reduces[1] to

$$\sigma = \{\sigma_1^2 - \sigma_1\sigma_2 + \sigma_2^2\}^{1/2}$$
$$\epsilon = \frac{2}{\sqrt{3}}\{\epsilon_1^2 + \epsilon_1\epsilon_2 + \epsilon_2^2\}^{1/2} \tag{2}$$

where the subscripts 1, 2 designate the principal directions. The material is assumed to be incompressible, or

$$\epsilon_1 + \epsilon_2 + \epsilon_3 = 0 \tag{3}$$

The assumption will be made that the material is characterised by the Ludwik power-law strain-hardening, or

$$F(\epsilon) = \epsilon^n \tag{4}$$

in equation (1), where n is the strain-hardening exponent.

Static Solution

The pressure-radius relationship for infinite cylinders subjected to monotonically increasing internal static pressures has been given previously.[2] This solution will be outlined briefly. For this case, subscript 1 refers to the circumferential direction, subscript 2 the axial direction, and subscript 3 the through-thickness direction. The following system of equations is used to obtain the solution:

(*a*) Strain-displacement relations (finite strains)

$$\epsilon_1 = \log\frac{R}{R_0} = \log r$$
$$\epsilon_3 = \log\frac{H}{H_0} = \log h \tag{5}$$

[1] R. Hill, *The Mathematical Theory of Plasticity*, Oxford University Press, London, England, 1956.

Contributed by the Applied Mechanics Division for presentation at the Winter Annual Meeting, New York, N. Y., November 29–December 4, 1964, of THE AMERICAN SOCIETY OF MECHANICAL ENGINEERS.

Discussion of this paper should be addressed to the Editorial Department, ASME, United Engineering Center, 345 East 47th Street, New York, N. Y. 10017, and will be accepted until one month after final publication of the paper itself in the JOURNAL OF APPLIED MECHANICS. Manuscript received by ASME Applied Mechanics Division, December 4, 1963. Paper No. 64—WA/APM-16.

[2] N. L. Svenson, "The Bursting Pressure of Cylindrical and Spherical Vessels," JOURNAL OF APPLIED MECHANICS, vol. 25, TRANS. ASME, vol. 80, 1958, pp. 82–96.

Nomenclature

H = shell thickness, in.
H_0 = initial shell thickness, in.
h = H/H_0, dimensionless shell thickness
n = strain-hardening exponent
P_d = applied dynamic internal pressure, psi
P_s = applied static internal pressure, psi
P_0 = initial peak dynamic pressure, psi
p = $PR_0/\sigma_0 H_0$, dimensionless pressure ratio
R = shell radius, in.
R_0 = initial shell radius, in.
r = R/R_0, dimensionless shell radius
t = time, sec
T = $[\gamma R_0^2/2\sigma_0]^{1/2}$, time factor sec
t_0 = dynamic load duration, sec
γ = unit mass of material
ϵ = effective strain
$\epsilon_1, \epsilon_2, \epsilon_3$ = principal strains
σ = effective stress, psi
σ_0 = strength measure, psi
$\sigma_1, \sigma_2, \sigma_3$ = principal stresses
τ = t/T, dimensionless time scale,

(*b*) Incompressibility, equation (3)

$$r = 1/h \tag{6}$$

(*c*) Plane-strain condition in axial direction

$$\epsilon_2 = 0 \tag{7}$$

(*d*) Flow law associated with Mises yield condition

$$\frac{\epsilon_2}{\epsilon_1} = \frac{2\sigma_2 - \sigma_1}{2\sigma_1 - \sigma_2}, \quad \text{or } \sigma_2 = \frac{\sigma_1}{2} \tag{8}$$

(*e*) Effective stress and strain, equation (2)

$$\sigma = \frac{\sqrt{3}}{2}\sigma_1, \qquad \epsilon = \frac{2}{\sqrt{3}}\epsilon_1 \tag{9}$$

(*f*) Stress-strain law, equations (1) and (4)

$$\sigma = \sigma_0 \left\{ \frac{2}{\sqrt{3}} \log r \right\}^n \tag{10}$$

(*g*) Equilibrium condition

$$\sigma_1 = \frac{PR}{H} \tag{11}$$

These equations are combined to lead to the dimensionless pressure-radius relation

$$p = \left(\frac{2}{\sqrt{3}}\right)^{n+1} \frac{\log^n r}{r^2}$$

and (12)

$$p^* = \frac{2}{\sqrt{3}} \left(\frac{n}{\sqrt{3}\, e}\right)^n$$

$$r^* = e^{n/2}$$

where asterisked quantities refer to quantities at instability. This relationship is shown graphically in Fig. 1.

Dynamic Solution

The equation of motion for the system can be written as

$$2\pi R(P_d - P_s) = 2\pi R H \gamma \frac{d^2R}{dt^2} \tag{13}$$

which in dimensionless form becomes

$$\frac{d^2r}{d\tau^2} = \frac{1}{2h}(p_d - p_s) \tag{14}$$

where p_d and p_s are the dimensionless applied pressure and static resistance, respectively. Substituting equation (6) into equation (14) the equation of motion becomes

$$\frac{d^2r}{d\tau^2} = \frac{r}{2}(p_d - p_s) \tag{15}$$

Solutions of Dynamic Problems

The problem at hand is to determine the maximum displacement that the shell achieves when a given internal pressure pulse is applied. Since only plastic deformations are being considered, it is necessary to determine the displacement when the shell velocity first becomes zero.

The dynamic pressures to be considered here are initially peaked, linearly decaying pressure pulses of the form

$$p_d = \begin{cases} p_0\left(1 - \dfrac{\tau}{\tau_0}\right) & \text{for } 0 \le \tau \le \tau_0 \\ 0 & \text{for } \tau_0 \le \tau \end{cases} \tag{16}$$

where p_0 is the initial peak pressure and τ_0 is the pulse duration.

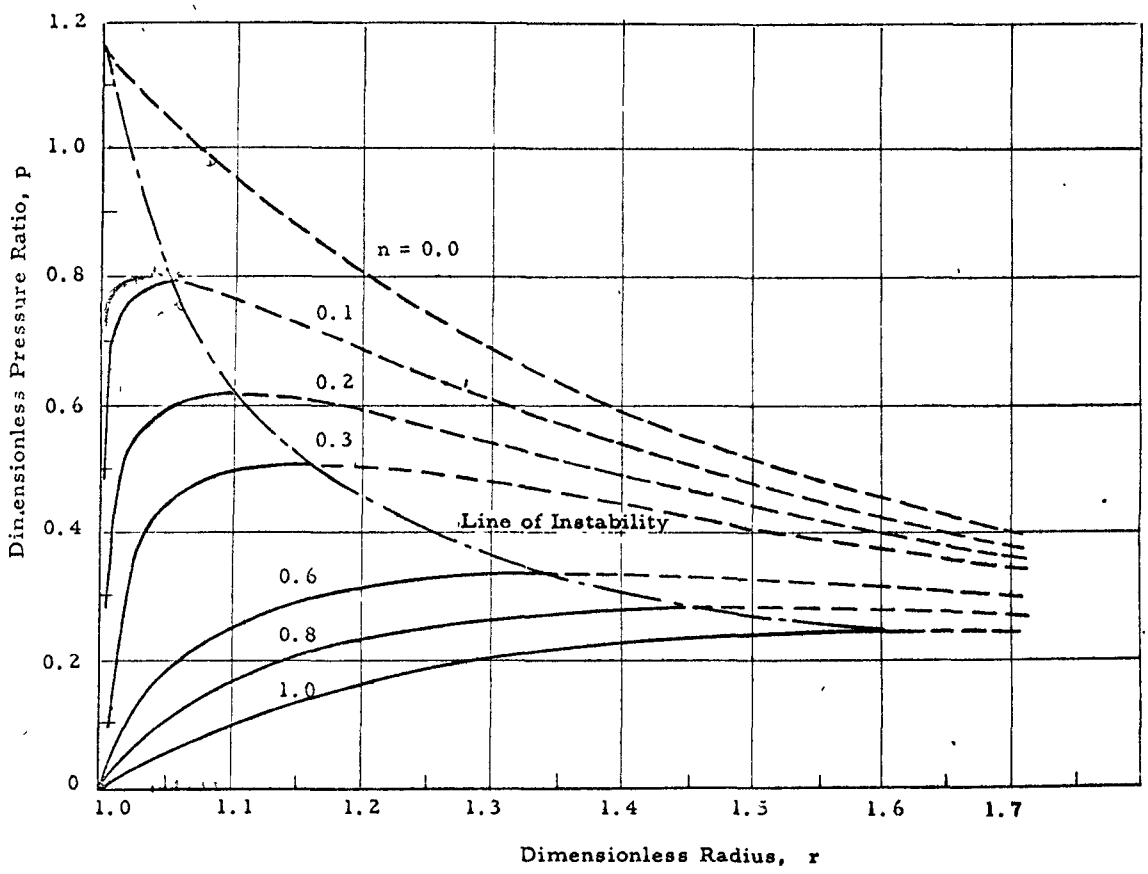

Fig. 1 Pressure-radius relation for various values of hardening exponent

-40a-

Table 1 Stress-strain properties in simple tension

Material	Strength coefficient, σ_0, psi	Hardening exponent, n	Yield stress, psi
A212 Grade B firebox steel....	155,000	0.245	32,000
A285 Grade B firebox steel...	117,000	0 278	27,500
T-304 stainless steel.....	171,000	0.724	36,800
A302 steel.....	133,000	0.197	52,190
USS T-1 steel.....	178,700	0.087	119,800
0.15 percent carbon steel.....	108,000	0.285	32,700

Although this is a rather approximate idealization of the actual pressure that would be felt by the shell, it allows for a representative evaluation of the relative effects of the load parameters p_0 and τ_0 on the response.

A first integral to equation (15) can be obtained from the relation

$$\frac{d}{d\tau}\left(\frac{dr}{d\tau}\right)^2 = 2\,\frac{dr}{d\tau}\,\frac{d^2r}{d\tau^2}$$

This leads to the relationship

$$(r')^2 = \int_1^r r\{p_0[1 - g(\tau)] - p_s\}dr + (r_0')^2 \qquad (17)$$

where primes designate differentiation with respect to τ; r_0' is the initial shell velocity, and

$$g(\tau) = \begin{cases} \tau/\tau_0 & \text{for} \quad 0 \le \tau \le \tau_0 \\ 1 & \text{for} \quad \tau_0 \le \tau \end{cases} \qquad (18)$$

At the maximum radius, r_{max}

$$r' = 0$$

so that

$$p_0 = \frac{\displaystyle\int_1^{r_{max}} rp_s dr - (r_0')^2}{\left(\dfrac{r_{max}^2 - 1}{2}\right) - \displaystyle\int_1^{\tau_{max}} rg(\tau)\,\frac{dr}{d\tau}\,d\tau} \qquad (19)$$

where τ_{max} is the dimensionless time at which the maximum radius is reached. Thus, equation (19) yields the peak dynamic pressure required to achieve a given final radius. For power law-hardening,

$$\int_1^{r_{max}} rp_s dr = \left(\frac{2}{\sqrt{3}}\right)^{n+1} \frac{\log^{n+1} r_{max}}{(n+1)} \qquad (20)$$

The remaining integral in equation (19) cannot be evaluated in closed form, and numerical integration techniques must in general be used.

For particular loading cases, however, complete solutions can be obtained, these being the extreme cases of a step pulse ($g = 0$) and the impulse ($g = 1$). For an impulsive load applied to the shell, equation (17) reduces to

$$(r_0')^2 = \int_1^{r_{max}} rp_s dr \qquad (21)$$

where the impulse is related to the initial velocity by

$$I = \left\{\frac{2\pi\gamma R_0^2 H_0}{T}\right\} r_0' \qquad (22)$$

If a linearly decaying pressure pulse of peak magnitude, p_1, and duration τ_0 is applied to the shell, and it is further assumed that this pulse is applied impulsively (actually it is applied over a finite time τ_0), the total impulse applied to the shell (area under the pressure-time curve) is

$$I = \{2\pi\sigma_0 H_0 T\}\,\frac{p_1\tau_0}{2} \qquad (23)$$

Equating equations (22) and (23), the initial velocity is found to be

$$r_0' = \frac{p_1\tau_0}{4} \qquad (24)$$

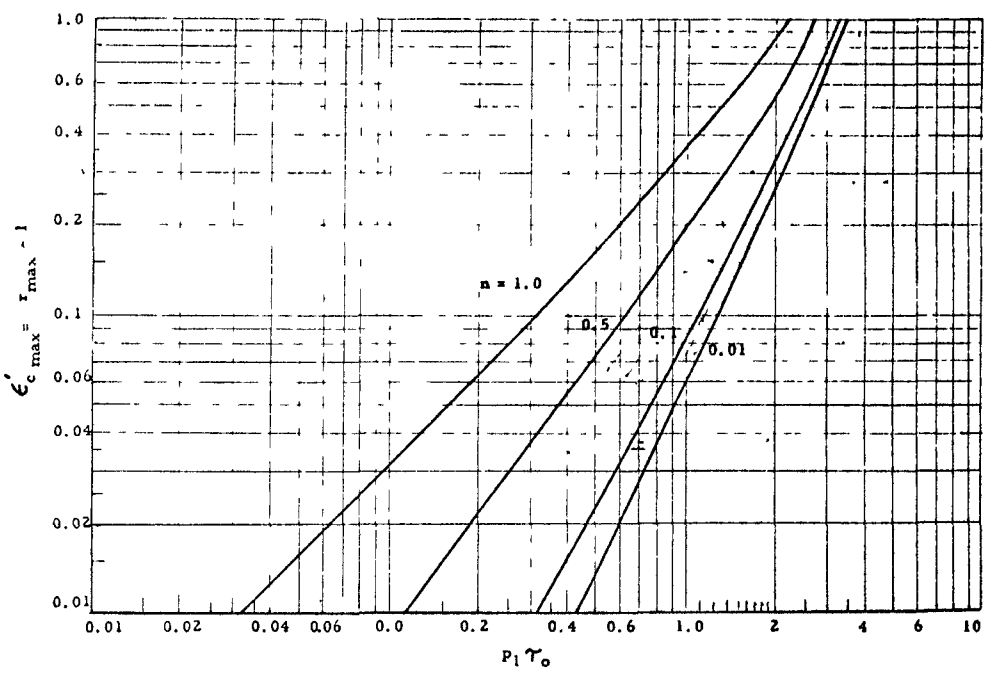

Fig. 2 Values of $p_1\tau_0$ as a function of maximum strain

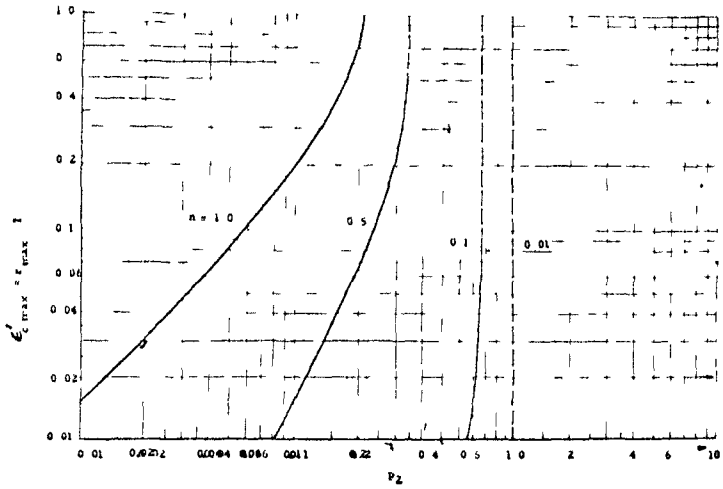

Fig. 3 Values of p_2 as a function of maximum strain

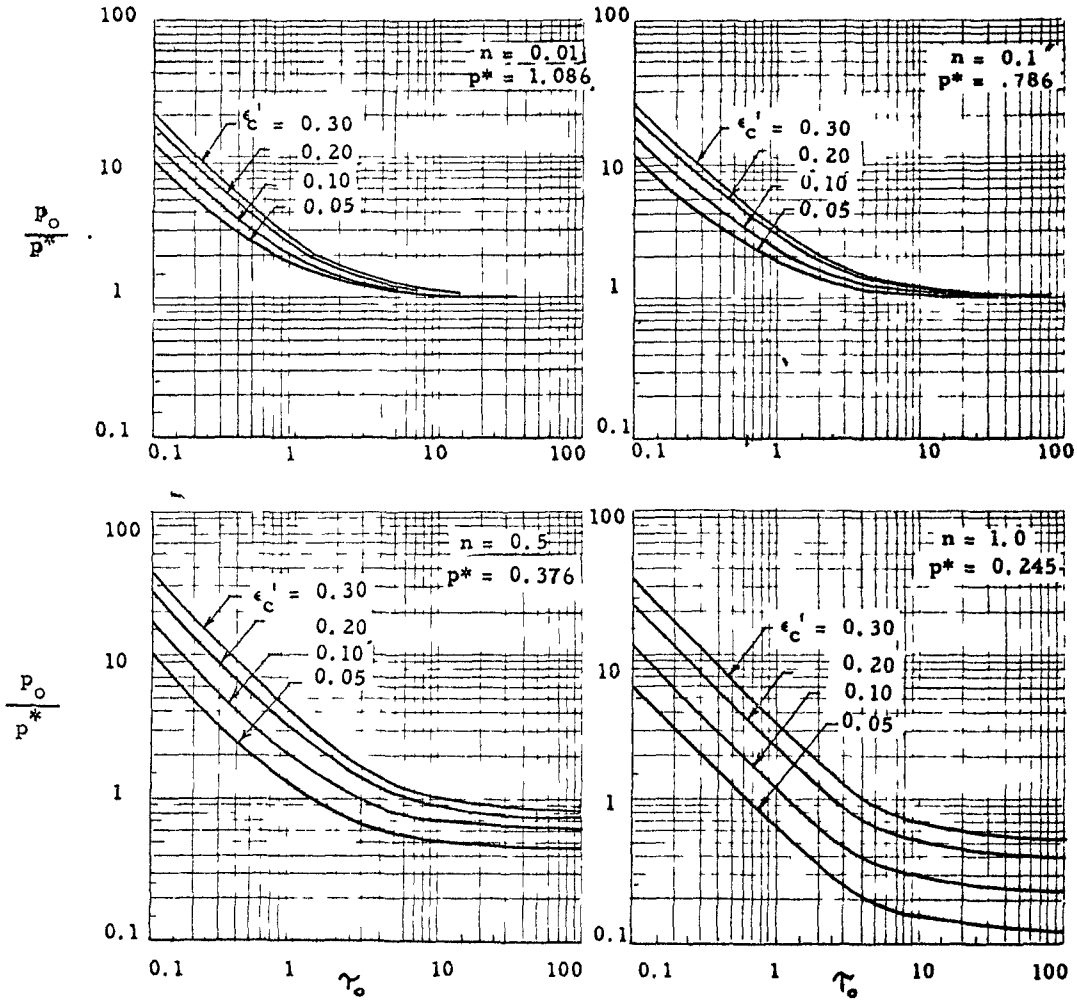

Fig. 4 Damage pressure ratios

Substituting into equation (21) we obtain

$$p_1 = \frac{4}{\tau_0} \left\{ \int_1^{r_{max}} r p_s dr \right\}^{1/2} \tag{25}$$

For the case of a step pulse of magnitude p_2 applied to the shell, the solution from equation (19) is

$$p_2 = \frac{2}{(r_{max}^2 - 1)} \left\{ \int_1^{r_{max}} r p_s dr - (r_0')^2 \right\} \tag{26}$$

This equation does not, however, completely solve the problem for the step pulse By referring to Fig. 1, we note that the static strength of the cylinder decreases for $r > r^*$. From the equation of motion, the shell acceleration is proportional to the difference between the dynamic pressure and the static strength. Therefore, if $r > r^*$ and if $p_d > p_s$, the shell will continue to accelerate and never stop. The maximum value of a step pulse that can be tolerated may be found by satisfying simultaneously both equation (26) and the condition

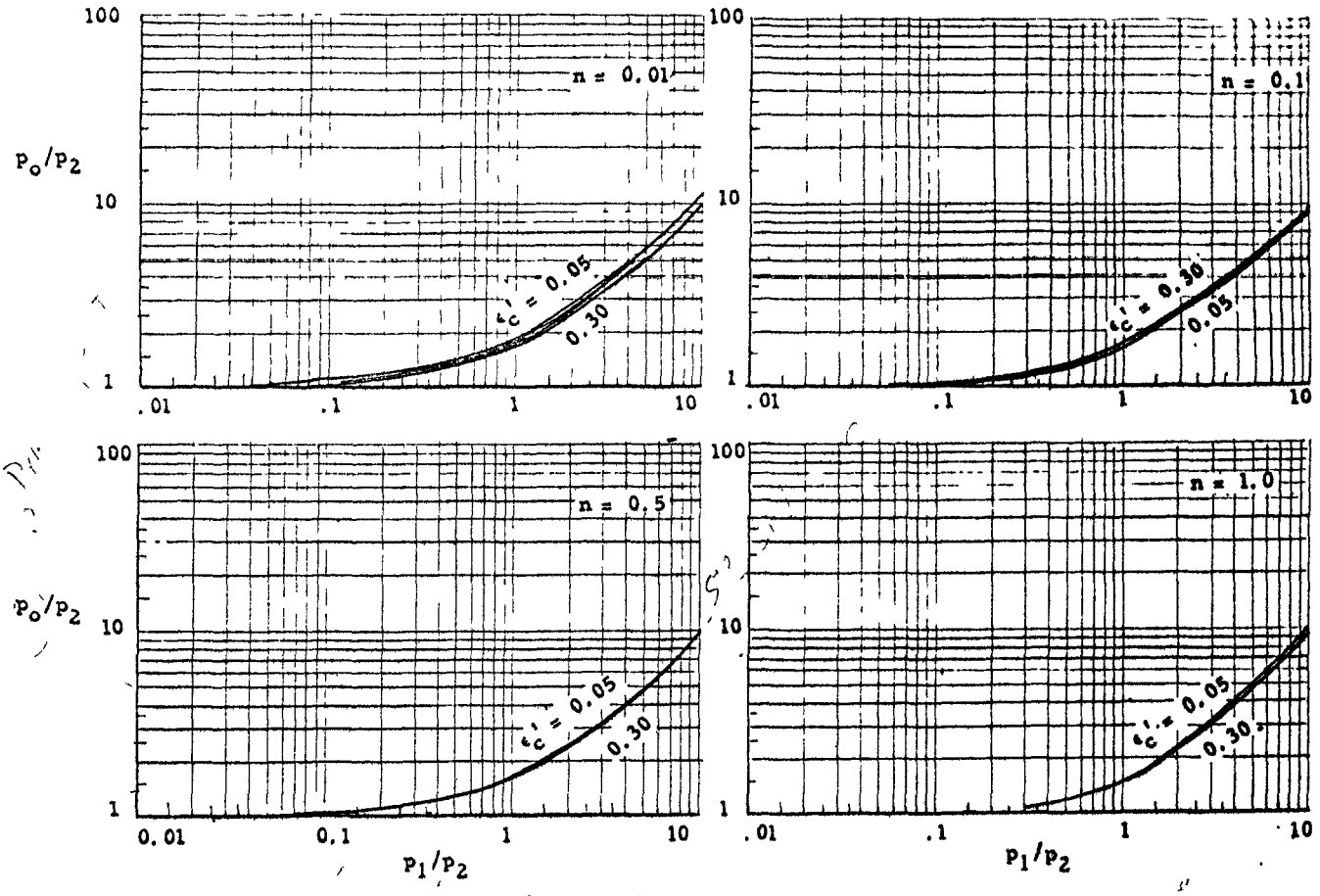

Fig. 5 Ratios p_0/p_2 versus p_1/p_2 for various hardening exponents

$$p_d = p_s \tag{27}$$

In this case, the shell will have zero velocity and zero acceleration. Thus, the shell motion will stop and the vessel will be able to sustain the step pulse applied to it.

Summary

As mentioned, the solution to the equation of motion cannot be obtained in analytic form for linearly decaying pulse, but must be derived numerically. This was done using a simple Runge-Kutta numerical integration scheme. In all cases, the numerical results shown are for values of the hardening exponent, n, of 0.01, 0.1, 0.5, 1.0, the range covering the values of most interest for ductile materials. Typical values of these parameters for several metals are shown in Table 1.[3]

The conventional or engineering definition of strain may be written as

$$\epsilon_c' = \frac{R - R_0}{R_0} = r - 1 \tag{28}$$

This form, a familiar measure of strain, is used as the parameter defining the final or maximum strain achieved at the end of the shell motion. The numerical results following are shown for strains in the range of 5 to 30 percent, the general range of interest.

In Fig. 2, the required load applied impulsively, p_1, to produce a given final strain is shown for the various values of the hardening exponent. Similarly, Fig. 3 presents the required step pulse, p_2, to produce a given final strain. The dotted portions of these curves indicate the maximum allowable value of the step pulse, as explained previously.

Fig. 4 shows the ratio of the peak dynamic pressure p_0 to the static burst strength p^*, required to produce a given final strain, as a function of the load duration. Naturally, the longer the duration of the load, the smaller the pressure required to develop the strain, while for short-duration loads, the required pressure p_0 approaches the impulsive pressure p_1. In addition, it may be noted from these curves that, for long-duration loads, the peak pressure may be significantly less than the static burst strength of the shell, particularly for high values of the hardness exponent. Thus, for these conditions, the dynamic strength of the cylinder may be much less than its static strength.

These results are essentially replotted in Fig. 5, presenting in this case the ratio of the peak pressure to the step-pulse pressure, p_0/p_2, as the ordinate, and the ratio of the impulsively applied pressure to the step-pulse pressure, p_1/p_2 as the abscissa. It may be noted that this technique essentially "collapses" the results shown in Fig. 4 into a single curve. The error, in so doing, is for the most part less than 10 percent over the range of interest of strains. Thus, if a maximum allowable strain is selected, together with an anticipated load duration, the parameters p_1 and p_2 may be computed from equations (20) and (21) (or alternatively from Figs. 2 and 3), from which the dynamic strength of the shell may be obtained from Fig. 5.

From these curves, it may be noted that for short-duration loads ($p_1/p_2 > 10$), the applied load acts essentially as an impulse, while for long-duration loads ($p_1/p_2 < 0.1$), the applied load acts essentially as a step pulse.

Acknowledgment

This research was performed for the United States Atomic Energy Commission under Contract No. AT (11-1)-578 with IIT Research Institute, Chicago, Ill.

[3] J. Marin and T.-L. Weng, "Strength of Thick-Walled Cylindrical Pressure Vessels," Department of Engineering Mechanics, The Pennsylvania State University, University Park, Pa., September, 1961.

Printed in U. S. A.

7.2 DYNAMIC STRENGTH OF STEAM GENERATOR SHELL

WORK-ENERGY METHOD OF ANALYSIS:

For times longer than approximately 10^{-1} to 1 second following the beginning of a reaction, depending on leak size, the reaction products will have reached the gas surge volume over the sodium and the rupture disc will have operated to relieve the pressure. During time less than 10^{-2} sec. the hydrogen bubble pressure exceeds the static strength of the steam generator vessel, and a dynamic analysis is required to demonstrate that the steam generator shell will not rupture. If it can be shown that the work required to deflect the vessel out to instability strain during any assumed time is always greater than the total energy available at that time from the reaction of sodium and water, the steam generator shell will not fail.

The total energy entering the steam generator as a result of a number of leaking tubes is the sum of the energy in the hot pressurized water entering the vessel, plus the energy released by the reaction of the water with sodium. A hydrogen bubble will be formed and a portion of the energy will appear as heat that raises the temperature of the sodium, hydrogen, and other reaction products. The remainder of the energy appears as the pressure of the hydrogen bubble. A portion of this pressure energy is dissipated in accelerating the sodium up through the steam generator tube bundle, and the remainder of the energy remains as potential energy in the high pressure hydrogen

bubble. This potential energy is available to act on the steam generator liner and shell.

The APDA calculations predict the hydrogen bubble pressure and volume at various times based on very conservative assumptions. These calculations presume that all of the energy of the reaction goes into the reaction products -- no heat is carried away by the flowing sodium. The calculations account for the energy used in accelerating the sodium up through the tube bundle. The bubble pressure calculated by APDA is therefore available to distort the steam generator shell.

CALCULATION OF ENERGY AVAILABLE FROM REACTION:

The pressure volume relationship of the hydrogen bubble has the characteristics of a non-flow process where the work or energy, for a change in volume, can be represented as follows:

$$E = \int P \, dv$$

If the pressure and volume vs. time curves plotted from the APDA data are divided into two time zones, 0 to 10^{-3}, and 10^{-2} to 6×10^{-2} sec., the curves can be approximated very closely as straight lines on log-log plots, as shown on Fig. 2, and the equations for the lines can be easily determined.

These equations are as follows:

Pressure:

$P = 106.3 \; T^{-0.568}$ $\quad (10^{-4} < T < 10^{-3})$

$P = 168.5 \; T^{-0.502}$ $\quad (10^{-3} < T < 6 \times 10^{-2})$

Volume:

$v = 14.57 \times 10^6 \; T^{1.572} \qquad (10^{-4} < T < 10^{-3})$

$v = 8.399 \times 10^6 \; T^{1.492} \qquad (10^{-3} < T < 6 \times 10^{-2})$

Where:

P = Hydrogen bubble pressure psi

v = Hydrogen bubble volume, in^3

N = Number of ruptured tubes

T = Time, sec.

The equations for volume were differentiated with respect to time and the expression for P dv written and integrated for each of the time zones. The resulting summation of bubble energy from the beginning of the leak to any time were plotted on Fig. 1. These energies were compared to the energy to deflect the Steam Generator shell to instability strain in the same time interval.

ENERGY REQUIRED TO DEFLECT STEAM GENERATOR SHELL:

The work required to deflect the steam generator shell to instability was calculated. The instability strain for this vessel is that strain beyond which the vessel can no longer withstand the same internal pressure, (because of thinning). The instability strain corresponds to the strain at the maximum stress point on a conventional stress-strain curve. For this analysis of the assumed simultaneous failure of a large number of tubes it was felt that allowing some yielding of the liner and shell are permissible as long as it can be shown that the shell does not go to failure.

In the dynamic analysis of the liner and shell it is assumed that the pressure developed because of the sodium-water reaction will accelerate the liner and shell outward together. (A separate calculation was made for the shell only as if there were no liner.)

The energy available in the hydrogen bubble will be dissipated in the work of accelerating the vessel and in the strain energy within the material of the vessel wall itself. If it is presumed that the vessel strains to instability, but does not fail, the outward velocity of the shell must be brought to zero at or before the instability strain is reached. The kinetic energy represented by this velocity must also finally go into strain energy.

Strain energy is determined from the following equation:

$$E = \int_0^{\varepsilon_i} \sigma \, d\varepsilon$$

This can be represented graphically as the area under a conventional stress-strain curve. If the energy to instability is considered the curve would be as follows:

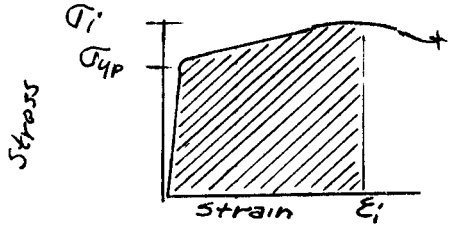

By neglecting the strain elastic portion of the stress-strain curve it was possible to approximate the strain energy by multiplying the strain at instability by the average of the yield point stress and instability stress. The product is strain energy in inch-pounds per cubic inch of metal.

At very short time intervals the pressure from the hydrogen bubble will not have progressed outward far enough to load the whole shell so that the strain energy available is only the strain energy in the portion of the shell affected. For this analysis it was assumed that the reaction occurred at a spot right on the shell, and that the pressure pulse traveled outward from this spot at 5000 ft/sec. The intersection of this pressure front and the vessel can therefore be approximated as a circle whose radius is increasing at a rate of 5000 ft/sec. The strength of the shell shown on Fig. 1 for times from 10^{-4} to approximately 5×10^{3} sec. is based on the strain energy in this circular piece of shell.

At some time interval between 10^{-3} and 10^{-2} sec. the pressure front has moved outward so that the whole shell will be affected. The APDA calculations predict the bubble pressure, or the maximum pressure that will exist within the Steam Generator shell at any time. The displacement of the sodium upward through the tube bundle by the hydrogen bubble can be considered to be a one dimensional transient flow problem for times longer than 10^{-2} seconds, and the pressure will vary linearly with distance from a maximum at the hydrogen bubble to essentially zero at the sodium surface at the top of the steam generator. The Steam Generator shell will not be affected uniformly because of the varying pressure. For this analysis it was assumed that the shell was deflected to instability at the worst location and proportionally less at other locations. For calculating the strength of the liner

and shell, half of the total strain energy to shell instability was assumed for times 10^{-2} seconds and longer. It is felt that this is a conservative assumption.

DISCUSSION OF RESULTS:

By referring to Fig. 1 it will be noted that the shell and liner can withstand the simultaneous rupture of 25 tubes in the worst location. It is of interest that the 1" vessel can withstand the rupture of these 25 tubes if the effect of the liner is ignored completely.

It will be noted that the bubble energy curves are not plotted beyond certain times, 6×10^{-2} sec. for the 25 tube leak). At these times the APDA calculations predict that the hydrogen bubble will have reached the inert gas space through one or the other of the parallel paths. The rupture disc will operate and relieve the reaction products beyond that time.

PROTOTYPE STEAM GENERATOR
VESSEL STRENGTH VS. BUBBLE ENERGY

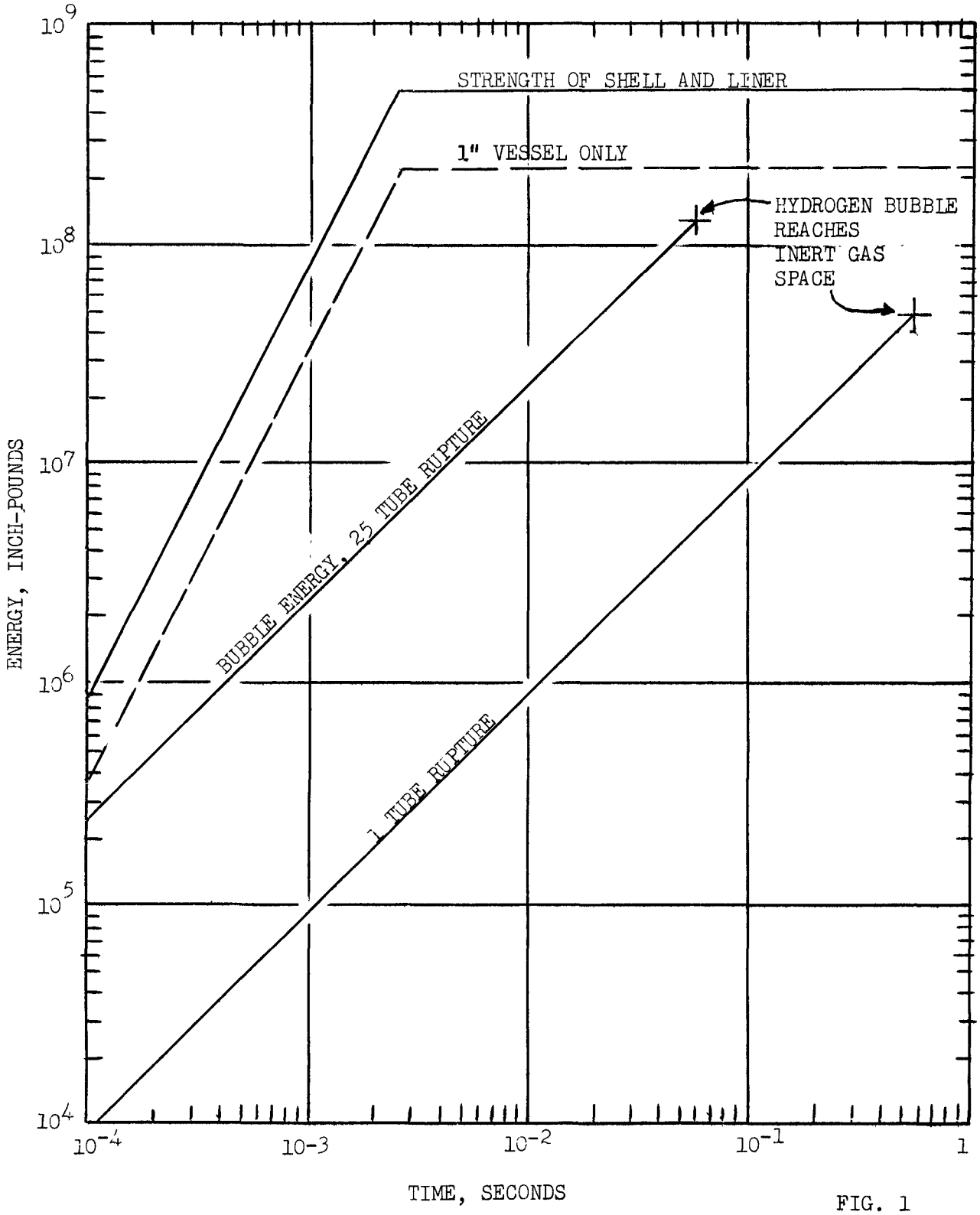

FIG. 1

HYDROGEN BUBBLE PRESSURE AND VOLUME, WORST CASE
(APDA CASE XVI DOWNCOMER ANNULUS)

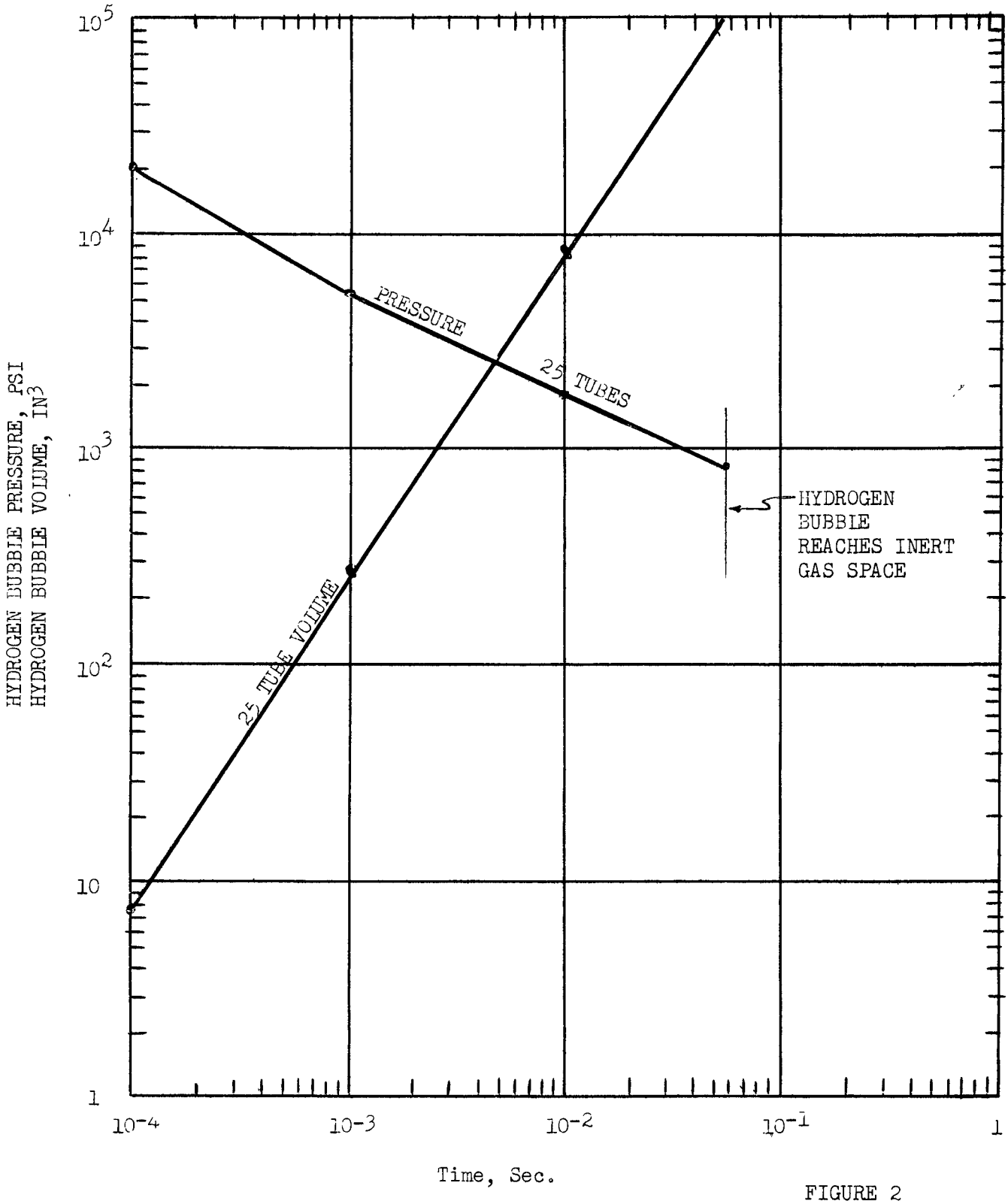

FIGURE 2

APPENDIX:

Sample Calculations -- Dynamic Strength of Steam Generator Shell, Work-Energy Method Analysis:

A. Energy available in Hydrogen Bubble

The hydrogen bubble is a non-flow thermodynamic process for which the equation for work or energy is as follows:

$$E = \int P \quad dv$$

where: E = energy, in-lb.

P = pressure, psi

dv = differential change in volume, in^3

If it is possible to write expansions for both p and dv in terms of the same variable the expression can be integrated.

The APDA curves for hydrogen bubble pressure and volume at the worst case location within the steam generator can be approximated very closely by straight lines on log-log plots if the total time interval is divided into two smaller zones. The equations for each straight line can be readily determined. They all have the form $y = K \quad X^n$.

The equations for pressure are:

1. $P = 106.3 \quad T^{-0.568}$ for time interval $10^{-4} < T < 10^{-3}$ sec.
2. $P = 168.5 \quad T^{-0.502}$ $10^{-3} < T < 6 \times 10^{-2}$

The equations for hydrogen bubble volume are:

1. $v = 14.57 \times 10^6 \quad T^{1.572}$ $10^{-4} < T < 10^{-3}$
2. $v = 8.399 \times 10^6 \quad T^{1.492}$ $10^{-3} < T < 10^{-2}$

Where: P = hydrogen bubble pressure, psi

v = hydrogen bubble volume, in^3

N = Number of ruptured tubes

T = Time, sec.

The equations for volume can be differentiated with respect to time to produce the following:

1. $dv = (14.57 \times 10^6)(1.572)\, T^{0.572}\, dT \qquad 0 < T < 10^{-3}$

2. $dv = (8.399 \times 10^6)(1.492)\, T^{0.492}\, dT \qquad 10^{-3} < T < 10^{-2}$

The expressions for P dv can be written and integrated as follows:

1. $E = 2435 \times 10^6 \int_0^{10^{-3}} T^{.004}\, dT \qquad 0 < T < 10^{-3}$

$= 2425 \times 10^6 \left[T^{1.004} \right]_0^{10^{-3}}$

in a similar manner:

2. $E = 2.132 \times 10^9 \left[T^{0.99} \right]_{10^{-3}}^{10^{-2}} \qquad 10^{-3} < T < 10^{-2}$

The energy for each of the time intervals can be calculated for any assumed number of ruptured tubes. The energy for individual time intervals can be summed together to give the total bubble energy at any time after beginning of a leak.

Bubble Energy, in-lb.

Time	Number of Tubes Ruptured
Sec.	25
10^{-4}	2.325×10^5
10^{-3}	2.38×10^6
10^{-2}	2.249×10^7

B Strength of Steam Generator Shell

Work-Energy Basis

1. To determine manner of loading shell assume:

a. Leak and consequent sodium-water reaction occurs immediately adjacent to vessel wall.

b. Pressure pulse travels outward from the leak site at sonic velocity in sodium or 5000 ft/sec.

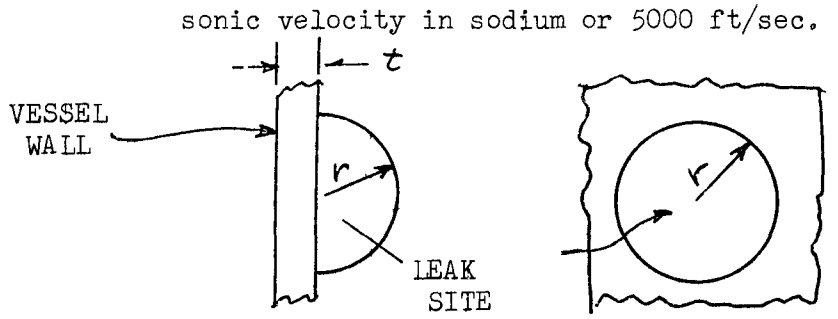

The projection of the pressure pulse on the vessel wall can be approximated as a circle whose radius is increasing at a rate of 5000 ft/sec or 60,000 in/sec.

Therefore $r = 60{,}000\ T$ where r is the radius, in

T is time from beginning of reaction, sec.

The area of the shell that is affected by the reaction is $\pi r^2 = \pi(60{,}000T)^2$ until the time it is long enough that the whole shell is affected. This occurs between 10^{-3} and 10^{-2} seconds for times longer than 10^{-2} it is assumed that the whole shell is affected.

3. Strain energy in 1/2" liner at vessel instability

Liner strain at vessel instability

$$\varepsilon_i = 0.145$$

2

Stress at this strain @ 700F

$$= 96{,}000 \quad \varepsilon^{0.044}$$

$$= 96{,}000 \quad (0.145)^{0.044}$$

$$= 88{,}200 \text{ psi}$$

Yield point stress for this thickness plate @ 900F

$$yp = 43{,}500 \text{ psi}$$

To get a good approximation for strain energy to instability we should multiply the strain at instability by the average of the stress at yield point and at instability. $E = \sigma_{avg}\, \varepsilon_i$

$$\sigma_{yp} = 43{,}500$$

$$= \underline{88{,}200}$$

$$avg = 65{,}850 \text{ psi}$$

$$= 0.145$$

Strain Energy to Instability, $E = (65{,}800)\ (0.145) = 9{,}550$ in-lb/in^3

3. Strain Energy in 1" vessel at instability

$$\varepsilon_i = 0.052$$

$$\sigma_i = 103{,}000 \quad \varepsilon^{0.098}$$

$$\sigma_i = 103{,}000 \quad (0.052)^{0.098}$$

$$\sigma_i = 77{,}000 \text{ psi}$$

Yield point stress for 1" plate @ 800F =

$$\sigma_{yp} = 45{,}000$$

To approximate Strain energy $E = \sigma_{avg.}\, \varepsilon_i$

$$\sigma_{yp} = 45{,}000$$

$$\sigma_i = \underline{77{,}000}$$

$$\sigma_{avg} = 61{,}000 \text{ psi}$$

Strain energy

$$E = \sigma_{avg}\, \varepsilon_i$$

$$= (61{,}000)\ (0.052) = 3{,}170 \text{ in-lb/in}^3$$

For times longer than 10^{-2} seconds the whole vessel will be affected, but it will not be loaded uniformly. Because the sodium is incompressible it is displaced upward through the steam generator by the expanding hydrogen bubble. At the longer times, such as are of concern here, the flow dynamics reduce to a one dimensional transient flow problem. The pressure will be a maximum at the hydrogen bubble and will decrease linearly to the sodium surface at the inert gas space.

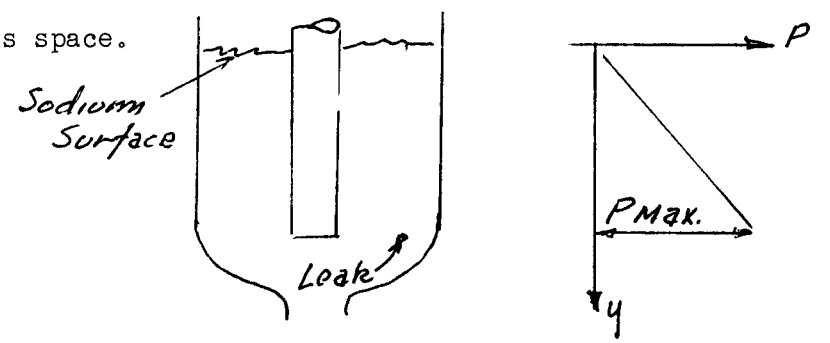

The vessel shell will be loaded in a similar manner. To account for the non-uniform absorbtion of energy in the shell, the total strain energy in the liner and shell to instability was divided by two to get the strength of the liner and shell for times 10^{-2} sec. and longer. These values are compared to the maximum hydrogen bubble energy.

4. Energy absorbed in 1/2" liner to vessel instability

$$E = 9550 \text{ in-lb/in}^3$$

To find volume of vessel affected

$$v = \pi (60{,}000\ T)^2\ t \qquad t = \text{thickness, in}$$

$t = 0.5''$ $\qquad$ T = Time, sec.

Time	$(60{,}000T)^2$	v (in^3)
10^{-4}	36	56.52
10^{-3}	3600	5.652×10^3
10^{-2}	3.6×10^5	5.652×10^5

But the volume of the complete liner (metal volume)

$$= (\pi)\ (6.6.25)\ (.5)\ (25)\ (12) = 3.122 \times 10^4$$

so between 10^{-3} and 10^{-2} the whole liner is affected by the pressure.

Therefore the energy can be evaluated as follows:

$$E = 9550v$$

Time	V (in^3)	E (in-lb)
10^{-4}	56.52	5.40×10^5
10^{-3}	5.652×10^3	5.40×10^7
10^{-2}	3.122×10^4	2.98×10^8

5. Energy absorbed in 1" vessel to instability

$$E = 3170 \text{ in-lb/in}^3$$

Volume of vessel affected

$$v = (\pi)\ (60{,}000\ T)^2\ t \qquad t = \text{thickness in}$$

$$T = \text{Time sec.}$$

Volume of complete shell

$$v = \pi(72)\ (1.0)\ (25)\ (12) = 6.790 \times 10^4 \text{ in}^3$$

Time (sec)	v (in^3)	E (in-lb)
10^{-4}	1.13×10^2	3.58×10^5

10^{-3}	1.13×10^{4}	3.58×10^{7}
10^{-2}	6.79×10^{4}	2.15×10^{8}

Sum up liner and vessel energy absorption

Time	10^{-4}	10^{-3}	10^{-2}
Liner	5.40×10^{5}	5.40×10^{7}	2.98×10^{8}
Vessel	3.58×10^{5}	3.58×10^{7}	2.15×10^{8}
Total	8.98×10^{5}	8.98×10^{7}	5.13×10^{8}

5.0 LOCALIZED BULGE ANALYSIS OF THE STEAM GENERATOR SHELL

INTRODUCTION:

During the initial stages of a major sodium-water reaction, the possibility of vessel failure, caused by localized bulging, must be investigated to verify the soundness of the vessel design.

This analysis provides that verification by comparing the energy required to strain to instability one square inch of vessel area to the energy per square inch of the hydrogen bubble distributed on a spherical area of radius equal to or greater than the distance from the center of the reaction to the vessel surface area under study.

SUMMARY OF CONCLUSION:

The vessel complex, or the shell and liner combination, is found to be of satisfactory design, on the basis of a localized bulge failure. When the hydrogen bubble reaches the gas space at .06 seconds after initiation of reaction the vessel complex can contain to its instability up to twenty-five tubes rupturing instantaneously. See Fig. 1 for graphical representation.

DESCRIPTION OF PROBLEM & SIMPLIFYING ASSUMPTIONS:

A localized bulging failure is developed when a tube or group of tubes near the liner and shell rupture instantaneously. Vessel rupture is represented by the instability strength of the vessel complex or the liner and shell combination. The apparent problem is to determine how many tubes must rupture to produce enough energy to strain the complex to instability. Using the instability strength is conservative since

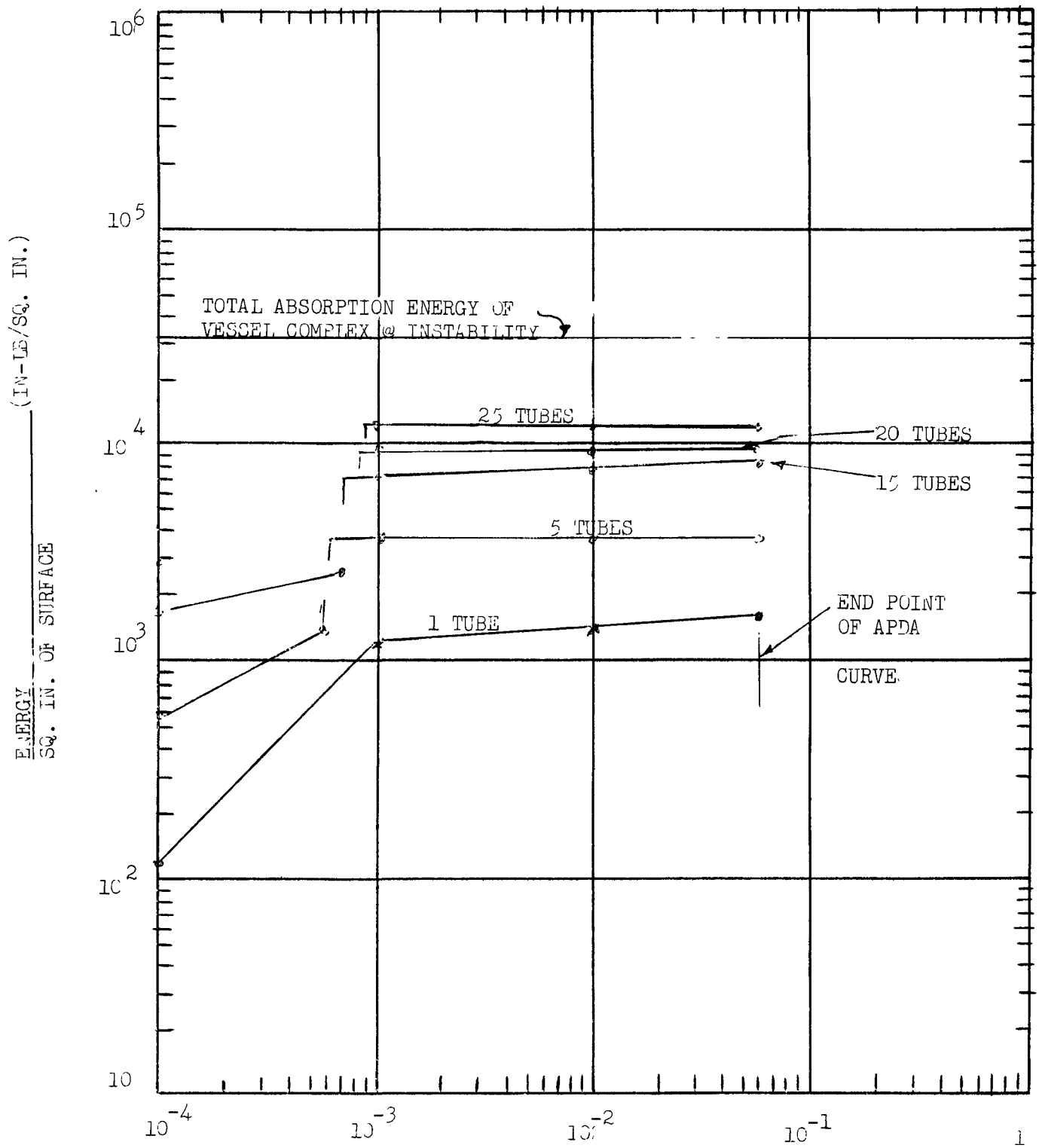

FIG. 1 (COMPARISON OF ABSORPTION ENERGY CAPACITY OF VESSEL COMPLEX WITH HYDROGEN BUBBLE ENERGY

the shell can withstand a great deal more energy input before fracture occurs. This fact is obvious when the energy input the complex can withstand per unit area is defined by the area under the engineering stress-strain curve from which the energy residing in the strains beyond instability or ultimate tensile strength can be compared to the energy up to instability.

The necessary assumptions, most of which are conservative, required to simplify the mathematical model are:

1. The tube ruptures are instantaneous severings of all the quantity of tubes being studied and the ruptures occur simultaneously.
2. The liner appears as a rigidly held plate to a nearby rupturing tube. This is assumed in conjunction with APDA's method of computing pressure-time and volume-time plots.
3. The hydrogen bubble expands isothermally; therefore, it is assumed no energy is dissipated in heat to surrounding medium and the hydrogen behaves as an ideal gas. The total energy released would be a direct function of the number of tubes rupturing.
4. In any combination of tube ruptures the tubes next to the liner are included, since their effect is presumed to be the most severe.
5. The total energy within the hydrogen bubble is assumed to be distributed uniformly over the surface of the bubble.

6. Each tube rupture forms its own bubble which can grow to a maximum radius of 1.25 or half the maximum distance between adjacent tubes in the downcomer section. At this radius the bubbles combine and the total surface area is assumed to immediately attain the value of one sphere of volume equal to the total of the smaller spheres.

7. The energy per unit area received by the liner at a preselected unit area is given by the distribution of the total energy of each bubble over the spherical surface area with a radius equal to the distance from the center of each rupturing tube to the center of the selected unit area. The total energy applied to the selected area would be the summation of the energies applied by the individual bubbles.

8. It is to be assumed that the work available from the bubble will be transferred instantaneously to the liner at its initial radius. In this manner the decay of available work per square inch can be neglected as the liner and shell expand.

9. The energy delivered to the liner is assumed to be uniform over the area considered and has the magnitude of the energy delivered to the point on the liner closest to the centroid of the reaction.

10. The geometry of arrangement of the ruptured tubes will only effect its relation with the liner, since the shell will re-

ceive only the kinetic energy of the liner.

11. Assumption seven is correct only until assumption six supercedes it. In this case the energy applied to the selected area is the energy per unit area of the sphere described in assumption six. This sphere is assumed to have the energy of all the reactions distributed over its surface.

12. During deformation of the liner and shell, beneficial strain-hardening will occur due to two factors. The first is due to elevated temperatures and the second is due to the rapid loading conditions. This strain-hardening is approximated by the Ludwik power strain-hardening law.

DESCRIPTION OF ANALYSIS:

Phase I: Determination of the liner and shell energy absorption capacity up to shell instability.

According to Cole, a simple approximation to the state of plastic deformation, that is reasonably accurate, is formulated in which as Cole states, "it is assumed that a definite elastic limit exists, below which Hooke's law applies and above which the plate acts like a membrane under constant tension determined by the yield stress under tension at the elastic limit." This is the condition present when a perfect plastic behavior of the material can be achieved. Since this is never the true case and is just an idealization for simplification by Cole in his dis-

cussion, an adjustment to correct the situation is the injection of the effect of strain hardening. The proper conditions are achieved by substituting the average stress between the material's yield stress and the final stress at the shell instability, for the yield stress mentioned by Cole. The final stress is computed by the Ludwik power strain hardening law.

In order to incorporate the temperature strain hardening, plots for yield stress vs. temperature, strength co-efficient vs. temperature, and strain hardening exponent vs. temperature, were constructed from Lehigh University data at room temperature, and from B&W Alliance Research data at elevated temperatures. Curves for Croloy 2-1/4 were made for 1/2" and 1 in. plate and values of σy, k, and n, were obtained at shell temperatures. These values are incorporated in the calculation of the average plastic stress, σp, between yield and shell instability.

Cole develops an equation for the plastic work, Wp, done by the applied forces in creating permanent plastic deformation. This equation, $Wp = (\sigma p)\ (h)\ (\Delta A)$, as the B&W utilizes it, incorporates the average plastic stress. The "h" represents the plate thickness and the ΔA represents the change in area of the surface facing the charge or explosion. The thickness is considered constant in this equation, but, since this is not true, due to thinning, it should be corrected. If the equation, $\varepsilon_1 + \varepsilon_2 + \varepsilon_3 = 0$, were a true condition for triaxial strain, ε_3, would equal the negative summation of the remaining strains that were

produced by tensile stresses. This would yield $\varepsilon_3 = -(\varepsilon_1 + \varepsilon_2)$. A reduction in thickness can now be expressed as h (ε_3).

When dealing with a localized bulge failure, the greatest interest is generated in determining the amount of energy transferred from the surface of the hydrogen bubble to a limited area of the liner and shell or vessel complex, the label for the combination. Hence, Cole's equation, is revised to read: The plastic work per square inch of liner or shell area required to strain that square inch of area to shell instability is given by the average plastic stress times the liner or shell thickness reduced by the thickness strain times the change in area of that one square inch.

One more qualification for use of the formula is the selection of the square inch area on the liner and its later projection to the shell. That area is chosen as the closest area to the centroid of the quantity of rupturing tubes. The equation thus far defined is:

$$\frac{Wp}{\text{sp.in.}} = (\sigma p) \quad (h - h\varepsilon h) \; (\Delta A) \; \frac{\text{in.-lb.}}{\text{sq.in.}}$$

This equation, however, is useless until the strain at shell instability is determined for both the liner and the shell.

Since it is desirable, because of simpler strain calculations, to work with static conditions, proof is required to indicate that static results would be conservative in comparison to the dynamic situation. Dynamic strain hardening improves the range of allowable stresses. For

a given stress, less strain occurs under rapid loading, and conversely for a given strain a higher stress is required with dynamic conditions. If the static strain at instability is considered, the static stress for this value on a dynamic stress strain curve would yield a strain below instability; therefore, the use of static conditions will be slightly conservative.

The inside radius of the shell at instability is determined from the dimensionless derivative of pressure to radius, evaluated at a derivative value equal to zero. (See Appendix C for derivation.) Assuming for the moment that the entire shell is loaded, the circumferential strain or effective strain can be calculated from the change in radius. For a localized bulge the axial strain is equal to the circumferential strain or, in other words, a condition of balanced biaxial tension exists. This is true for a major portion of the bulged area and is a precise condition at the center of the bulge.

The change in area per square inch for the energy equation can now be defined as $(1 + \epsilon)^2 - 1$. This area will have to be computed for the liner at a radius equal to the inside shell radius at instability minus, for simplification, the original liner thickness.

For the total energy absorption capacity of the vessel complex, the absorption energy of the liner and shell at shell instability are added. Phase one of the analysis is now complete.

<u>Phase II:</u> Determination of the amount of energy from the hydrogen

bubble available to do work on the selected square inch of vessel complex.

The APDA curves in Section 3.0 Fig. 1 provide the relationship between pressure and time and between volume and time for the worst case single tube rupture. Development of curves for pressure and volumes at other locations for one, five, fifteen & twenty tube failures provide the correlation for pressure-time curves caused by any quantity of tube failures. The equation for the energy in the hydrogen bubble is derived from the pressure and volume equations by the relation $E = \int_{To}^{T} PdV$.

Curve fitting for various time intervals produces the equations:

Time Interval

10^{-4} to 10^{-3} sec.

$$P = 21.26 \sqrt{N}\, T^{-0.568}$$

$$V = 2.914 \times 10^{6} \sqrt{N}\, T^{1.572}$$

$$E = 97.0 \times 10^{6} \quad N\, T^{1.004}$$

10^{-3} to 10^{-2} sec.

$$P = 33.7 \sqrt{N}\, T^{-0.502}$$

$$V = 1.679 \times 10^{6} \sqrt{N}\, T^{1.492}$$

$$E = 85.3 \times 10^{6} \quad N.T^{0.99}$$

Values of volume and energy are tabulated in Appendix C, Table II. Figure 1 in Section 3.0 contains a plot of the volume, and Figure 1 in Section 4.0 contains a plot of the energy.

The values for the volume and energy at specific times are used to compute the energy received from the hydrogen bubble by a square inch of liner area. In so doing assumptions 1 to 11 are taken into account.

These considerations produce the following conditional equations for available energy from <u>each</u> tube rupture.

Eqn. 1 For $r_b \leq r_s$

$$W_a/\text{Sq. In.} = E/4\pi (r_s)^2 = 0.07955\ E/(r_s)^2$$

Where r_d = bubble radius, and r_s = radius to liner surface area considered.

Eqn. 2 $r_s < r_b \leq 1.25''$

$$W_a/\text{Sq. In.} = E/4\pi (r_b)^2 = 0.07955\ E/(r_b)^2$$

Eqn. 3 For r_b 1.25"

$$\text{Total } W_a/\text{Sq. In.} = E_{total}/4\pi (r_b)^2 = 0.07955\ E\ total/(r_b)^2$$

Two more conditions are necessary for proper representation of the energy available.

1. An instantaneous changeover between equations 2 and 3 is required by assumption 11 at the elapsed time for which the bubble radius equals 1.25". These times are found in Appendix C, Table I.

A tabulation of energies available for various tube failure combinations is found in Appendix C, Table III. Values from this table are plotted in Figure 1 for comparison to the vessel complex capacity.

<u>CONCLUSION:</u>

By referring to the plots in Fig. 1, it can be seen that vessel instability will not occur for less than twenty-five simultaneous tube ruptures. It will also be noted that the APDA analysis stops at .06 seconds. This point in time represents the emptying of sodium from one

of the flow paths available. This occurs when the hydrogen bubble enters the gas space and actuates the rupture disk, thereby relieving the pressure.

Hence it has been demonstrated that the steam generator will not rupture on occurrence of up to a twenty-five tube leak rate reaction.

R E F E R E N C E S

1. "Underwater Explosions" by Robert H. Cole, Princeton University Press, Princeton, New Jersey, 1948.

2. "Effects of Tube Leaks in Sodium-Heated Steam Generators" by M.A. Salmon, Armour Research Foundation of Illinois Institute of Technology, NAA-SR-8140, August 31, 1962.

APPENDIX C

PART 1. - Derivation of formula for the shell instability strain.

In Section 0 comparison of static vs. dynamic conditions was made, in which it was demonstrated that if static material properties were used the results would be conservative. This derivation will follow the same procedure given by M.A. Salmon in his discussion of an "Infinite Cylinder Subjected to Static Internal Pressures". He determines the burst radius (at instability) from the solution for a maximum value of the pressure-radius curve. This, of course, is accomplished by setting the derivative equal to zero.

Some adjustments to his discussion must be made to account for the conditions of localized bulging. The first change will represent the condition of balanced biaxial stress and strain, and the second change involves the use of the Ludwik power strain hardening law in place of the linear strain hardening law.

Normally the equilibrium condition of a typical shell element (Fig. 1) would produce the equations:

$$\sigma_\theta = \frac{pr}{h}, \qquad \sigma_x = \frac{\sigma_\theta}{2}$$

Where it is assumed in thin shell theory that σ_r is negligible. But with balanced biaxial stresses (Fig. 2) σ_x must $= \sigma_\theta$.

The following dimensionless notation will be employed:

$$\rho = \frac{\text{deformed radius}}{\text{initial radius}} = \frac{r}{r_o}$$

$$\eta = \frac{\text{deformed thickness}}{\text{initial thickness}} = \frac{h}{h_o}$$

$$\sigma_\theta = \bar{\sigma}_x = \frac{\text{circumferential stress}}{\text{strength co-efficient}} = \frac{\sigma_\theta}{K}$$

$$\alpha = \text{dimensionless pressure ratio} = \frac{pr_o}{Kh_o}$$

The stress equations can now be rewritten, becoming

$$\bar{\sigma}_\theta = \bar{\sigma}_x = \frac{pr}{h} \approx \frac{pr_o}{Kh_o} \cdot \frac{r/r_o}{h/h_o} = \frac{\alpha\rho}{\eta}$$

For large strains, the natural strain is given by

$$\epsilon_\theta = \epsilon_x = \log \frac{L}{L_o} = \text{lob} \frac{2\pi r}{2\pi r_o} = \log \frac{r}{r_o} = \log \rho$$

If plastic strains are assumed to satisfy the condition of incompressibility then:

$$\epsilon_\theta + \epsilon_x + \epsilon_h = 0$$

and $$\epsilon_h = -(\epsilon_\theta + \epsilon_x) = -2\epsilon_\theta$$

but ϵ_h can also be defined as

$$\epsilon_h = \log \frac{h}{h_o} = \log \eta$$

A thickness to displacement relation can now be expressed

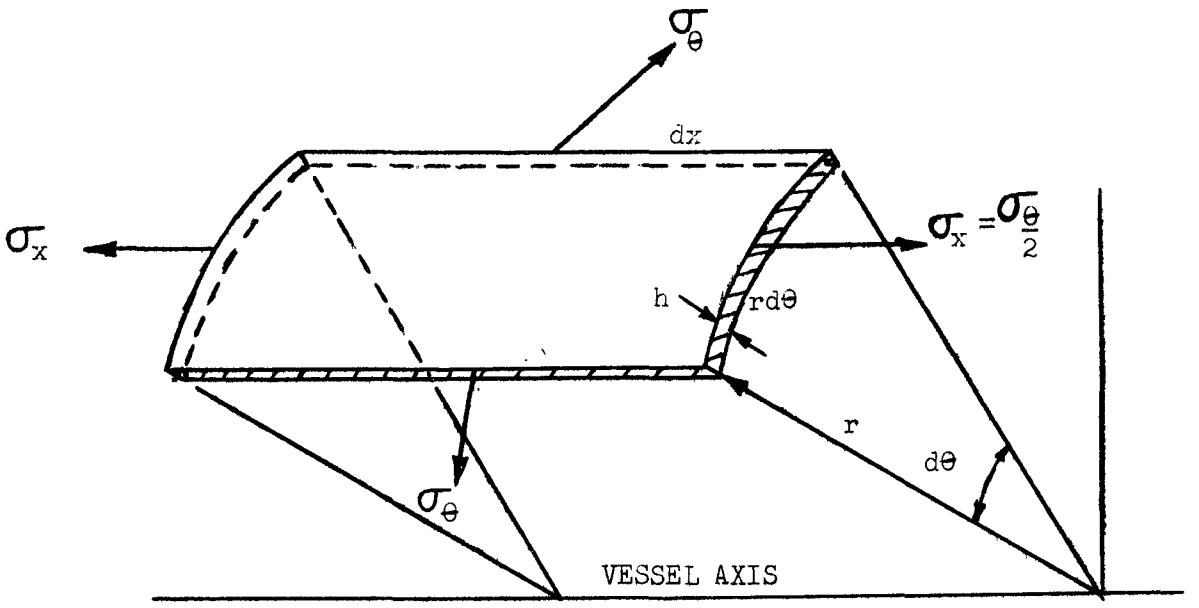

FIG. 1 STRESS CONDITION IN NORMAL STATICALLY LOADED SHELL ELEMENT

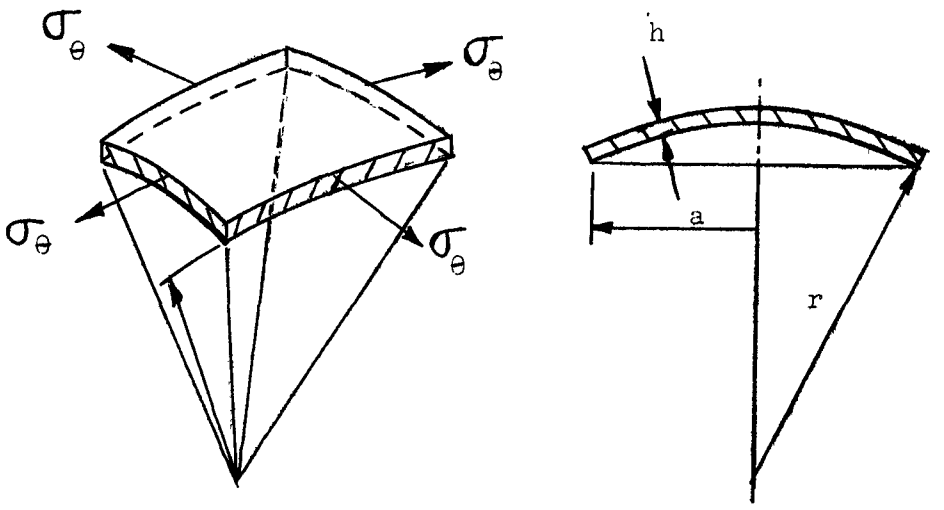

(a) STRESSES IN AN ELEMENT

(b) SPHERICAL DEFORMATION

FIG. 2 "TANGENTIAL STRESSES FOR A PLATE IN PLASTIC TENSION"

$$\epsilon_h = -2\,\epsilon_\theta$$

$$\log \eta = -2 \log \rho$$

or $\eta = \frac{1}{\rho^2}$

Cosnider now the stress situation at yield. The maximum shear strain energy or the maximum distortion energy theory gives the equation for effective stress at yield point as

$$2\,\sigma_{yp}^2 = (\sigma_1 - \sigma_2)^2 + (\sigma_2 - \sigma_3)^2 + (\sigma_1 - \sigma_3)^2$$

or

$$2\,\sigma_{yp}^2 = (\sigma_\theta - \sigma_x)^2 + (\sigma_\theta - \sigma_r)^2 + (\sigma_x - \sigma_r)^2$$

which reduces to

$$2\,\sigma_{yp}^2 = \sigma_\theta^2 - 2\,\sigma_\theta\sigma_x + \sigma_x^2 + \sigma_\theta^2 + \sigma_x^2$$

$$\sigma_{yp} = (\sigma_\theta^2 - \sigma_\theta\sigma_x + \sigma_x^2)^{\frac{1}{2}}$$

since $\sigma_r \doteq 0$.

Substituting $\sigma_x = \sigma_\theta$

$$\sigma_{eff} = (\sigma_\theta^2 - \sigma_\theta^2 + \sigma_\theta^2)^{\frac{1}{2}} = \sigma_\theta$$

Developing effective strain in the same manner from the defining equation of effective strain

$$\epsilon = \sqrt{2/3}\,(\epsilon_1^2 + \epsilon_2^2 + \epsilon_3^2)^{\frac{1}{2}} =$$

$$= \sqrt{2/3}\,(\epsilon_\theta^2 + \epsilon_\theta^2 + (-2\,\epsilon_\theta)^2)^{\frac{1}{2}}$$

$$= 2/3\,(6\,\epsilon_\theta^2)^{\frac{1}{2}}$$

$$= 2\epsilon_\theta$$

Since Groloy 2-1/4 is a strain hardening material, the stress-strain behavior may be expressed analytically by:

$$\sigma = K \quad F(\epsilon)$$

Where σ is defined as the effective stress under triaxial stress conditions, K is the constant strength co-efficient, and ϵ is the effective strain.

Using the equation, $\bar{\sigma}_\theta = \frac{\alpha\rho}{\eta}$,

together with $\sigma = K \quad F(\epsilon)$,

$\frac{\sigma}{K} = \bar{\sigma} = \bar{\sigma}_\theta$, $\epsilon = 2\epsilon_\theta$, and $\eta = \frac{1}{\rho^2}$,

the pressure-radius relation can be developed.

$$\alpha = \frac{\bar{\sigma}_\theta \eta}{\rho} = \frac{\bar{\sigma}\,\rho^{\frac{1}{2}}}{\rho} = \frac{1}{\rho^3}\,\frac{\sigma}{K} = \frac{1}{\rho^3}\quad F(\epsilon)$$

$$\alpha = \frac{1}{\rho^3}\quad F(2\epsilon_\theta) = \frac{1}{\rho^3}\quad F(2\log\rho)$$

which for power strain hardening becomes

$\alpha = \frac{1}{\rho^3}\ (2\log\rho)^n$ where n is the strain hardening exponent.

Solving for α max, $\frac{d\alpha}{d\rho}$ is set = 0.

$$\frac{d\alpha}{d\rho} = \frac{d}{d\rho}\left[\frac{(\log\rho^2)^n}{\rho^3}\right]$$

$$= \frac{\rho^3 n\,(\log\rho^2)^{n-1}\left(\frac{1}{\rho^2}\right)(\log e)\,(2\rho) - \log\rho^2)\,(3\rho^2)}{}$$

$$n(\log e)\ 2\rho^2\ (\log\rho^2)^{n-1} - 3\ (\log\rho^2)^n\rho^2 = 0$$

$$\frac{2n\log e}{(\log \rho^2)} = 3$$

$$\log \rho^2 = 2/3\ n \log e$$

$$\rho^2 = e^{2/3\ n}$$

$$\rho = e^{n/3}$$

$$\frac{r}{r_o} = \rho$$

$$r = r_o e^{n/3}$$

which for the shell at 800°F, where $n = 0.098$ and $r_o = 36''$, becomes

$$r = 36e^{\frac{0.098}{3}} = 36e^{0.033} = 36\ (1.0335) = 37.206''$$

and $\rho = 1.0335$

$$\epsilon = \rho - 1 = 0.0335$$

APPENDIX

PART 2. - Determining the vessel complex's energy absorption capacity.

The equations to be used are:

$$\frac{\text{Wp req'd}}{\text{sq. in.}} = (\sigma_p \text{ psi})\,(h_o - h_o \epsilon_h)'' \left(\frac{\Delta A \text{ sq. in.}}{\text{sq. in.}}\right)$$

$$\frac{\Delta A}{\text{sq. in.}} = (1 + \epsilon)^2 - 1^2$$

and from Part 1.

$$\epsilon_h = 2\epsilon$$

Section A. Energy absorption capacity of shell

$$\epsilon = 0.-335$$

$$\epsilon_h = 0.0670$$

$$\frac{\Delta A}{\text{sq. in.}} = (1.0335)^2 - 1 = 0.068 \frac{\text{sq. in.}}{\text{sq. in.}}$$

$$h_o = 1.0''$$

$$\sigma_p = \text{ave. plastic stress} = \frac{\sigma_i + \sigma_y}{2}$$

σ_y from Section 10.7 Fig. 3 @ 800°F for h = 1" is 48,000 psi.

From Section 10.7 on strain hardening σ is found by

$$\sigma = K\epsilon^n$$

for the shell @ 800°F, K and n, from Section 10.7 Figs. 1 & 2, are 103,000 psi and 0.098 respectively. Hence,

$$\sigma_i = 1.03 \times 10^5\,(0.0335)^{0.098}$$

$= 1.03 \times 10^5$ antilog (0.098 log 0.0335)

$= 73{,}768$ psi

and $\sigma p = \frac{76{,}768 + 48{,}000}{2} = 62{,}384$ psi

$\frac{Wp \text{ req'd}}{\text{sq. in.}} = (\sigma p)\ (h_o - h_o \epsilon_h)\ (\Delta A)$

$= (62{,}384)\ (1.0 - 1.0\ (0{,}0670)\ (0.068)$

$= (62{,}384)\ (0.068)\ (.933)$

$= 3.958 \frac{\text{in. lb.}}{\text{sq. in.}}$

$\frac{We \text{ req'd}}{\text{sq. in.}} = \frac{\sigma_y \quad h}{2} \Delta A$

$= \frac{48{,}000}{2}\ 1\left[\left(1 + \frac{48{,}000}{30 \times 10^6}\right)^2 - 1\right]$

$= 38 \frac{\text{in-lb}}{\text{sq.in.}}$

Total work req'd on shell/sq.in. = 3996 $\frac{\text{in-lb}}{\text{sq. in.}}$

Section B Energy absorption capacity of liner at shell instability

$r_o = 32.625''$

$h_o = 0.5''$

$r = 37.026'' = 0.5'' = 36.706$

$\rho = \frac{36.706}{32.625} = 1.125$

$\epsilon = \rho - 1 = 0.125$

$\epsilon_h = 0.250$

$\frac{\Delta A}{\text{sq.in.}} = (1.25)^2 - 1 = 0.5625 \frac{\text{in-lb}}{\text{sq.in.}}$

σ_y from fig. 3 @ 900°F = 65,000 psi

K from fig. 1 = 96,000 psi

n from fig. 2 = 0.044

$$\sigma_f = 0.96 \times 10^5 \, (0.125)^{0.044}$$

$$= 0.96 \times 10^5 \text{ antilog } (0.044 \log 0.125)$$

$$= 87{,}600 \text{ psi}$$

$$= \frac{87{,}600 + 65{,}000}{2} = 76{,}300 \text{ psi}$$

$$\frac{\text{Wp req'd}}{\text{sq. in.}} = \sigma_p \, (h_o - h_o \epsilon_h) \, (\Delta A)$$

$$= (76{,}300) \, (0.5 - 0.5 \, (0.250)(0.5625)$$

$$= (76{,}300) \, (0.375) \, (0.5625)$$

$$= 16{,}095 \, \frac{\text{in. - lb.}}{\text{sq. in.}}$$

$$\frac{\text{We req'd}}{\text{sq. in.}} = \frac{\sigma_y}{2} \, h \, \Delta A = \frac{65{,}000}{2} \cdot \frac{1}{2} \cdot \left[\left(1 + \frac{65{,}000}{30 \times 10^6}\right)^2 - 1 \right]$$

$$= 70 \, \frac{\text{in. - lb.}}{\text{sq. in.}}$$

Total work req'd. on liner/sq. in. = 16,165 $\frac{\text{in. - lb.}}{\text{sq. in.}}$

Section C

Total work capacity of vessel complex

$$W_{T/\text{sq.in.}} = 3996 + 16{,}165 = 20{,}161 \, \frac{\text{in. - lb.}}{\text{sq. in.}}$$

PART 3. - Computation of energy available from the hydrogen bubble to do work on vessel complex.

Conditional Equations

1. For $r_b \leq r_s$

$$\frac{W_a}{SQ.IN.} = 0.07955\ E/r_s^2$$

2. For r_s r_b 1.25"

$$\frac{W_a}{sq.\ in.} = 0.07955\ E/r_b^2$$

3. For $r_b > 1.25$

$$\text{Total } \frac{W_a}{SQ.In.} = 0.07955\ E\ \text{total}/(r_b\ \text{equiv})^2$$

Since the bubble radius r_b is a function of time, the times for cut off of (2) can be found for any quantity of rupturing tubes. This is done in Table I with the following equations:

$$r_b = 1.25''$$

$$V = (N)\ 8.18 = 2.914 \times 10^6\ \sqrt{N}\ \ T^{1.572}$$

$$\text{Log } T = \frac{1}{1.572} \log \left(\sqrt{N}\ 2.81 \times 10^{-6} \right)$$

From the equations for volume and energy, values can be tabulated for various times and quantities of rupturing tubes. See Table II. The equations for Table II are:

$$V = 2.914 \times 10^6\ \sqrt{N}\ \ T^{1.572}$$

$$E = 97.0 \times 10^6\ \ N\ \ T^{1.004}$$

Sample Calculations for Table II:

1 TUBE

@ 10^{-4} sec. $V = 2.914 \times 10^{6} \times 1 \times 10^{-6.288} = 2.914 = 1.5$

$E = 97 \times 10^{6} \times 1 \times 10^{-4.016} = 1.941 \times 10^{1.984} = 97 \times 96.38 = 9{,}300$

@ 10^{-3} sec. $V = 2.914 \times 10^{6} \times 1 \times 10^{-4.716} = 2.914 \times 10^{1.284} = 2.914 \times 19.23 = 55.7$

$E = 97 \times 10^{6} \times 1 \times 10^{-3.012} = 97 \times 10^{2.988} - 97 \times 9728 = 94.000$

From Table II and the conditional equations a computation table can be formed to find the work available for various times and tube ruptures. See Table III. These values are plotted on Fig. 1, Section 5.0 with end conditions approximated for APDA information.

TABLE I

Computation Table for Instantaneous Changeover Time Between Equations 2 and 3

N	$\sqrt{N}$	$\sqrt{N}(2.81 \times 10^{-6})$	$\mathrm{Log}(N2.81\times10^{-6})$	$\mathrm{Log}(N2.81\times10^{-6})$	$\frac{\mathrm{Log}(N2.81\times10^{-6})}{1.572}$	Log T	T
2	1.414	3.99×10^{-6}	4.60097 - 10	- 5.39903	- 3.43447	6.56523 - 10	3.675×10^{-4}
3	1.732	4.87×10^{-6}	4.68753 - 10	- 5.31247	- 3.37943	6.62057 - 10	4.174×10^{-4}
5	2.236	6.29×10^{-6}	4.79865 - 10	- 5.20134	- 3.30874	6.69126 - 10	4.912×10^{-4}
10	3.162	8.9×10^{-6}	4.94939 - 10	- 5.05061	- 3.21286	6.78714 - 10	6.125×10^{-4}
15	3.873	1.085×10^{-5}	5.03543 - 10	- 4.96456	- 3.15812	6.84188 - 10	6.948×10^{-4}
20	4.472	1.257×10^{-5}	5.09934 - 10	- 4.90066	- 3.11747	6.88253 - 10	7.630×10^{-4}
25	5.000	1.405×10^{-5}	5.14768 - 10	- 4.85232	- 3.08672	6.91328 - 10	8.190×10^{-4}

TABLE II
Tabulation of Volumes & Energies at Selected Times for
Given Quantities of Tube Ruptures

N	$T = 10^{-4}$ sec.		$T = 10^{-3}$ sec.		$T = 10^{-2}$ sec.	
	V ¿³	E"#	V ¿³	E"#	V ¿³	E"#
1	1.5	9.3×10^3	5.57×10	9.4×10^4	1.739×10^3	8.9×10^5
2	2.12	1.86×10^4	7.88×10	1.86×10^5	2.46×10^3	1.78×10^6
3	2.59	2.79×10^4	9.64×10	2.82×10^5	3.01×10^3	2.67×10^6
5	3.35	4.65×10^4	1.245×10^2	4.7×10^5	3.89×10^3	4.45×10^6
10	4.74	9.3×10^4	1.76×10^2	9.4×10^5	5.49×10^3	8.9×10^6
15	5.810	1.39×10^5	2.2×10^2	1.4×10^6	6.74×10^3	1.34×10^7
20	6.708	1.86×10^5	2.49×10^2	1.88×10^6	7.78×10^3	1.78×10^7
25	7.5	2.33×10^5	2.79×10^2	2.35×10^6	8.695×10^3	2.23×10^7

TABLE III

N	N/r_s	r_s	T	$V(t)^3$	$^3V(t)$/tube	r_b	$\frac{r_b}{r_s}$	Eqnn. No.	r_b^2 or r_s^2	E(t)"#	W_a/" $\frac{"\#}{in.^2}$
1	1	2-1/2	10^{-4}	1.5	1.145	0.71	<1	1	6.25	9.3×10^3	118
			10^{-3}	55.7	3.82	2.36	<1	I	6.25	9.4×10^4	1196
			10^{-2}	1739.0	12.1	7.5	>1	3	56.25	8.91×10^5	1259
			6×10^{-2}	25185	29.3	18.2	>1	3	332.0	5.3×10^6	1265
5	1	2-1/2	10^{-4}	3.35	1.5	.93	<1	1	6.25	4.65×10^4	591
			10^{-3}	124.5	4.99	3.1	>1	3	9.6	4.7×10^5	3894
			10^{-2}	3890	15.73	9.8	>1	3	95.5	4.45×10^6	3707
			6×10^{-2}	56300	38.5	24.9	>1	3	623	2.65×10^7	3384
			4.912×10^{-4}	40.9	3.45	2.14	<1	1	6.25	1.03×10^5	1310

N	T_s	T	$V(t)^3$	$^3V(t)$/tube	r_b	$\frac{r_b}{r_s}$	Eqn. No.	$r_b^2 + r_s^2$	E(t)"#	W_a/" "#/"
15	2-1/2	10^{-4}	5.80	1.8	1.14	<1	1	6.25	1.39×10^5	1769
		10^{-3}	216.0	6.0	3.7	>1	3	14.4	1.4×10^6	7734
		10^{-2}	6733	18.9	11.8	>1	3	139.5	1.34×10^7	7669
		6×10^{-2}	97516	44.4	27.6	>1	3	763	7.9×10^7	8237
		6.948×10^{-4}	122	4.96	3.02	>1	3	9.1	2.53×10^5	2210
20	2-1/2	10^{-4}	6.708	1.865	1.18	<1	1	6.25	1.86×10^5	2367
		10^{-3}	249	6.29	3.9	>1	3	15.2	1.88×10^6	9839
		10^{-2}	9777	19.75	12.3	>1	3	151.0	1.78×10^7	9377
		6×10^{-2}	112,627	48.4	29.5	>1	3	870	1.06×10^8	9692
25	2-1/2	10^{-4}	7.5	1.96	1.21	<1	1	6.25	2.33×10^5	2966
		10^{-3}	279	6.52	4.05	>1	3	16.4	2.35×10^6	11399
		10^{-2}	8695	20.55	12.8	>1	3	164.0	2.23×10^7	10817
		6×10^{-2}	125925	50.1	31.1	>1	3	961	1.32×10^8	10927

6.2.5 CORROSION OF MATERIALS OF CONSTRUCTION IN PRODUCTS OF A SODIUM WATER REACTION

CORROSION OF MATERIALS OF CONSTRUCTION IN PRODUCTS OF A SODIUM-WATER REACTION:

In addition to the problem of withstanding the high pressures and temperatures due to a large sodium-water reaction there is the problem of rapid corrosion of material of construction in the high temperature reaction product. A small leak is much more credible than the very large leaks assumed in the vessel strength analysés. Leaks in pressure tubing usually start small. The heat generated by the sodium-water reaction will be confined to a small area around the leak site, and little or no increase in the bulk temperature and pressure of the sodium will occur. Early detection and dumping of the water from the Steam Generator are the best way to minimize damage to the Steam Generator.

Two separate research projects have been carried out on the small leak and corrosion problem. As part of Subcontract No. 1 under this Contract APDA has investigated the corrosion of adjacent tubes due to the impingement of reacting high pressure water and sodium from a small leak. The results from these experiments are reported in APDA 176 "Analysis of the Babcock & Wilcox Full-Size Steam Generator for a Sodium-Water Reaction." Very briefly these tests show that erosion-corrosion from reacting water and sodium can produce severe thinning of adjacent tubes in a few seconds.

A separate general corrosion project was conducted by B&W Research Center. This project was directed to determine the corrosion rate for Croloy 2-1/4 steel in the products of a sodium-water reaction. The results of this investigation are reported in B&W Research Report BAW-1280-30.

Corrosion rates were determined for various concentrations of NaOH in water and in sodium at various temperatures. The tests were conducted under gently stirred conditions to isolate the effect of corrosion from the effects of erosion and other phenomina near an actual reaction. The corrosion of Croloy 2-1/4 steel in NaOH in sodium was found to be quite low and should not prove to be a problem. Corrosion in aqueous NaOH is very rapid, especially at high temperature.

Fig. 1 shows the trend of corrosion rate with temperature. At a given temperature concentration of NaH had a minor effect on corrosion rate. Since temperatures of 1800-2300F have been observed in reaction zones it can be seen that corrosion alone can result in a loss of about .001" of tube wall per hour. The other effects due to the reaction increase the corrosion rate greatly and make early detection and dumping of the water very important.

Fig. 2 shows the steam pressure decay curve after beginning of isolation and dump. The dump valve is a 2½" valve at the feedwater inlet side of the Steam Generator. It will be noticed that the pressure drops to approximately 134 psi in 0.5 sec. for the case where the steam generator is 350F isothermal. This case resulted in the highest water leak rate and was used in the vessel strength calculations. It can be seen that it is a worst case for a small leak and corrosion. The longest dump time occurs for 20% load operation, and is also shown on Fig. 2.

A simplified schematic diagram for an isolation and dump system for one steam generator is shown on Fig. 3. In addition to sealing off

the connections to the steam and feedwater headers, and opening a dump valve; this system shows a nitrogen system that will help purge the water from the tubes and will prevent the pressure inside the tubes from falling below the pressure on the sodium side of the tubes. This will prevent forcing sodium back through the tube leak and prevent contamination of the whole water system.

Since severe local erosion and corrosion can occur in a few seconds, and since it can take as much as 25 seconds for the water pressure to decay after the isolation and dump operation has begun, it can be appreciated that early, reliable detection of a leak is of greatest importance. Development work is now in progress by others on leak detection devices, and is outside the scope of this Contract.

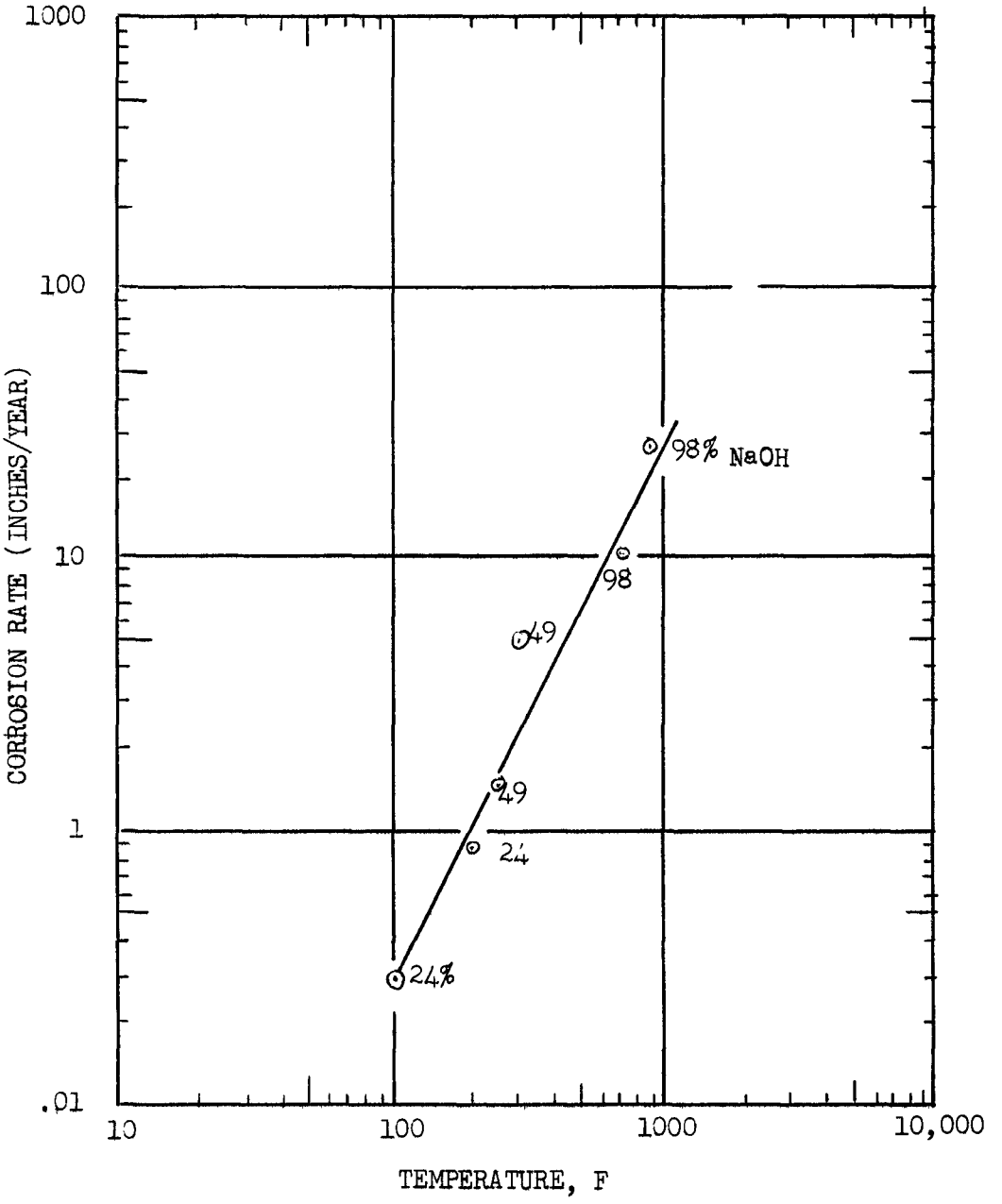

CORROSION OF CROLOY 2-1/4 STEEL IN AQUEOUS NaOH

FIG. 1

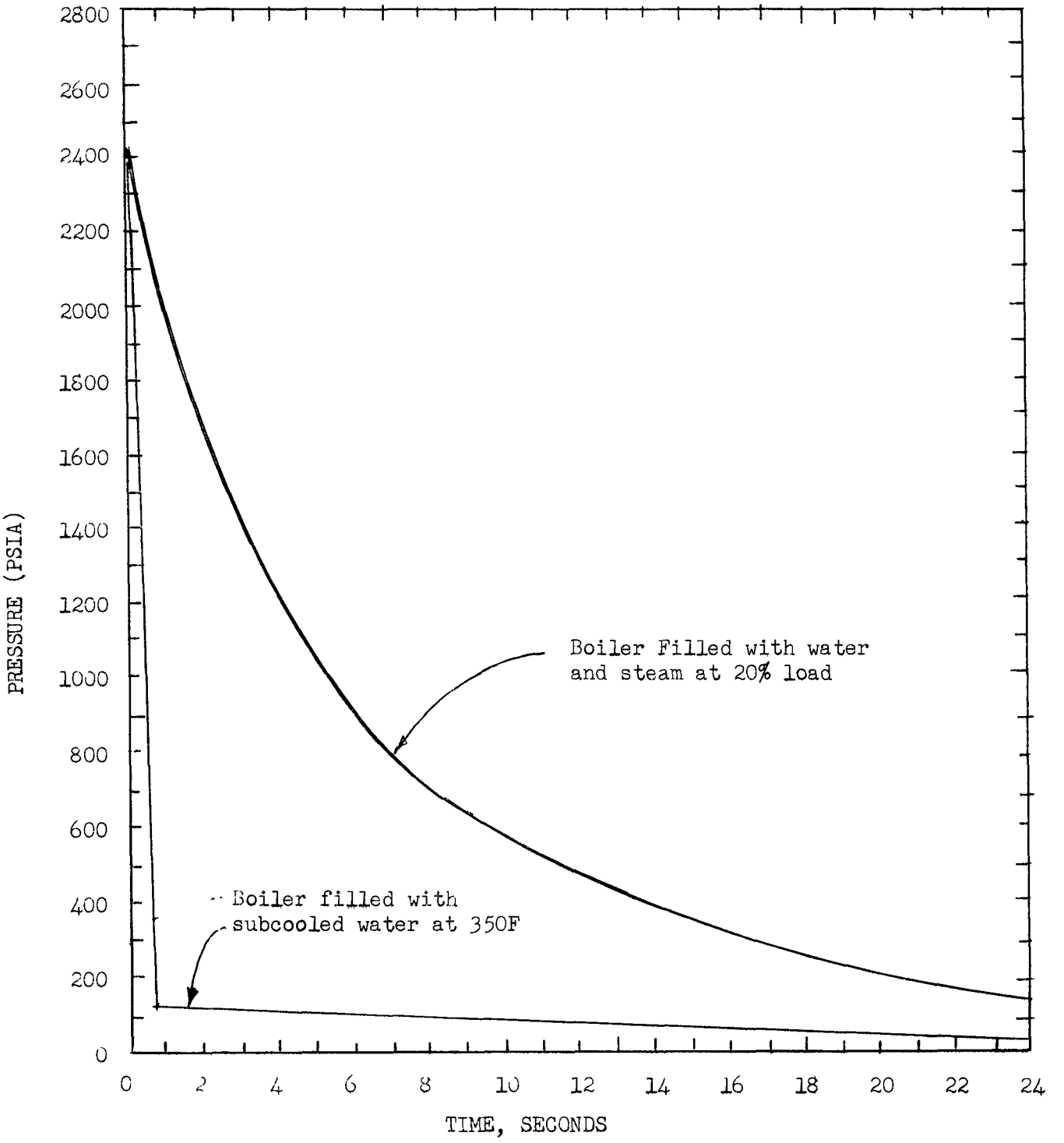

PRESSURE VS. TIME FOR DUMPING OF WATER
FROM PROTOTYPE STEAM GENERATOR

FIG. 2

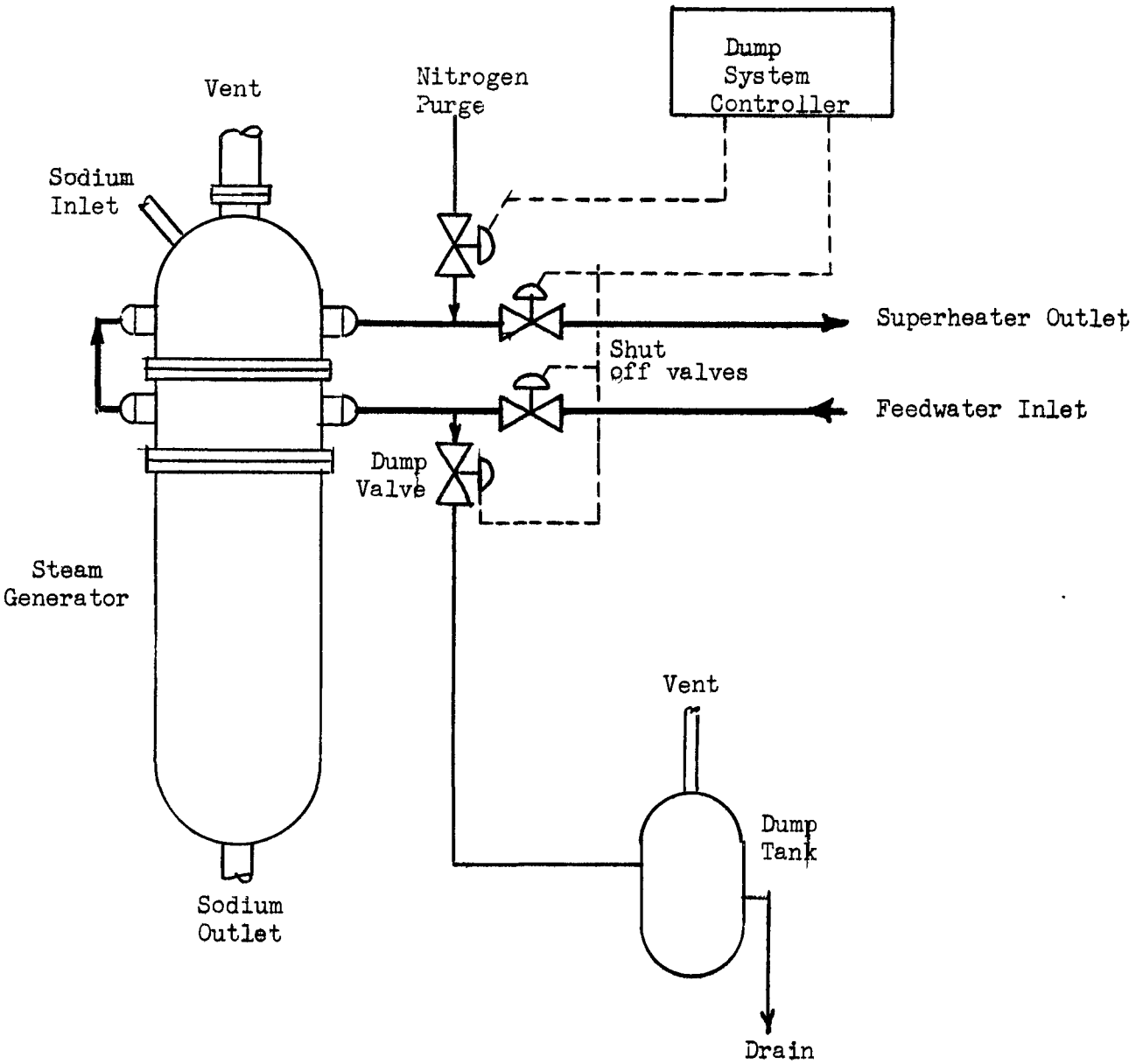

SCHEMATIC DIAGRAM OF ISOLATION AND DUMP SYSTEM

FIG. 3

[redacted] STRAIN HARDENING DATA

Evaluation of Strain Hardening Coefficient and Strength Coefficient for 2-1/4 Croloy Material at Temperatures.

"The process of changing the mechanical properties of a metal by plastic deformation is termed strain hardening.[1] After the yield limit of a metal is exceeded structural changes begin to take place in the metal and ever higher stresses are required to continue the deformation." This process is related to the stress-strain relationship in the plastic range. An increase in rate of loading or decrease in temperature would increase the rate of strain hardening. Strain hardening becomes less apparent with increase in temperature.[2]

The engineering stress-strain relationship which relates conventional stress to conventional strain proves to be quite useful in the elastic range of the metal; however, it leaves much to be desired when considering the plastic range where the cross section is constantly changing during the loading.

In the plastic region of the stress-strain diagram it has been found empirically that:

$$\sigma = K \varepsilon^{n}$$

where

σ = true stress, psi
K = strength coefficient
ε = natural strain in/in
n = strain exponent

References: 1 Behavior of Metals under Impulsive Loads by Rinehart & Pearson, American Society of Metals.

2 High Velocity Forming of Metals - American Society of Tool & Manufacturing Engineers.

This equation then accounts for the increase in stress due to the property changes in the plastic range of the metal.

When $\varepsilon = 1$,

then $\sigma = K(1)^{n} = K$

Therefore the strength coefficient can be found from experimental results by evaluating K on the curves of log σ vs. log ε where strain (ε) = 1.

Experimental data was obtained for 2-1/4 Croloy material from Lehigh University for the strain hardening exponent and the strength coefficient under room temperature conditions. To satisfy strain hardening effects for high temperature values actual temperature conditions were obtained from the Babcock & Wilcox Alliance Research Center. These values for the Lehigh & Alliance results are given below.

LEHIGH UNIVERSITY (ROOM TEMPERATURE)

Condition	Code	(strain hardening exponent)	K (strength coefficient)
SA387D Cooled at 0.3°F/sec.	SC-1	0.171	179,000
	SC-2	0.179	176,000
A387D Cooled at 0.3°F/sec. and Tempered at 1350°F One Hour	SF-1	0.168	142,000
	SF-2	0.169	140,000

By inspection use = .17 & K = 160,000

Alliance Research Data

For plates normalized and stress relieved as follows:

Austenitize @ 1700F - Air Cool

Stress Relieve @ 1315F for one hour - Air Cool

Plate Thick (in.)	Test Temp. (F)	Strain Hardening Exponent	Strength Coefficient K (psi)
$1\frac{1}{2}$	900	.10	89,000
1	900	.09	91,000
$\frac{1}{2}$	700	.07	115,000
$\frac{1}{2}$	1015	.03	76,000

Fig. 1 is a plot of the strength coefficient value for the $\frac{1}{2}$" & 1" plate. Since only two points were available for the 1" plate it was plotted to the same configuration as the $\frac{1}{2}$" plate for which three points were available.

Fig. 2 is a plot of the strain hardening coefficients for the same thickness plates.

Representative temperatures were selected for this report. On this basis, values of "n" and "K" can be chosen for both plate thicknesses and the strain hardening equation for each can be stated. However, these equations only account for temperature conditions, since a rapid loading device that would reliably serve at high temperatures was not available. This testing difficulty is the major obstacle to the complete utilization of beneficial strain hardening. Hence, a compromise to the situation was necessitated which resulted in a power equation for high temperature while neglecting any additional effects of rapid loading. Higher stresses would have been allowed if loading conditions were considered, so the compromise is conservative.

The strain hardening equations for the liner and shell are:

For the liner:

$$= (96{,}000 \text{ psi}) \; (\epsilon)^{0.044}$$

and for the shell,

$$= (103{,}000 \text{ psi}) \; (\epsilon)^{0.098}$$

Another matter to be commented upon is the effect of temperature on the yield stress. This is necessary because the energy calculations are based on the area under the true stress strain curve. The area is computed by the average plastic stress which is defined as the average stress between the yield stress and the stress at shell instability.

THE BABCOCK & WILCOX CO.

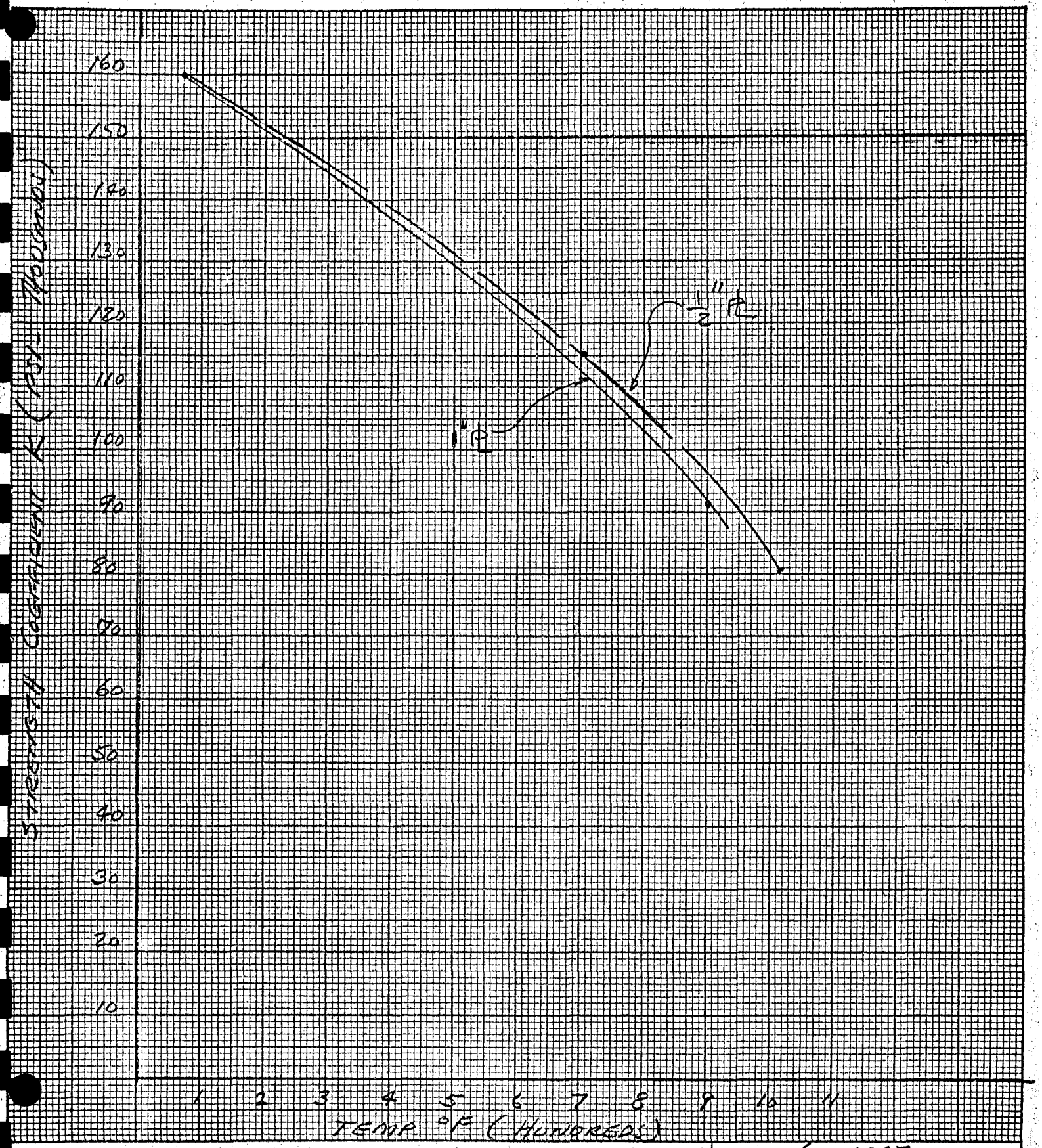

CUSTOMER	JOB NO. 610-0067
SUBJECT STRENGTH COEFFICIENT -K- FOR 1" & 1/2" THK. — 2 1/4 CROLOY PLATE	FIG 2
	BY J.H
	DATE

FORM 3026 15M 8-27-58 K+E ALBANENE 195T TRACING PAPER 52132

THE BABCOCK & WILCOX CO.

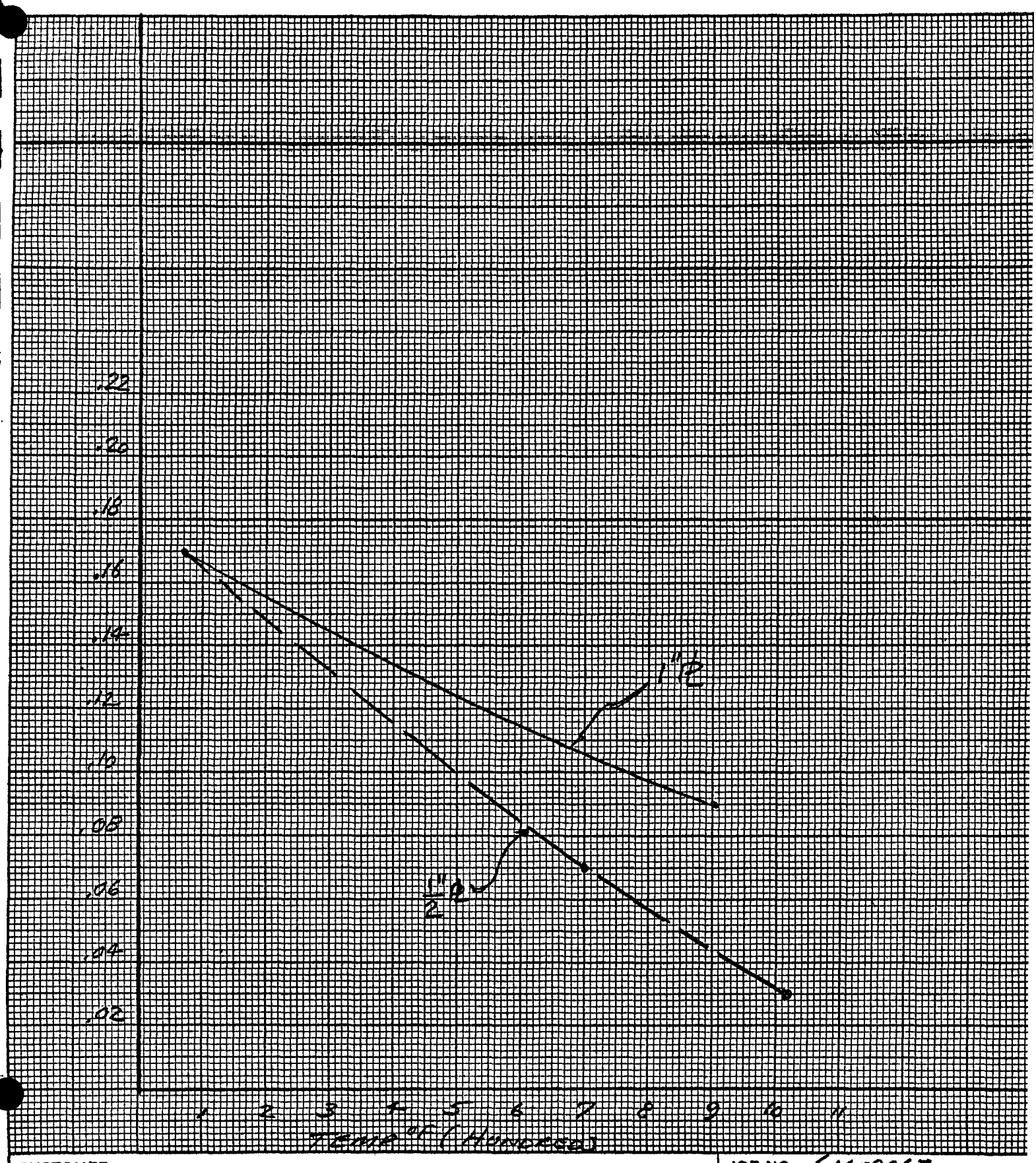

CUSTOMER	JOB NO. 610-0667
SUBJECT STRAIN HARDENING EXPONENT (n) FOR 1/2"-1" THK PLATE - 2 1/4 CROLOY	FIG 2
	BY J.H.
	DATE

FORM 3026 15M 6-27-56 K+E ALBANENE 1967 TRACING PAPER 52132

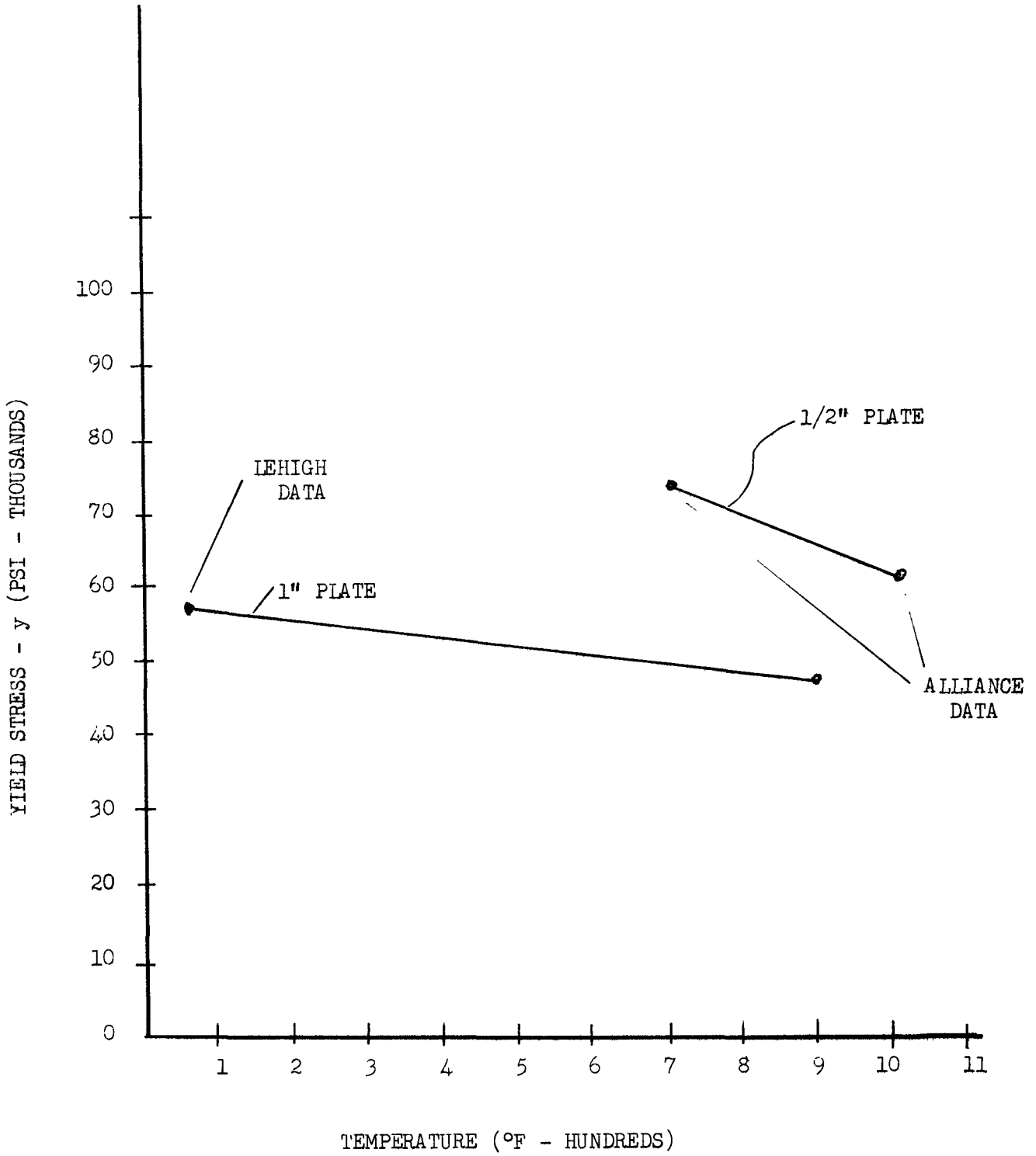

FIG. 3 YIELD STRESS VS. TEMPERATURE
FOR 1" & 1/2" PLATES OF CROLOY 2-1/4

8.0 STRUCTURAL ANALYSIS OF THE CENTER PIPE ASSEMBLY UNDER EXTERNAL PRESSURE.

STRUCTURAL ANALYSIS OF THE CENTER PIPE ASSEMBLY UNDER EXTERNAL PRESSURE

The 30 inch center pipe assembly forms the core around which the helical coils are wound. It also serves as a relief path for any sodium-water reaction products that may be generated. A sodium-water reaction within the coil area will produce an external loading on the center pipe. It is, therefore, necessary to determine the capability of the center pipe to withstand an external pressure and further what effect a possible collapse of the pipe would have on the safety of the unit.

A study of the structural capabilities of the 30 inch center pipe for the Full-Size Unit concluded that this pipe would fail by elastic buckling due to the external pressure loading generated by a one tube failure. It was further concluded that this collapsing and closing off of the relief path would not appreciably increase the internal pressure. This is mainly due to the limiting assumption of two flow escape paths used in the mathematical model to predict the hydrogen bubble pressures. When the center pipe is plugged any one of the other available exits may be assumed to take over the relieving function.

Since the center pipe, the coil tubes and coil diameters in the Prototype Steam Generator are exact models of the Full-Size Unit it will only require correlation of Prototype with the Full-Size Unit to establish the effect of the pressure on the center-pipe assembly.

The worst case pressure in the Full-Size Unit for a one tube failure are as follows:

time (sec)	pressure (psi)
10^{-4}	2600
10^{-3}	800
10^{-2}	270
3×10^{-2}	185

By comparison for the Prototype APDA Case II for a reaction at the top of the downcomer annulus, for a one tube rupture with relief down the boiler downcomer annulus and up the center pipe; up both downcomer boxes yields the following:

time (sec)	pressure (psi)
10^{-4}	3400
10^{-3}	980
10^{-2}	280
10^{-1}	165
5×10^{-1}	120 (rupture disk burst).

For APDA Case XVI, which is considered to be the worst case in the Prototype, a 25 tube rupture at the top of the downcomer annulus with the center pipe blocking flow yields the following pressures:

time (sec)	pressure (psi)
10^{-4}	20,000
10^{-3}	5,400
10^{-2}	1,700
6×10^{-2}	960 (bubble reaches gas space)

The increase in pressure for any number of ruptured tubes relates to the square root of the number of tubes; therefore a one tube rupture for Case XVI would give the following pressures:

time (sec)	pressure (psi)
10^{-4}	4000
10^{-3}	1080
10^{-2}	340
6×10^{-2}	192

The equation for the minimum critical pressure for a long thin walled tube is characterized by the equation for critical or collapse pressure for a uniform-static condition from "Advanced Mechanics of Materials" by Seely & Smith.

$$P_{CR} = \frac{2E}{1- \quad ^2} \left(\frac{t}{d}\right)^3 \qquad \text{Eq(707)}$$

The solution of this equation for the Full-Size Unit shows the critical collapse pressure to be 99 psi. This will be also true of the Prototype configuration.

Conclusion: A comparison of the worst hydrogen bubble pressure for the Prototype and the Full-Size Unit shows that the center pipe in the Prototype can be expected to collapse and may plug-off with a one tube rupture. This is of very little concern as it relates to the calculation affecting the shell, liner and other portions of the vessel, since the pressure being used as the worst case does account for center pipe blocked.

9.0 STRUCTURAL ANALYSIS OF THE BOILER COIL SUPPORTS UNDER SODIUM-WATER REACTION CONDITIONS.

1.0 INTRODUCTION:

A tube failure in the boiler tube bundle assembly will produce a Na/H_2O reaction with resulting high hydrogen bubble pressures. During the early times of the reaction there is the possibility of large loadings on the structural elements of the coil support bars adjacent to the segment containing the reaction. These loadings could result in failures due to induced moments and shears producing a possible continuing chain of events and progressive reactions. Since the integrity of the tubes is of prime importance in a sodium-water system the problem in the coil support system resolves itself about:

1. The prediction of the pressure acting upon the supports.
2. The relative strength of the tubing and the supporting elements.

2.0 PREDICTION OF THE PRESSURE DIFFERENTIAL ACROSS THE BOILER COIL SUPPORT BARS:

Figure 6 shows a plot of the spatial distribution of the hydrogen bubble pressure across the boiler coil support bars at any time. The discussion on the methods used in the derivation of this pressure relationship is shown in the Structural Analysis of the Center Pipe. (For the full size unit).

The differential reaction pressures, in terms of percentage of the maximum pressure, across the support bars adjacent to the segment in which the reaction occurs are as follows:

distance from top of support bar	differential pressure (percentage of maximum pressure)
d (ft.)	P_{diff} (%)
1	10
3	28
5	42
7	26
9	10

The maximum worst case pressure for each condition of time at the center of the coil is as follows: (Values from APDA Curve #XVI and from Fig. 1 of Section 10.3.

t (sec)	max - press. (psi)
10^{-4}	20,000
10^{-3}	5,400
10^{-2}	1,700
6×10^{-2}	960

Assuming the maximum worst case pressure acts at the center of the boiler coil.

The following table gives the maximum pressure differential that can be expected across the boiler coil supports at various distances from the top of the support bar.

distance below top of support bar	t(sec)	Pressure Differential (psi) for 25 tubes failing simultaneously
1	10^{-4}	2000
3		5600
5		8400
7		5200
9		2000
1	10^{-3}	540
3		1512
5		2268
7		1404
9		540
1	10^{-2}	170
3		476
5		714
7		442
9		170
1	6×10^{-2}	96
3		269
5		403
7		250
9		96

Figure 1, a plot of these values shows that the pressures are approaching a steady state value at times in the range of 10^{-3} and 10^{-2} seconds.

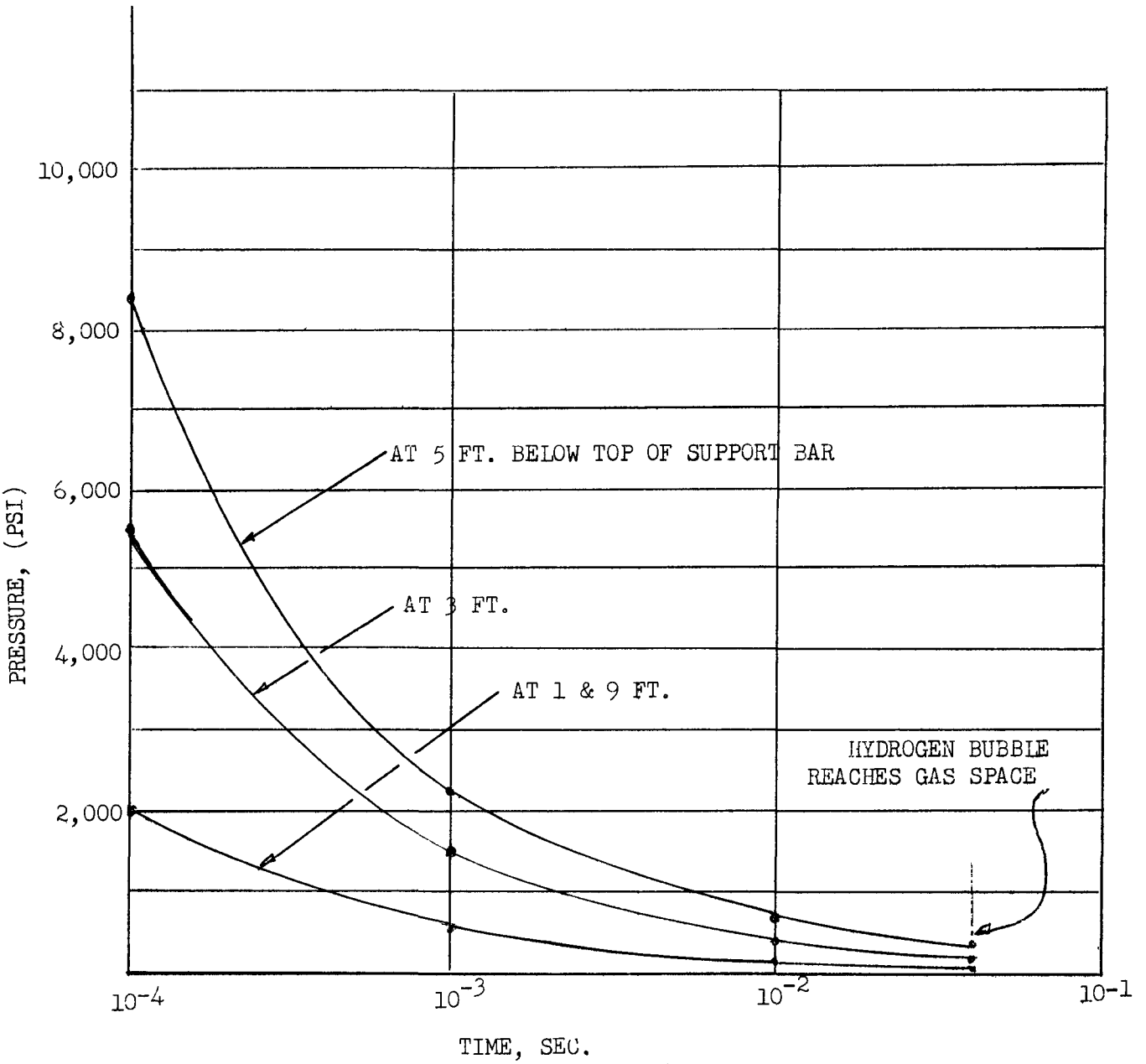

FIG. 1 PRESSURE DIFFERENTIAL ACROSS THE BOILER COIL SUPPORT BARS AT VARIOUS LOCATIONS BELOW THE TOP OF THE BARS.

3.0 CALCULATION OF THE TENSION STRENGTH OF THE WELD CONNECTING THE CLAMPING BARS TO THE COIL SUPPORT BARS:

Refer to the top view of the boiler coil support bars in Figure Number 2. Assuming that the differential pressure across the support bars cause piece number 2 to translate with respect to number 1 and 3, and thereby places the weld in tension. Consider the allowable stress to be equal to the short time ultimate tensile stress, for a condition of failure.

Short time tensile strength of SA-387 GRD D 1000°F = 57,500 psi (from Steel at Elevated Temperatures. U.S. Steel).

The tensile area of the weld is taken as:

$$A_w = .1875'' \times .375'' = 0.070 \text{ in}^2$$

The force the weld can withstand for short time tension is then:

$$F = .070\ (57,500) = 4025\#$$

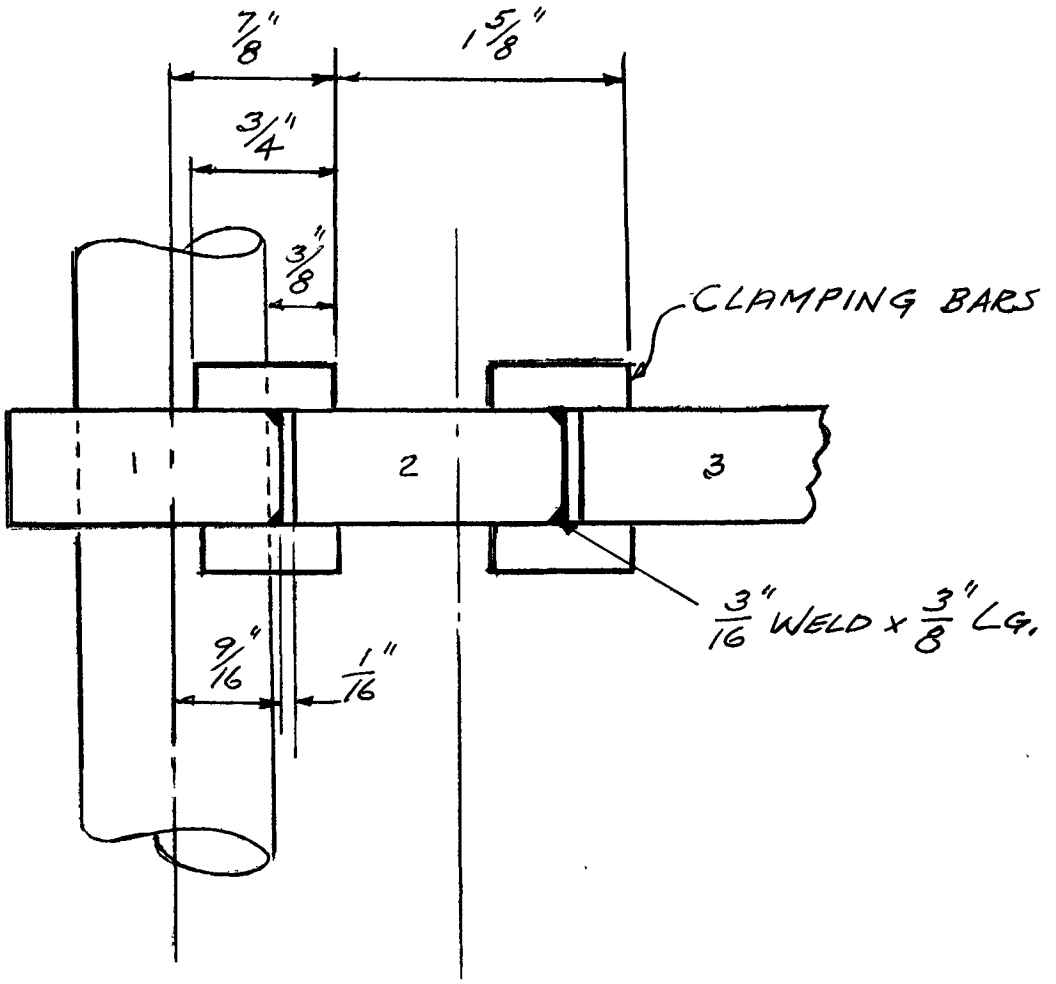

FIG. 2 BOILER COIL SUPPORT BARS.

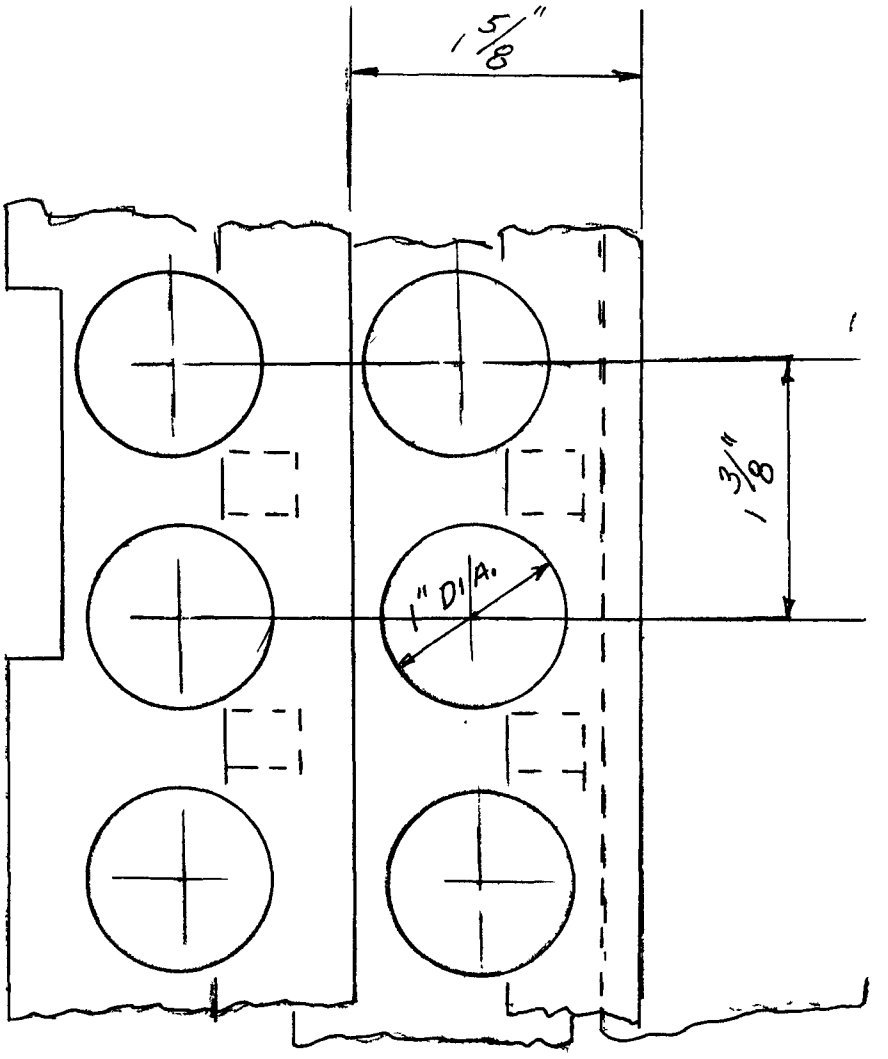

FIG. 3 BOILER COIL SUPPORT BARS.

The load acting on the clamping bar to produce a tension failure in the weld will then be:

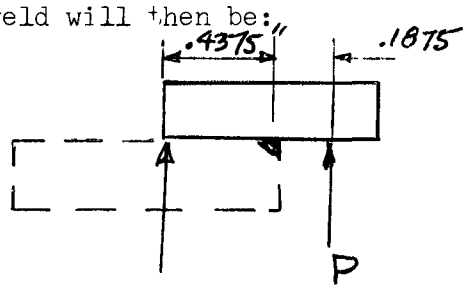

$$\Sigma M = .4375 - .625P$$
$$(.4375)(4025) = .625P$$
$$.625P = 1761$$
$$P = 2818\#$$

The force per unit area is (See Figure 3 side view of boiler coil support bars.):

$$A = (1.625 \times 1.375 - .7854(1^2) = 1.449 \text{ in}^2$$

$$p = \frac{2818}{1.449} = 1945 \text{ psi}$$

Comparing this value with the expected pressure differential across the support bars at times above 10^{-3} where the values are approaching a steady state condition it can be concluded that the weld will be satisfactory for 25 tubes rupturing simultaneously. On the basis of the dynamic analysis for the vessel shells it can be concluded that at shorter times, at and below 10^{-3}, the dynamic strength will be greater than the static strength by a factor of 5 to 1, or better. This would lead to the conclusion that the weld which connects the clamping bars to the coil support bars are satisfactory for a simultaneous failure of 25 tubes.

4.0 CALCULATION OF THE SHEAR STRENGTH OF THE WELD CONNECTING THE CLAMPING BAR TO THE COIL SUPPORT BAR:

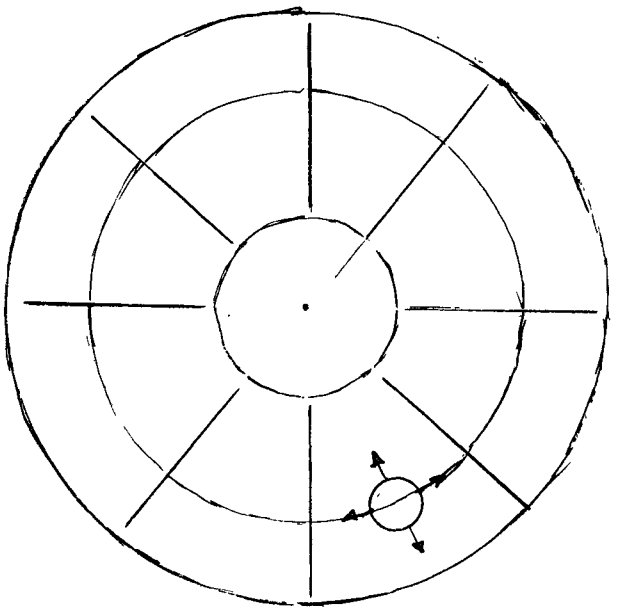

PLAN VIEW THROUGH BOILER SUPPORTS

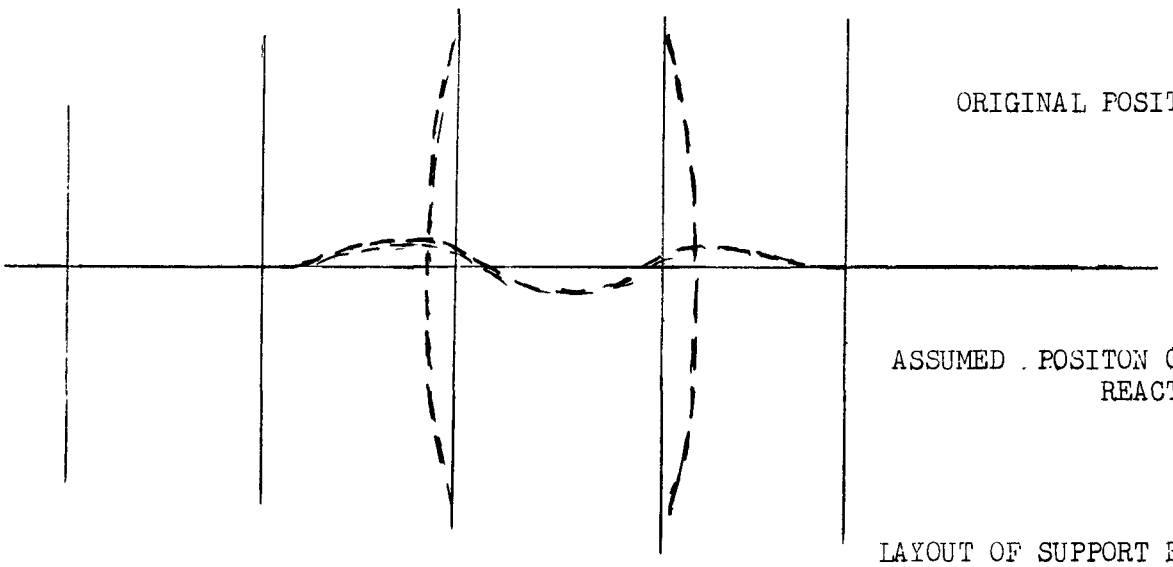

With a reaction as shown in the preceding sketches, it is possible that the coil support bars might deform in the manner shown. In such deformation the tubes will attempt to maintain their perpendicularity with the support bars. In so doing there will be resisting forces produced in the weld and a local moment induced in the tube.

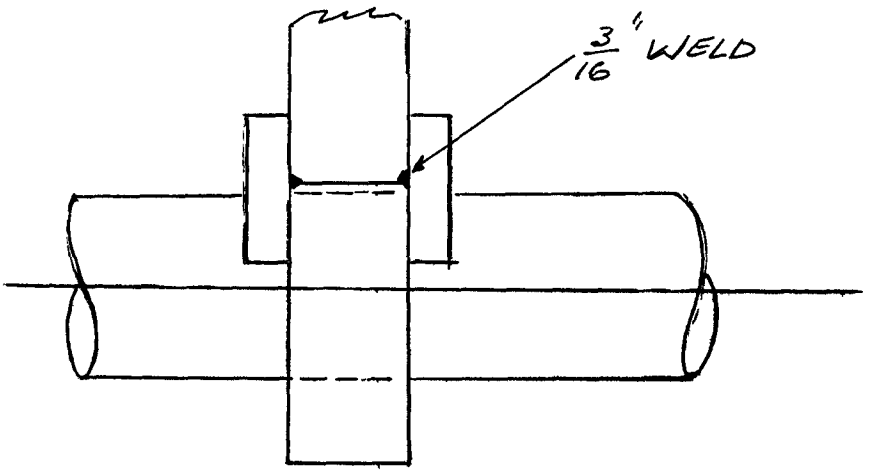

FIG. 4

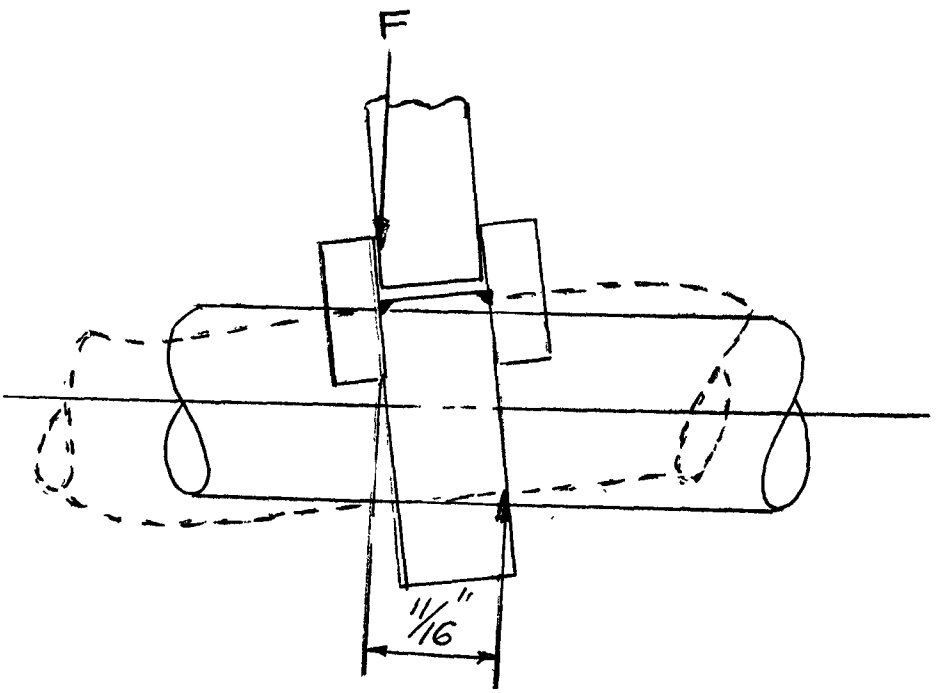

FIG. 5

Fig. 4 indicates the position of the coil support bar on the tube in its normal as erected state.

Fig. 5 indicates the position the support might assume during sodium-water reactions.

It is evident from this picture that there are two main considerations:

1. The shear strength of the weld to failure versus the shear capacity of the tube.
2. The bending of the tube due to the moment applied by the binding action of the tube.

Considering the maximum shear force on the weld first.

The allowable shear stress will be taken as 1/2 the ultimate strength since we are considering a failure condition.

Shear = 1/2 Ultimate

In the boiler coil section there are three major differences in temperature and tube thickness.

1" O.D. x 120" THK	Temp 700F
1" O.D. x 145" THK	Temp 850F
1" O.D. x 165" THK	Temp 1000F

Ultimate @ 700F	=	70,000 psi*
Ultimate @ 850F	=	65,000
Ultimate @ 1000F	=	57,500

* Short time tensiles from Pg. 41 Steels at Elevated Temperature Service, U.S. Steel.

The area of shear for the weld = .070 in^2, F the force the weld will take in shear is:

@ 700F $\quad F = .070 \times \frac{70,000}{2} = 2450\#$

@ 850F $\quad F = .070 \times \frac{65,000}{2} = 2275\#$

@ 1000F $\quad F = .070 \times \frac{57,500}{2} = 2103\#$

5.0 CALCULATION OF SHEAR STRENGTH OF THE BOILER TUBES:

Considering the tube to be in direct shear calculate the force required to shear the tube.

The shear area of the tubes is as follows:

1" O.D. x .120" THK = $.7854\ (1^2 - .760^2) = .331\ in^2$

1" O.D. x .145" THK = $.7854\ (1^2 - .710^2) = .390\ in^2$

1" O.D. x .165" THK = $.7854\ (1^2 - .670^2) = .433\ in^2$

Force required to shear the tubes is:

.120" THK @ 700°F $\quad F = .331 \times \frac{70,000}{2} = 11,585\#$

.145" THK @ 850°F $\quad F = .390 \times \frac{65,000}{2} = 12,675\#$

.165" THK @ 1000°F $\quad F = .433 \times \frac{57,500}{2} = 12,449\#$

It is evident from the values for the shear strength of the weld versus the shear strength of the tube that the weld will fail and peel away from the support before causing failure in the tube.

All of the above is considered at a static state condition. Dynamically the weld will be much stronger for transient conditions as will the tube.

6.0 CALCULATION OF THE STRESSES DUE TO MOMENT AND LONGITUDINAL PRESSURE:

Considering next the bending moment on the tube produced by the couple.

The moment on the tubes is the product of the force the weld can take, for each tube condition, times the moment arm of the couple.

@ 700°F M = 2450# x .6875" = 1684 in -lbs.

@ 850°F M = 2275 x .6875 = 1564 in -lbs.

@ 1000F M = 2013 x .6875 = 1384 in -lbs.

The moment of inertia for each tube is:

1" O.D. x .120" THK $I = .049087\ (1^4 - .760^4) = .033\ in^4$

1" O.D. x .145" THK $I = .049087\ (1^4 - .710^4) = .037\ in^4$

1" O.D. x .165" THK $I = .049087\ (1^4 - .670^4) = .039\ in^4$

The stresses from the moments (which are caused by the restraining action of the coil bars and welds) are for

1" O.D. x .120" THK @ 700F = $= \frac{Mc}{I} = \frac{1684\ (.5)}{.033} = 25{,}515$ psi

1" O.D. x .145" THK @ 850F = $= \frac{1564(.5)}{.037} = 21{,}135$ psi

1" O.D. x .165" THK @ 1000F = $= \frac{1384\ (.5)}{.039} = 17{,}743$ psi

Longitudinal stress in tubes.

1" O.D. x .120" THK $\frac{PR}{2t} = \frac{2825\ (.380)}{2\ (.120)} = 4{,}475$ psi

1" O.D. x .145" THK $= \frac{2800\ (.355)}{2\ (.145)} = 3{,}428$ psi

1" O.D. x .165" THK $= \frac{2775\ (.335)}{2\ (.165)} = 2{,}815$ psi

Total Bending + Pressure Stress

1" O.D. x .120" THK	25,515 + 4,475 = 29,990 psi
1" O.D. x .145" THK	21,135 + 3,428 = 24,563 psi
1" O.D. x .165" THK	17,743 + 2,815 = 20,558 psi

Short time yield strength from Steels for Elevated Temperature Service for 2-1/4 Croloy

@ 700 = 33,000 psi

@ 850 = 30,000

@ 1000 = 28,000

7.0 CONCLUSIONS:

Based on the predicted pressure differentials across the coil support bars it can be concluded that the weld connecting the clamping bars to the support bars will be satisfactory, in tension, for the total number of tubes in the boiler section (25), rupturing simultaneously. It has been established that the welds on the clamping bars will fail before the tubes are affected in shear or before the applied moment causes failure stresses in the tubes.

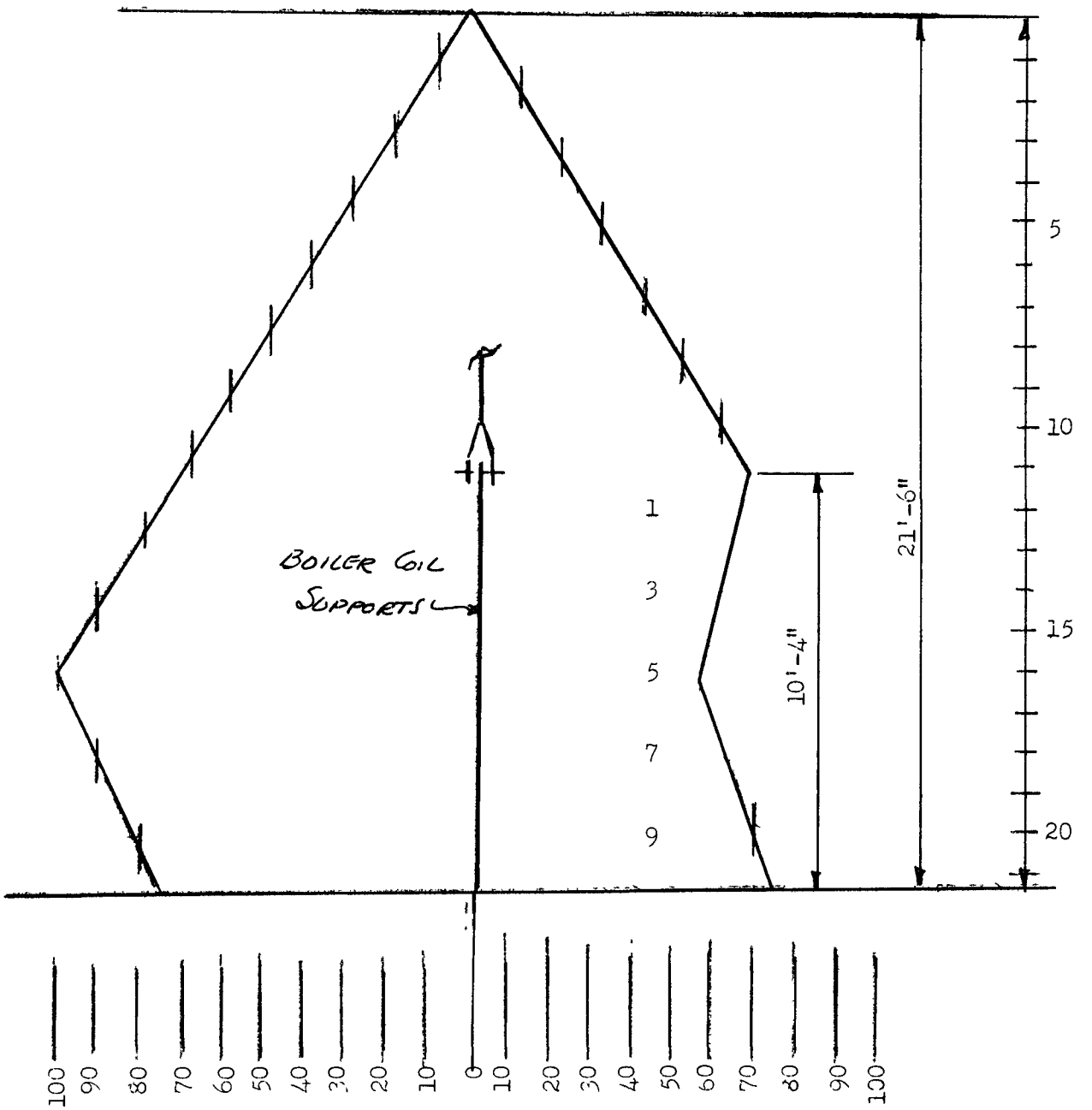

FIG. 6 SPATIAL DISTRIBUTION OF HYDROGEN BUBBLE PRESSURE (FOR ANY TIME) FOR BOILER COIL SUPPORT BARS, REACTION AT CENTER OF COIL BUNDLE.

10.0 ANALYSIS OF THE TUBE VIBRATION SUPPORTS AND BAFFLES.

ANALYSIS OF TUBE SUPPORTS AND BAFFLES DURING A SODIUM-WATER REACTION:

A sodium-water reaction in the boiler downcomer region will produce pressure differentials across the vibration plates and baffles. These plates are used to control the tube vibration and the natural convection flow of the fluid sodium. They have been staggered to provide an escape path for the reaction products up through the unit. These staggered plates will lengthen the path of travel for the flow of these products. Figure 1 shows the actual distance to the sodium level in the unit. Figure 2 shows the total distance through the tortuous path of the staggered plates. Because pressure drop is a linear function of length the pressure at any time in the downcomer annulus will be a maximum of the reaction, and will decay linearly to the sodium surface.

The following tabulation gives the hydrogen bubble pressure for various numbers of tubes rupturing simultaneously. These pressures are for a reaction half-way up the downcomer annulus and is considered as the worst case. Values for tubes 1 - 20 were obtained by using the approximation factor based on the square root of the number of tubes.

TABLE I

PRESSURE (PSIA) AT VARIOUS TIMES

NO. OF TUBES	10^{-4} SEC.	10^{-3} SEC.	10^{-2} SEC.
1	4000	1080	340
5	8944	2414	760
10	12640	3412	1074
15	15480	4179	1315
20	17854	4827	1520
25	20000	5400	1700

The pressure, in terms of percentage of the maximum pressure, at the various locations in the boiler downcomer area (locations indicated on Fig. 2) are as follows:

TABLE II

Location	Pressure %	Pressure Diff. Between Points	
		Points	Press. %
1	70		
2	80	1-2	10
3	90	2-3	10
4	100	3-4	10
5	78	4-5	22
6	64	5-6	14

Using the maximum differential percentage of 10%, and the actual pressures shown in Table I the expected differential pressure across the baffles and supports are as tabulated below: (This is for the baffles and supports in the lower downcomer region, below the downcomer boxes).

TABLE III

PRESSURE (PSIA)

NO. OF TUBES	10^{-4} (SEC.)	10^{-3} (SEC.)	10^{-2} (SEC.)
1	400	108	34
5	894	241	76
10	1264	341	107
15	1548	418	132
20	1784	483	152
25	2000	540	170

Maximum Pressure Loadings the Vibration Plates & Gusset Can Sustain.
(Below the Downcomer Boxes)

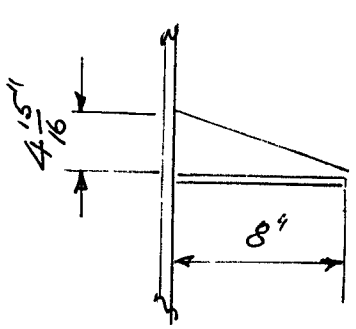

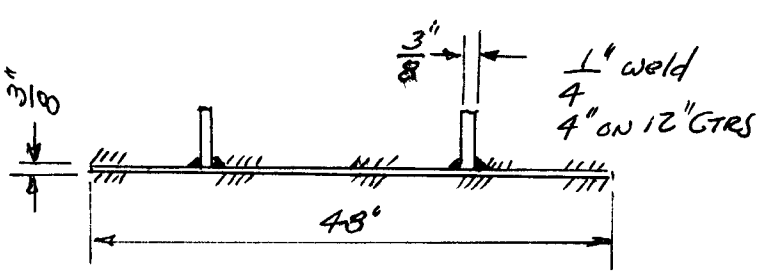

$$M = \frac{p \times 48 \times (8)^2}{2} = 1536p$$

$$y = \frac{(48 \times .375 \times .1875) + 2(4.94 \times .375 \times 2.85)}{18.0 \qquad 2(1.85)} = .644''$$

$$I = \frac{48\ (.375^3)}{12} + (48)\ (.375)\ (467^2) + 2\left(\frac{.375\ 4.94^3}{12}\right) + .375\ (4.94)$$

$$(2.151^2) = 20.4\ in^4$$

The bending stress due to the loading is:

$$= \frac{Mc}{I} = \frac{1536\ pc}{I}$$

The allowable short time tensile stress σ_T for Type 304 Stainless Steel @ 900°F = 60,000 psi (Steels @ Elevated Temperature (U.S. Steel).

$$p = \frac{\sigma_A I}{311c} = \frac{60,000 \times 20.35}{1536 \quad \times 2.47} = \underline{322}\ psi$$

The preceding analysis is based on a static loading solution. The following plot of the expected differential pressures for several conditions of tube failure shows that a steady-state condition is being approached at a time of 10^{-2} and the analysis is valid at this time.

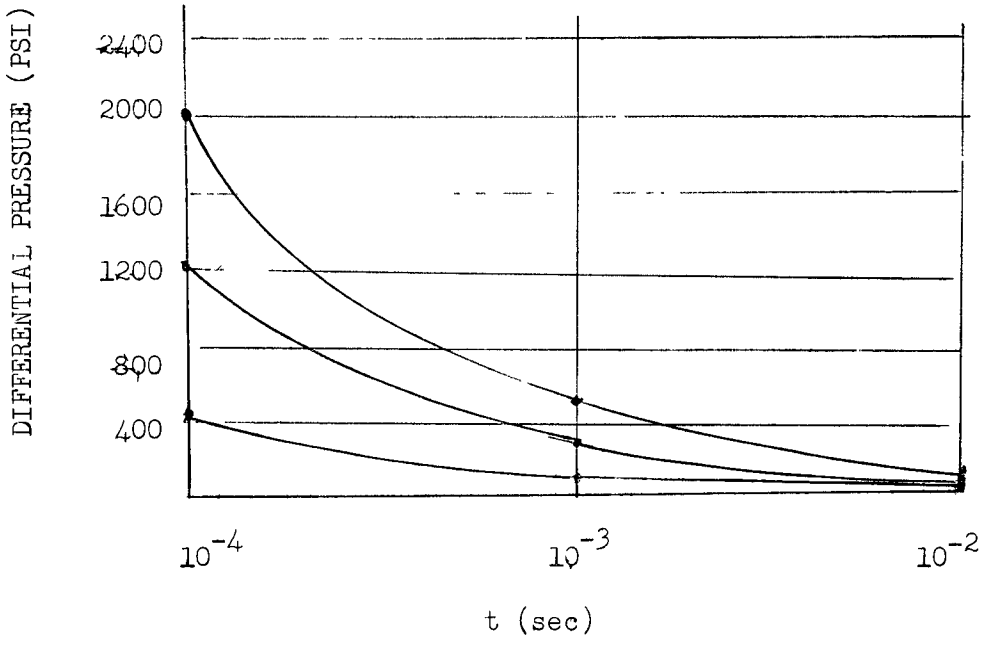

At times of 10^{-4} and 10^{-3} it is evident that the static solution, as such, is not wholly satisfactory.

It is recognized that for the longer duration loads a smaller pressure is required to develop the strain, while for shorter duration loads the required pressure to develop the strain approaches the impulsively applied pressure.

Based on the calculation made for the shell and liner (impulse-momentum method) in Section 4.1 it is possible to make a correlation between the dynamic capabilities and the static solution of the vibration plates and baffles.

The static strength of the shells was shown to be 3647 psi. The total dynamic pressure strength for the shells at the three times of interest are:

$$10^{-4} = 93{,}643 \text{ psi}$$

$$10^{-3} = 15{,}203 \text{ psi}$$

10^{-2} = 4,163 psi

The apparent increase in strength at a time of 10^{-4} is 25 times greater than the static strength, and 4.2 times greater at a time of 10^{-3}. To introduce conservatism into this analysis these factors are reduced by a factor of 1-1/2.

By applying these factors to the calculated static value it is possible to state that the vibration plates will be satisfactory for the following number of simultaneous tube failure.

time (sec.)	Allowable Static Pressure (PSI)	Dynamic Multiplier	Allowable Dynamic Pressure (PSI)	Satisfactory For Simultaneous Rupture of
10^{-4}	322	16.6	5350	25 tubes
10^{-3}	322	2.8	900	25 tubes
10^{-2}	322	1.0	322	25 tubes

This shows the vibration plates to be good for a simultaneous rupture of 25 tubes.

Using the max. value of 22% and the pressures shown in Table 1 the expected differential pressures across the baffles and supports in the downcomer boxes are as tabulated below:

TABLE IV

PRESSURE (PSIA)

NO. OF TUBES	10^{-4} SEC.	10^{-3} SEC.	10^{-4} SEC.
1	880	238	75
5	2200	530	168
10	2780	750	238
15	3400	915	290
20	3920	1060	334
25	4400	1190	380

Maximum Pressure Loading the Vibration Plates & Gussets Can Sustain (In Downcomer Boxes).

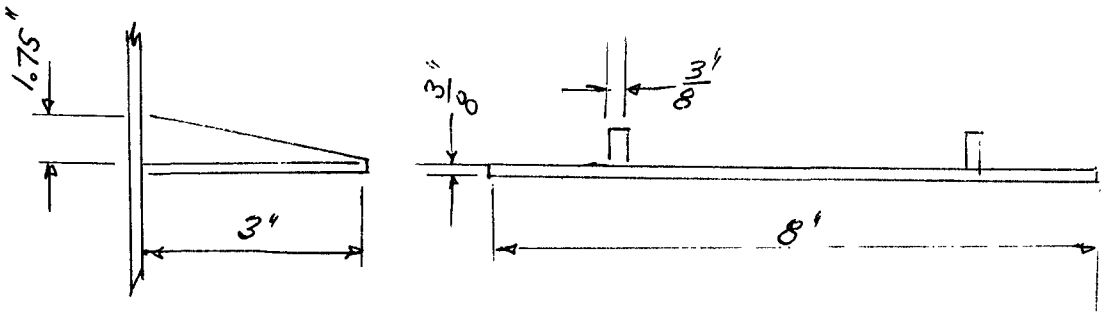

$$M = \frac{p \times 8 \times 5^2}{2} = 100p$$

$$y = \frac{8 \times .375 \times .1875 + 2(1.75 \times .375 \times 1.25)}{3 \qquad 2(.656)}$$

$$= \frac{2.21}{4.312} = .51$$

$$I = \frac{8 \times .375^3}{12} + 8 + .375\ (.32^2) + \frac{2(.375 \times 1.75^2)}{12} + .375 \times 1.75 \times .74^2$$

$$.053 + .315 + .175 + .36 = .90$$

$$p = \frac{60{,}000 \times .90}{100 \quad \times 1.25} = 430 \text{ psi}$$

Using the same factors as used in the previous analysis we get the following results:

time sec.	Allowable Static Pressure (PSI)	Dynamic Multiplier	Allowable Dynamic Press. (PSI)	Satisfactory for Simultaneous Rupture of
10^{-4}	430	16.6	7100	25 tubes
10^{-3}	430	2.8	1200	25 tubes
10^{-2}	430	1.0	430	15 tubes

Both the calculation for the vibration plates and convection plates in the downcomer area in the vicinity of the boiler coil section as well as in the downcomer boxes are good for a simultaneous rupture of total number of tubes (25) in the boiler section.

MAXIMUM LOADING THE WELDS ON VIBRATION PLATES CAN SUSTAIN WELD IN SHEAR:

$$\text{Max. Load} = (p)\ (48)\ (8) = 384p$$

Using an allowable in shear of $\frac{1}{4}$ the short time tensile strength.

Material Type 304 Stainless Steel

tensile @ 900F = 60,000 psi

Allowable = 15,000 psi

$$384p = A = 15{,}000 \times 68\ (.707)\ (.250) = 180{,}285$$

$$p = \frac{180{,}285}{384} = 470 \text{ psi}$$

Comparing the pressure the welds will sustain to failure with the bubble pressure in Table III shows that at the longer times, at 10^{-2}, when the pressure is decaying to a steady state value the welds are good for 25 tube failing simultaneously. This again is a static loading analysis and on the same basis as used on the plates the following will be nearer to the true dynamic strength of the welds.

time (sec)	Allowable Static Pressure (PSI)	Dynamic Multiplier	Allowable Dynamic Pressure (PSI)	Satisfactory for Simultaneous Rupture of
10^{-4}	470	16.6	7800	25 tubes
10^{-3}	470	2.8	1310	25 tubes
10^{-2}	470	1.0	470	25 tubes

CONCLUSIONS:

The vibration plates and baffles will be satisfactory for the simultaneous rupture of 25 tubes with a factor of safety of 1-1/2. This has been shown to be true by solving the problem with static methods of analysis and correlating this with the results of the dynamic strength of the shells to obtain the apparent dynamic strength capabilities of these plates and baffles.

FIG. 1 LAYOUT OF VIBRATION PLATES & CONVECTION BAFFLES IN THE BOILER DOWNCOMER ANNULUS PROTOTYPE STEAM GENERATOR

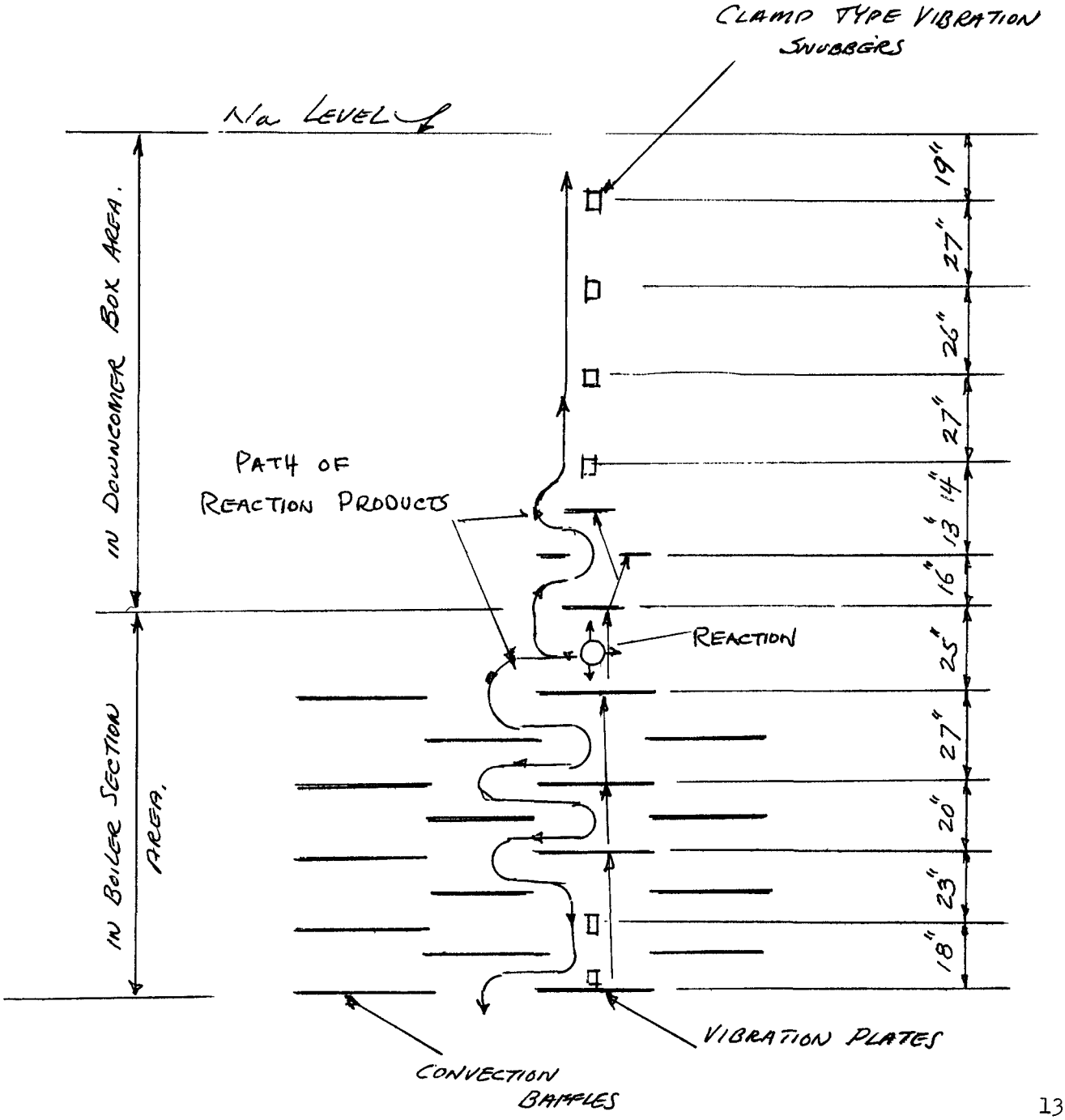

FIG. 2
LAYOUT OF TOTAL DISTANCE
TRAVELED THROUGH THE DOWNCOMER
VIBRATION PLATES & BAFFLES

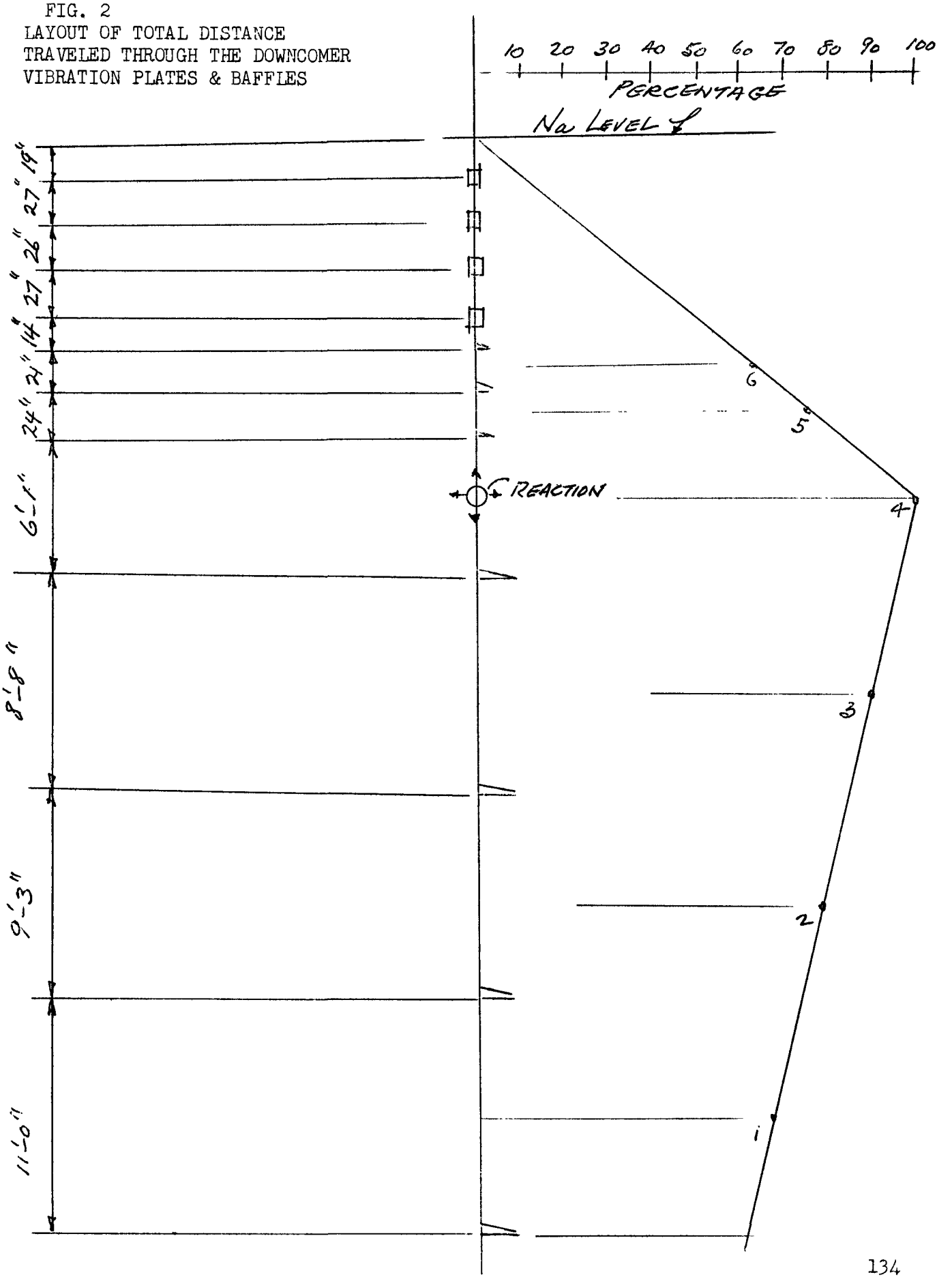

11.0. CREDIBILITY OF OVERHEATING THE SHELL AND LINER DURING A SODIUM-WATER REACTION.

CREDIBILITY OF OVERHEATING THE SHELL AND LINER DURING A SODIUM-WATER REACTION:

The APDA analysis of the Sodium-Water Reaction assumes that the hydrogen is generated at a temperature of 1800°F. Using 1800°F as the reaction boundary condition at the inside of the liner and the shell the transient temperature gradients have been calculated using the analysis of "Conduction of Heat in Solids by Carslaw & Jaeger. These are shown graphically for the shell and liner in Figure 1. It should be noted that the 1800°F was applied to both the inside of the liner and shell. For the actual case this would not be true. The liner would see the 1800°F at the inner surface; however the insulating value of the gas in the space between the liner and outer shell would create a lag in the transfer of the temperature to the outer shell. The temperature of 1800°F applied at the inner surface of both the shell and liner provides a conservatism in the shell calculations.

For the times of concern at 10^{-4} to 1 sec. when the reaction pressures are at the highest values the liner will see only a skin effect and the outer shell will be at the operating temperature. Therefore, there is no concern for a diminishing in the strength of the shell material at the times of high reaction pressures within the shell.

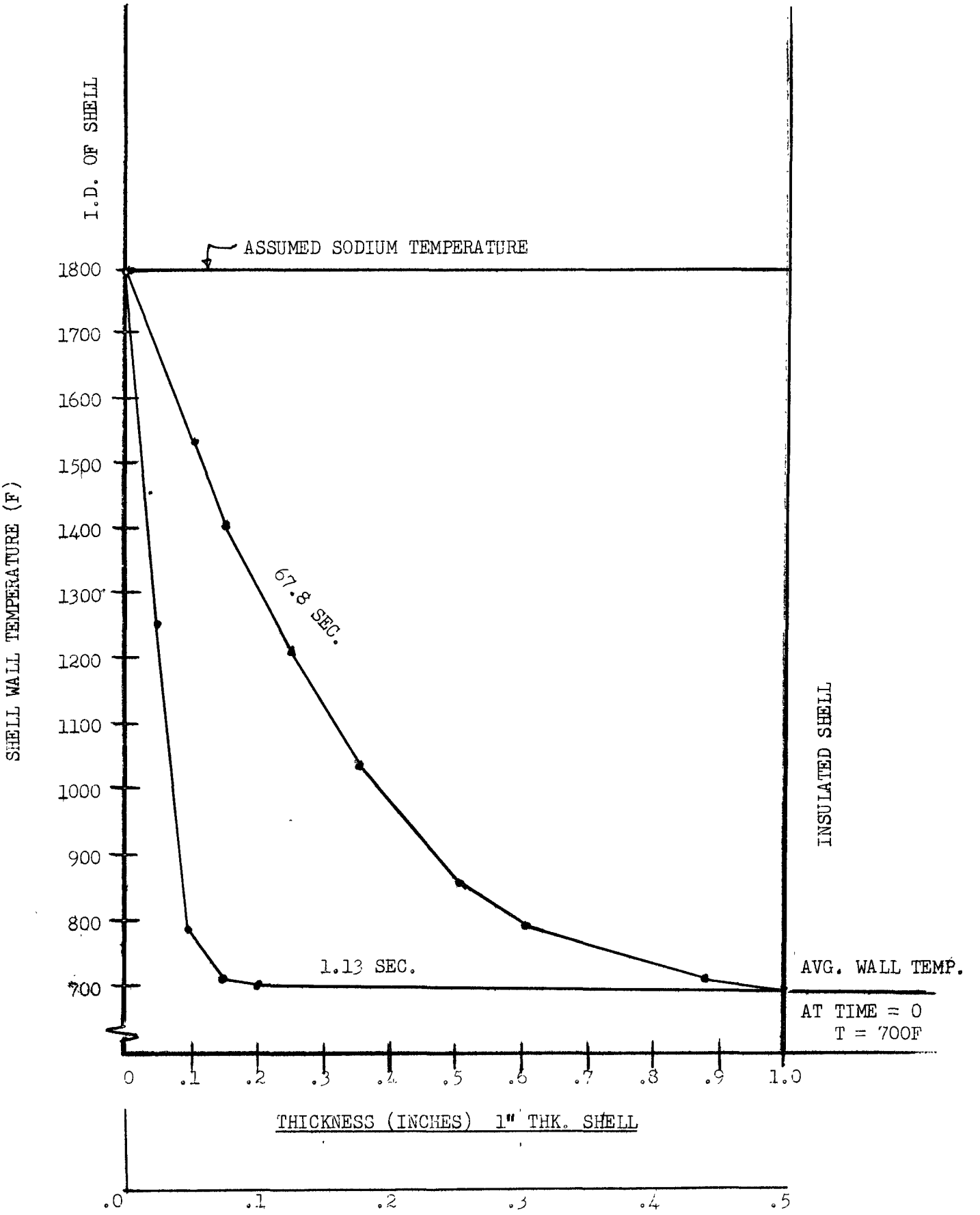

FIG. 1 TRANSIENT TEMPERATURE GRADIENTS IN SHELL, PROTOTYPE